Universität Rostock

Traditio et Innovatio

Analysis and numerics of the full viscous quantum hydrodynamic system with barrier potential

Dissertation

zur Erlangung des Grades

doctor rerum naturalium (Dr. rer. nat.)

am Institut für Mathematik

der Mathematisch-Naturwissenschaftlichen Fakultät

der Universität Rostock

vorgelegt von

Paul Thomas

Rostock, 2023

https://doi.org/10.18453/rosdok_id00004580

Gutachter:

Prof. Dr. Michael Dreher, Universität Rostock, Institut für Mathematik, Analysis-Differentialgleichungen
Prof. Dr. Ansgar Jüngel, Technische Universität Wien, Analysis nichtlinearer PDEs

Jahr der Einreichung: 2023

Jahr der Verteidigung: 2024

Danksagung

An dieser Stelle möchte ich Prof. Dr. Michael Dreher für die Möglichkeit danken an der Universität Rostock zu arbeiten und einen faszinierenden sowie fordernden Bereich der Analysis zu studieren. Weiterhin bin ich dankbar für die inspirierende Zusammenarbeit in der Lehre, in der die Vermittlung von Wissen angestrebt und die Ausbildung einer mathematischen Denkweise gefördert wurde.

Zusammenfassung

In dieser Arbeit soll das vollständige viskose quantenhydrodynamische Modell untersucht werden. Dazu werden zunächst reelle Potenzen von Operatoren und darauf aufbauend fraktionale Sobolev Räume sowie analytische Halbgruppen eingeführt. Zusätzlich geben wir eine Verknüpfung der analytischen Halbgruppe, basierend auf dem Laplace-Operator, zur Fundamentallösung der Wärmeleitungsgleichung. Unter Nutzung analytischer Halbgruppen und fraktionaler Sobolev Räume, sowie u.a. dem Satz von Gagliardo-Nirenberg, zeigen wir zum einen unter der Annahme weitestgehend allgemeiner Anfangsbedingungen und zum anderen unter speziellen Anfangsbedinung die Existenz milder Lösungen zu den viskosen quantenhydrodynamischen Gleichungen, die wir mit einem zusätzlichen Barrierepotential versehen. Wir zeigen weiterhin, dass diese Lösungen Hölder-stetig und stetig differenzierbar sind. Die analytische Betrachtung schließen wir mit dem linearisierten System und der Stabilitätsanalyse stationärer Lösungen ab, wobei wir die Instabilität des vollständigen viskosen quantenhydrodynamischen Systems für große Stromdichten zeigen.
Im zweiten Teil dieser Arbeit erklären wir zunächst die Diskretisierung von Ableitungen und beschreiben die Fortsetzungsmethode mittels Prediktor-Korrektor-Verfahren. Für das zeitabhängige Problem nutzen wir die Rückwärts-Euler-Zeitintegration und geben eine numerische Lösung für eine Spannung von $0V$. Abschließend geben wir Lösungen des stationären Systems und eine Strom-Spannungskurve an.

Abstract

In this work, we investigate the full viscous quantum hydrodynamic model. First, real powers of operators, fractional Sobolev spaces and analytic semigroups are introduced. Additionally, we give a relation of the analytic semigroup, based on the Laplace operator, to the fundamental solution of the heat conduction equation. Using analytical semigroups and fractional Sobolev spaces, as well as the Gagliardo-Nirenberg inequality, we show the existence of mild solutions to the viscous quantum hydrodynamic equations with an additional barrier potential, under the assumption of rather general initial conditions and special initial conditions. We further show that these solutions are Hölder continuous and continuously differentiable. We conclude the analytical consideration with the linearized system and the stability analysis of stationary solutions, whereby we show instability of the full viscous quantum hydrodynamic system for large current densities. In the second part of this thesis we explain the discretization of derivatives and the continuation method using a predictor-corrector scheme. The time dependent, spatially discretized problem is solved by backward Euler time integration and we give a numerical solution for a voltage of $0V$. Finally, we present solutions to the stationary system and the current-voltage characteristic.

Contents

Chapter 1

Introduction

Quantum technology is a key research field of the 21st century, with applications in e.g. communication, cryptography, computer science and measuring devices. One very important quantum effect, that was already exploited in experimental setups even before the Einstein-Podolsky-Rosen paradox was proposed in 1935, is quantum tunneling, which e.g. allows the α-decay. There are several applications of quantum tunneling today, for example tunnel field-effect transistor, nuclear fusion and scanning tunneling microscope. Furthermore, quantum tunneling is crucial for the resonant tunneling diode, which received increasing attention during the last 20 years, see [FSCM12, AS16, MKSA16, Fei19]. Such diodes show negative differential resistances and are able to create frequencies in the $Terahertz$ range, useful for ultra fast electronics.

Let us briefly investigate this phenomenon. Quantum tunneling allows particles, e.g. electrons, to tunnel through barriers. The most basic model is the tunneling of an electron through a single square barrier of finite height. In vacuum, a single electron can be described by a plane wave, when we neglect the normalization. Then, the corresponding stationary single particle Schrödinger equation in one space dimension, with the physical constants set to 1 for simplicity, is given by

$$\psi''(x) = (V(x) - E)\psi(x),$$

where ψ is the electron wave function, V is the square barrier potential and E is the energy of the electron, which is smaller than the barrier height. Now, let $a < b$, $U > 0$ and the barrier be

$$V(x) = \begin{cases} U, & a \leq x \leq b \\ 0, & else \end{cases} .$$

Using the continuity and smoothness conditions $\psi(a-0) = \psi(a+0)$, $\psi(b-0) = \psi(b+0)$,

$\psi'(a-0) = \psi'(a+0)$ and $\psi'(b-0) = \psi'(b+0)$, we obtain the wave function

$$\psi(x) = \begin{cases} \mathrm{e}^{\mathrm{i}kx} + R\mathrm{e}^{-\mathrm{i}kx}, & x < a \\ c\mathrm{e}^{\alpha x} + d\mathrm{e}^{-\alpha x}, & a \leq x \leq b \\ T\mathrm{e}^{\mathrm{i}kx}, & b < x \end{cases},$$

with wave vector k, $\alpha^2 = U - k^2 > 0$, some constants c, $d \in \mathbb{R}$, the reflection coefficient R and transmission coefficient T. Then, the transmission probability is given by

$$|T|^2 = \left[1 + \frac{U^2}{4k^2\alpha^2}\sinh^2(\alpha(b-a))\right]^{-1}.$$

The calculations are given in the appendix A. Remarkably, the electron can be observed behind the barrier. This result can only be obtained by the quantum mechanical approach.

If a second barrier is added, we observe the formation of a finite potential well between both barriers. For simplicity, let us have a look at a single electron in a box. Again, the stationary Schrödinger equation reads

$$\psi''(x) = (V(x) - E)\psi(x),$$

with the potential well of width L given by

$$V(x) = \begin{cases} 0, & 0 < x < L \\ \infty, & else \end{cases}.$$

Since the electron can not leave the box, we use the Ansatz $\psi(x) = A\cos(kx) + B\sin(kx)$ with the condition $\psi(0) = 0 = \psi(L)$. This gives the energy $E = k^2$ with $k = n\pi/L$. Therefore, inside the box are only discrete energy values allowed. The same holds true for the potential well with finite height, although the energy values can only be calculated numerically.

Combining the previous considerations, incorporating reflection and transmission at the boundary layers for incoming waves, one can calculate the transmission probability for a double square potential barrier, which is given by

$$|T|^2 = \frac{|T_1|^2|T_2|^2}{1 + |R_1|^2|R_2|^2 - 2|R_1||R_2|\cos(\phi)},$$

where ϕ includes the phase shifts for each reflection inside the potential well. The calculations of the transmission coefficient for a double barrier can be found in [XDZ12] and taking the absolute value gives the transmission probability for the double barrier setup. Since ϕ can be equal to 0, the transmission probability can be exactly 1 in case of identical barriers, and the double barrier system would be transparent to the electron. This effect is called resonance tunneling and occurs if the energy of the incoming electron is identical to an admissible energy value of the potential well.

If a voltage is applied to such a double barrier setting, the energy of the electrons on one side will be increased with increasing voltage until the first energy level of the well is reached, increasing the current to a maximum. Further raising the voltage actually decreases the current and one observes the negative differential resistance.

In a realistic setting, the potential barriers have a more complicated form, the electrons move through semiconductor materials and a sophisticated physical model becomes necessary in order to understand the flow of the electrons. There exists several models like the quantum Vlasov-, quantum Boltzmann-, quantum drift diffusion equations and the viscous quantum hydrodynamic model.

In this work, we study the full viscous quantum hydrodynamic model with an additional barrier potential - a system of nonlinear parabolic partial differential equations and a Poisson equation. We divide the work in two parts.

The first part covers the analytical results and we start by the introduction of knowledge from functional analysis in ch. 2. This includes Sobolev spaces and important theorems, like the Gagliardo-Nirenberg inequality, that we use regularly during the following proofs. Then, we define Banach scales and interpolation spaces, which complement the Sobolev spaces. Additionally, we give some results concerning fractional powers of operators. We conclude the first chapter with semigroups and the heat kernel. Especially the semigroup approach allows us to prove the existence of a solution to the given system of partial differential equations.

In ch. 3, we briefly introduce the full viscous quantum hydrodynamic system with barrier potential and formulate the problem, which we solve in the subsequent sections. Using the mathematical methods from the previous chapter, we present a solution to the parabolic problem for a variety of initial conditions and a special case, which is analogous to switching on the device. We finalize this chapter with our analysis of the linearized system and present results regarding the stability of stationary solutions.

During the second part of this work, ch. 4, we recapitulate the spatial discretization of differential equations and present a continuation method. With these fundamentals, we discretize the full viscous quantum hydrodynamic system, which will be solved by backward Euler time integration and continuation starting from an initial point. Additionally, we solve the stationary viscous quantum hydrodynamic equations for various applied voltages. The corresponding code, written in Matlab, is given in the appendix B. In the app. C we present our results for the isothermal case of the viscous quantumhydrodynamic system to test our algorithm. Lastly, in app. D, we give the Jacobian to the discretized full viscous quantum hydrodynamic system.

Chapter 2

Mathematical methods

For a given mathematical problem we need appropriate tools to solve them. In case of partial differential equations (PDEs) or systems of PDEs we choose our method based on the type of equation. The type of a PDE is determined by the number of derivatives, that is the order of the differential equation, linearity and homogeneity. Several subcategories concerning the order are possible, e.g. second-order PDEs can be elliptic, hyperbolic or parabolic. Examples for parabolic PDEs are the heat equation and other diffusion equations. A well known elliptic PDE is the Poisson equation. Furthermore, a PDE defined on a bounded domain is given with boundary and initial conditions, if the unknown is time dependent. Popular examples are Dirichlet-, Neumann- and Robin-type boundary conditions.

Since we will investigate a system of inhomogeneous parabolic PDEs with homogeneous Neumann boundary conditions coupled to a Poisson equation, where the nonlinear inhomogeneities depend on the unknown itself, methods like separation of variables or Fourier transform are insufficient. Also, the nonlinear perturbations may not be functions in the classical sense and a more general definition of functions becomes necessary.

Therefore, the following sections give a short introduction in functional analysis. In section 2.1 we recapitulate important theorems from functional analysis concerning Sobolev spaces. Then, we further expand our understanding of function spaces with the use of interpolation spaces and Banach scales in sec. 2.2, which follows [Ama95]. In sec. 2.3, semigroups are considered. Additionally, we have a quick look at the heat kernel in sec. 2.4, which finally connects the operator theory to more classical approaches like Duhamel's principle.

2.1 Function spaces

This section is a recap of basic knowledge concerning Lebesgue, Hölder and Sobolev spaces. By $\|.\|_{L^p(\Omega)}$ we denote the usual L^p norm on the set $\Omega \subset \mathbb{R}^n$ for $1 \leq p \leq \infty$. The Hölder spaces are denoted by $C^{k,\alpha}(\Omega)$, with $0 < \alpha \leq 1$, and we denote the well known Sobolev spaces by $W_p^k(\Omega)$, with $k \in \mathbb{N}$ and $1 \leq p \leq \infty$. Beside Young's and Hölder's inequalities we will use the following embedding theorems.

Theorem 2.1.1 (Gagliardo-Nirenberg inequality, [BM18]). *Let $\Omega \subset \mathbb{R}^n$ be a bounded Lipschitz domain, $1 \leq q, r \leq \infty$ and $m \in \mathbb{N}$. For $\alpha \in \mathbb{R}$ and $j \in \mathbb{N}$ with*

$$\frac{1}{p} = \frac{j}{n} + \left(\frac{1}{r} - \frac{m}{n}\right)\alpha + \frac{1-\alpha}{q},$$

and $j/m \leq \alpha \leq 1$ it holds

$$\|\partial^j x\|_{L^p(\Omega)} \leq C\|\partial^m x\|^{\alpha}_{L^r(\Omega)}\|x\|^{1-\alpha}_{L^q(\Omega)},$$

where C only depends on j, m, n, q, r, α and the domain.

These embeddings rely on the regularity of the domain Ω. There are several possible restrictions to the boundary, e.g. the cone condition or Lipschitz domains. We refer to [AF03] for further reading, where more conditions are explained in detail. Since we only consider bounded intervals on $\mathbb{R}$, we will not pursue this topic.

Theorem 2.1.2 (Sobolev-Embedding, [AF03]). *Let $\Omega \subset \mathbb{R}^n$, $k, l \in N$ with $k > l$ and $1 \leq p < q < \infty$ such that*

$$\frac{1}{p} - \frac{k}{n} = \frac{1}{q} - \frac{l}{n},$$

then the continuous embedding $W^k_p(\Omega) \hookrightarrow W^l_q(\Omega)$ holds.

Note, that the Sobolev embedding is a special case of the Gagliardo-Nirenberg inequality for $\alpha = 1$.

The previous inequalities show a trade-off between differentiability and integrability. Furthermore, we have a connection to continuous or continuous differentiable functions with the following theorem.

Theorem 2.1.3 (Morrey's inequality, [Eva10]). *Let $\Omega \subset \mathbb{R}^n$, $k \in \mathbb{N}$ and $1 < p < \infty$ with $kp > n$ such that*

$$\frac{1}{p} - \frac{k}{n} = -\frac{r+\alpha}{n}$$

with $\alpha \in (0, 1]$ and $r \in \mathbb{N}$. Then $W^k_p(\Omega) \hookrightarrow C^{r,\alpha}(\Omega)$.

Thus, if a function does have weak derivatives up to a sufficient order and being sufficiently integrable, it is a continuous function or even continuously differentiable. This is an important property, useful in the analysis of partial differential equations. We are able to prove existence of solutions with weak derivatives, study their regularity, or smoothness, and may be able to show continuity. For further reading about Sobolev spaces we refer to [AF03, Ren04, Eva10, Bré11, Bre13, Sch13], which have different level of detail, perspectives, proofs and several examples.

Now, given a nonlinear inhomogeneous PDE, we need appropriate function spaces in order to prove existence of solutions, highly depend on properties of the inhomogeneities and nonlinearities. With the previously mentioned relation between integrability and differentiability, how do we choose such a function space? First, we utilize fractional order and negative order Sobolev spaces to estimate the inhomogeneous and nonlinear parts of the PDE. Then, we choose a function space based on these estimates, which allows us to prove existence of a solution, although the term "solution" needs to be defined appropriately. The next section follows the theory of Amann [Ama95] in order to define fractional order Sobolev spaces and negative order Sobolev spaces in the context of Banach scales.

2.2 Banach scales and interpolation spaces

This section covers the concept of Banach scales and interpolation spaces to build fractional order Sobolev spaces. We follow closely [Ama95], which gives an abstract and general presentation of interpolation spaces, Banach scales, semigroups and applications. However, we will use more specific function spaces. This gives the reader a simpler introduction into this topic and prepares the following chapter. Basic definitions will be in a general frame and results are given for L^p- and Sobolev spaces. Starting with powers of operators and Banach scales we define fractional order Sobolev spaces and identify them as interpolation spaces of L^p-and Sobolev spaces later on.

Let us consider the linear differential operator $A = \nu\partial_x^2$ with $\nu > 0$ in $L^p(\Omega)$, with the domain $\Omega = (0, 1)$ and Neumann bondary conditions $\partial_x u = 0$ for $x = 0, 1$. Of course, the following can be applied to more general linear operator and domains. Since the resolvent operator $R_\lambda(A) = (\lambda - A)^{-1}$ is a linear bounded operator, see [Lun12] for proofs concerning general elliptic operators, and A has the spectrum $\sigma(A) \subset (-\infty, 0]$, we can define the sector $\Sigma_\delta = \{z \in \mathbb{C} : |\arg(z)| < \pi - \delta\}$ for some $\pi/2 > \delta > 0$. Actually, we give the following more specific definition.

Definition 2.2.1. *Let the linear operator A be closed and densely defined in the Banach space X. If the resolvent set of A contains a sector $\Sigma_\theta = \{z \in \mathbb{C} : |\arg(z - \omega)| \leq \theta\}$ for some $\theta \in (0, \pi)$, $\omega \in \mathbb{C}$ and the resolvent operator enjoys the estimate*

$$\|(\lambda - A)^{-1}\| \leq \frac{M}{|\lambda - \omega|}, \quad M > 0,$$

then we call A a sectorial operator of angle θ.

Note, that sectorial operators are already quite restricted in their properties. On the other hand, this gives us some properties that allow the utilization of Dunford's integral. Now, we can define negative fractional powers of the operator.

Definition 2.2.2. *Let A be a sectorial operator of angle $\theta > \pi/2$. The fractional powers $\alpha < 0$ of A are defined by*

$$A^\alpha = \frac{1}{2\pi \mathrm{i}} \int_\Gamma \lambda^\alpha R_\lambda(A) \mathrm{d}\lambda,$$

where Γ *is a curve in* Σ_δ *going from* $\infty e^{-i\psi}$ *to* $\infty e^{i\psi}$ *with* $\psi \in (\pi/2, \theta)$. *Furthermore, we define* $A^0 = 1$.

Let us give some important properties.

Lemma 2.2.1. *The integral in definition* (2.2.2) *does not depend on the choice of* Γ *and for* $\alpha > 0$ *there exists a constant* $C > 0$ *such that* $\|A^{-\alpha}\| \leq C$. *Furthermore, we have the relation*

$$A^{-\alpha}A^{-\beta} = A^{-(\alpha+\beta)}, \quad \alpha, \beta > 0.$$

Proof. Let X be a Banach space and A a sectorial operator of angle $\theta > \pi/2$ and w.l.o.g. $\omega = 0$. In case of $\omega \neq 0$ we can shift the path of integration by ω and use the estimate $|\lambda - \omega|^{-1} \leq C|\lambda|^{-1}$ for some constant $C > 0$.

We choose the curve $\Gamma = \Gamma_1 \cup \Gamma_2 \cup \Gamma_3$ given by

$$\begin{aligned}
\Gamma_1 &= \{\lambda \in \mathbb{C} : \lambda = re^{-i\psi}, \infty \geq r \geq \epsilon\}, \\
\Gamma_2 &= \{\lambda \in \mathbb{C} : \lambda = \epsilon e^{i\phi}, -\psi \leq \phi \leq \psi\}, \\
\Gamma_3 &= \{\lambda \in \mathbb{C} : \lambda = re^{i\psi}, \epsilon \leq r \leq \infty\},
\end{aligned}$$

with $\psi \in (\pi/2, \theta)$ and $\epsilon > 0$. Now, we show that $A^{-\alpha}$ defined by (2.2.2) is a bounded operator as follows

$$\begin{aligned}
\|A^{-\alpha}x\| &= \left\| \frac{1}{2\pi i} \int_\Gamma \lambda^{-\alpha} R_\lambda x \mathrm{d}\lambda \right\| \\
&\leq \frac{M}{2\pi} \left(2 \int_\epsilon^\infty r^{-(1+\alpha)} \mathrm{d}r \|x\| + \int_{-\psi}^{\psi} \epsilon^{-\alpha} \mathrm{d}\phi \|x\| \right) \\
&\leq C\|x\|,
\end{aligned}$$

where we used the estimate of the resolvent operator $\|R_\lambda x\| \leq M\|x\|/|\lambda|$.

Next, we will show independence of the choice of Γ. Let $R > 0$, $\pi/2 < \theta_\delta < \theta_\epsilon < \theta$ and $\Gamma_{\epsilon,R}$, $\Gamma_{\delta,R}$ be the curves given by

$$\begin{aligned}
\Gamma_{\epsilon,R,1} &= \{\lambda \in \mathbb{C} : \lambda = re^{i\theta_\epsilon}, R \geq r \geq \epsilon\}, \\
\Gamma_{\epsilon,R,2} &= \{\lambda \in \mathbb{C} : \lambda = \epsilon e^{i\phi}, \theta_\epsilon \geq \phi \geq -\theta_\epsilon\}, \\
\Gamma_{\epsilon,R,3} &= \{\lambda \in \mathbb{C} : \lambda = re^{-i\theta_\epsilon}, \epsilon \leq r \leq R\}, \\
\Gamma_{\delta,R,1} &= \{\lambda \in \mathbb{C} : \lambda = re^{-i\theta_\epsilon}, R \geq r \geq \delta\}, \\
\Gamma_{\delta,R,2} &= \{\lambda \in \mathbb{C} : \lambda = \delta e^{i\phi}, -\theta_\delta \geq \phi \geq \theta_\delta\}, \\
\Gamma_{\delta,R,3} &= \{\lambda \in \mathbb{C} : \lambda = re^{i\theta_\delta}, \delta \leq r \leq R\},
\end{aligned}$$

that we connect with the two curves

$$\Gamma_{R,1} = \{\lambda \in \mathbb{C} : \lambda = R\mathrm{e}^{\mathrm{i}\phi}, \theta_\delta \leq \phi \leq \theta_\epsilon\},$$
$$\Gamma_{R,2} = \{\lambda \in \mathbb{C} : \lambda = R\mathrm{e}^{\mathrm{i}\phi}, -\theta_\epsilon \leq \phi \leq -\theta_\delta\},$$

to obtain the closed curve Γ, as sketched in fig. 2.1. Since $\lambda^{-\alpha}R_\lambda x$ is holomorphic in the region enclosed by Γ for all $x \in X$ we have

$$\int_\Gamma \lambda^{-\alpha} R_\lambda x \mathrm{d}\lambda = 0.$$

We estimate the integral along the curve $\Gamma_{R,1}$ as follows

$$\left\| \int_{\Gamma_{R,1}} \lambda^{-\alpha} R_\lambda x \mathrm{d}\lambda \right\| \leq M \int_{\theta_\delta}^{\theta_\epsilon} R^{-\alpha} R R^{-1} \|x\| \mathrm{d}\phi = C \frac{\theta_\epsilon - \theta_\delta}{R^\alpha} \|x\|.$$

In the limit $R \to \infty$ the integral along $\Gamma_{R,1}$ vanishes and the same holds true for $\Gamma_{R,2}$, by analogous calculations. Now, let Γ_δ and Γ_ϵ be the limits of $\Gamma_{\delta,R}$ and $\Gamma_{\epsilon,R}$, respectively, for $R \to \infty$. Then, we obtain

$$\int_{\Gamma_\delta} \lambda^{-\alpha} R_\lambda x \mathrm{d}\lambda = - \int_{\Gamma_\epsilon} \lambda^{-\alpha} R_\lambda x \mathrm{d}\lambda.$$

Note, that Γ_ϵ is negative orientated while Γ_δ has positive orientation.

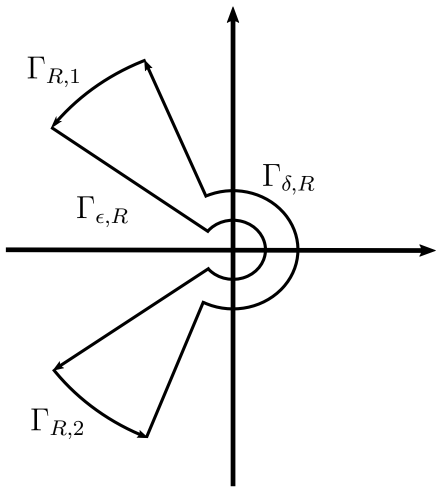

Figure 2.1: The closed integration path Γ in the complex plane.

Let us verify the semigroup property. For this, we use the resolvent identity

$$(\mu - \lambda) R_\lambda R_\mu = R_\lambda - R_\mu,$$

and calculate for two paths Γ and Γ', with Γ lying entirely to the left of Γ',

$$\begin{aligned}
A^{-\alpha}A^{-\beta}x &= \frac{1}{(2\pi\mathrm{i})^2}\int_\Gamma\int_{\Gamma'}\lambda^{-\alpha}\mu^{-\beta}R_\lambda R_\mu x\mathrm{d}\mu\mathrm{d}\lambda \\
&= \frac{1}{(2\pi\mathrm{i})^2}\int_\Gamma\int_{\Gamma'}\lambda^{-\alpha}\mu^{-\beta}\frac{R_\lambda x - R_\mu x}{\mu-\lambda}\mathrm{d}\mu\mathrm{d}\lambda \\
&= \frac{1}{(2\pi\mathrm{i})^2}\left(\int_\Gamma\int_{\Gamma'}\lambda^{-\alpha}\frac{\mu^{-\beta}}{\mu-\lambda}R_\lambda x\mathrm{d}\mu\mathrm{d}\lambda + \int_\Gamma\int_{\Gamma'}\mu^{-\beta}\frac{\lambda^{-\alpha}}{\lambda-\mu}R_\mu x\mathrm{d}\mu\mathrm{d}\lambda\right) \\
&= \frac{1}{2\pi\mathrm{i}}\int_\Gamma\lambda^{-(\alpha+\beta)}R_\lambda x\mathrm{d}\lambda \\
&= A^{-(\alpha+\beta)}.
\end{aligned}$$

The second integral vanishes, because $\lambda^{-\alpha}$ is holomorphic in $\mathbb{C}\setminus(-\infty,0]$ and Γ lies to the left of Γ', more precisely μ is outside of the region enclosed by Γ. □

For further reading concerning properties of fractional powers and calculations, we refer to [Ama95, Lun12, Ren04], with different frameworks and notations. Let us now define fractional powers of the operator A.

Definition 2.2.3. *The fractional power $\alpha > 0$ of a sectorial operator A of angle $\theta > \pi/2$ is defined by*

$$A^\alpha = \left(A^{-\alpha}\right)^{-1}.$$

Since $A^{-\alpha}$ is injective and therefore has an inverse, this definition is reasonable. See [Ren04] for details. From the definition and the previous lemma it follows, that $A^{\alpha+\beta} = A^\alpha A^\beta$ also holds for $\alpha, \beta > 0$. However, in the following chapter we consider the one dimensional Laplace operator with Neumann boundary conditions, hence A is not injective. Thus, definition (2.2.2) gives a representation for A^{-1}, such that $AA^{-1} = 1$, but $A^{-1}A \neq 1$.

Now, let us define Banach scales, especially power scales, using the previous results.

Definition 2.2.4. *Let $A = \mathrm{d}_x^2$, $0 < \alpha < 1$ and $\mathrm{D}(A^\alpha) = \mathrm{Range}(A^{-\alpha}) + \mathbb{R}$. Then, the fractional order Sobolev spaces on a domain Ω are defined by*

$$W_p^{2\alpha}(\Omega) = \left(\mathrm{D}\left(A^\alpha\right), \|.\|_{W_p^{\lfloor 2\alpha\rfloor}(\Omega)} + \|A^\alpha .\|_{L^p(\Omega)}\right),$$

with $\alpha \in \mathbb{R}$ and $1 \leq p < \infty$.

Note, that the spaces $W_p^{2\alpha}(\Omega)$ with $\alpha \in \mathbb{N}$ coincide with the previously introduced Sobolev spaces. Moreover, there are different definitions of fractional order Sobolev spaces, e.g. Bessel-potential spaces [AH96], Sobolev-Slobodeckij spaces [DNPV12], Besov spaces [AF03]. Each of these approaches has its benefits. Specific calculations and embeddings can be quite difficult using definition (2.2.4). On the other hand, estimates involving the semigroup generated by $A = \mathrm{d}_x^2$ need less effort.

Since the parameter α can be negative we immediately obtain negative fractional order Sobolev spaces. These coincide with the dual spaces of Sobolev spaces with $\alpha > 0$, more precisely $W_p^{-\alpha}(\Omega) = \big(W_{q,0}^{\alpha}(\Omega)\big)'$ with $\alpha > 0$ and $1/p + 1/q = 1$.

Theorem 2.2.2. *The fractional order Sobolev spaces $W_p^{\alpha}(\Omega)$ are Banach spaces.*

Proof. Let $(x_n)_{n\in\mathbb{N}}$ be a Cauchy sequence in $W_p^{\alpha}(\Omega)$ and define the sequence $(y_n)_{n\in\mathbb{N}}$ in $L^p(\Omega)$ by $y_n = A^{\alpha}x_n$. Since $L^p(\Omega)$ is a Banach space, there exists x, $y \in L^p(\Omega)$ such that $x_n \to x$ and $y_n \to y$ in $L^p(\Omega)$. Now define $\tilde{x} = A^{-\alpha}y$, then x and $\tilde{x}$ are equivalent up to some constant $c = x - \tilde{x}$ a.e. Hence, $x = \tilde{x} + c$, $x_n \to x$ and $y_n \to y = A^{\alpha}\tilde{x} = A^{\alpha}x$. $\square$

There are many properties of Banach scales, like continuous or dense injections, which we will not cover in this work. The main idea of the previous part was the introduction of fractional order Sobolev spaces without the use of real or complex interpolation. Now, we show that the fractional order Sobolev spaces defined via power scales are interpolation spaces w.r.t. the already known L^p- and Sobolev spaces. For this, we need to define interpolation spaces.

Definition 2.2.5. *Let A and B be Banach spaces. If there exists a locally convex space X, such that A and B are continuously embedded in X, we call (A, B) an interpolation couple.*

From this definition it follows that $A + B = \{x = a + b : a \in A, b \in B\}$ and $A \cap B$ are well defined.

Definition 2.2.6. *If (A, B) is an interpolation couple and*

$$A \cap B \hookrightarrow X \hookrightarrow A + B,$$

then X is called intermediate space w.r.t. (A, B).

Let us denote by $L(A, B)$ the set of linear bounded operators from the Banach space A into the Banach space B. We are now able to define interpolation spaces.

Definition 2.2.7. *Let (A_0, A_1) and (B_0, B_1) be interpolation couples. Furthermore, we have the intermediate spaces A and B w.r.t. (A_0, A_1) and (B_0, B_1). If for every operator $T \in L(A_j, B_j)$, $j = 0, 1$, it holds $T \in L(A, B)$, we call A and B interpolation spaces w.r.t. (A_0, A_1) and (B_0, B_1). Additionally, if there exists $c(\theta)$, $0 < \theta < 1$, such that*

$$\|T\|_{L(A,B)} \leq c(\theta)\|T\|^{\theta}_{L(A_0,B_0)}\|T\|^{1-\theta}_{L(A_1,B_1)},$$

then A and B are called interpolation spaces of exponent θ w.r.t (A_0, A_1) and (B_0, B_1).

The previous definition gives rise to interpolation inequalities.

Lemma 2.2.3. *Let A be an interpolation space of exponent θ w.r.t. to the interpolation couple (A_0, A_1). Then*

$$\|x\|_A \leq c(\theta)\|x\|_{A_0}^{1-\theta}\|x\|_{A_1}^{\theta}, \quad x \in A_0 \cap A_1.$$

Proof. This follows from definition (2.2.7) and using the operator $Ax = \lambda x$, with $\lambda \in \mathbb{C}$ (or $\mathbb{R}$) and $x \in A_0 \cap A_1$, see [Ama95] for details. $\square$

As a basic example we consider the spaces $L^1(\Omega)$ and $L^\infty(\Omega)$. Then, $(L^1(\Omega), L^\infty(\Omega))$ is an interpolation couple and every space $L^p(\Omega)$ with $1 < p < \infty$ can be understood as interpolation space w.r.t. $(L^1(\Omega), L^\infty(\Omega))$. From Hölder's inequality follows the corresponding interpolation inequality $\|x\|_{L^p(\Omega)} \leq \|x\|_{L^1(\Omega)}^{1/p}\|x\|_{L^\infty(\Omega)}^{1-1/p}$. Another example is the interpolation couple $(L^p(\Omega), W_p^k(\Omega))$. Sobolev spaces $W_p^{k'}(\Omega)$ with $0 < k' < k$, $k' \in \mathbb{N}$, are interpolation spaces w.r.t. $(L^p(\Omega), W_p^k(\Omega))$ and we already have the Gagliardo-Nirenberg inequality.

We close this section with the connection of fractional order Sobolev spaces defined via Banach scales to interpolation spaces.

Theorem 2.2.4. *Let $0 < \alpha < 1$ and $1 \leq p < \infty$. The fractional order Sobolev spaces $W_p^{k+2\alpha}(\Omega)$ given by definition (2.2.4) are interpolation spaces of exponent α w.r.t $(W_p^k(\Omega), W_p^{k+2}(\Omega))$.*

Proof. It suffices to prove the claim for $k = 0$ and repeat the process for the k-th derivative if $k > 0$.

We consider the interpolation couple $(L^p(\Omega), W_p^2(\Omega))$. First, we have $L^p(\Omega) \cap W_p^2(\Omega) = W_p^2(\Omega) \hookrightarrow L^p(\Omega) + W_p^2(\Omega) = L^p(\Omega)$. Next, let $x \in W_p^2(\Omega)$. Then we calculate

$$\|A^\alpha x\|_{L^p(\Omega)} = \|A^{\alpha-1}Ax\|_{L^p(\Omega)} \leq \|A^{\alpha-1}\|\|Ax\|_{L^p(\Omega)} \leq C\|x\|_{W_p^2(\Omega)}.$$

Thus, $W_p^2(\Omega) \hookrightarrow W_p^\alpha(\Omega)$. In the same manner we get for $x \in W_p^\alpha(\Omega)$

$$\|x\|_{L^p(\Omega)} = \|A^{-\alpha}A^\alpha x\|_{L^p(\Omega)} \leq \|A^{-\alpha}\|\|A^\alpha x\|_{L^p(\Omega)} \leq C\|x\|_{W_p^\alpha(\Omega)}.$$

We conclude $W_p^2(\Omega) \hookrightarrow W_p^\alpha(\Omega) \hookrightarrow L^p(\Omega)$.

Now, let (B_0, B_1) be an interpolation couple with intermediate space B, $T \in L(B_0, L^p(\Omega))$ and $T \in L(B_1, W_p^2(\Omega))$ and $\Gamma = \Gamma_1 \cup \Gamma_2 \cup \Gamma_3$ is the curve given by

$$\begin{aligned}
\Gamma_1 &= \{\lambda \in \mathbb{C} : \lambda = r\mathrm{e}^{-\mathrm{i}\psi}, \infty > r \geq \epsilon\}, \\
\Gamma_2 &= \{\lambda \in \mathbb{C} : \lambda = \epsilon\mathrm{e}^{\mathrm{i}\phi}, -\psi \leq \phi \leq \psi\}, \\
\Gamma_3 &= \{\lambda \in \mathbb{C} : \lambda = r\mathrm{e}^{\mathrm{i}\psi}, \epsilon \leq r < \infty\},
\end{aligned}$$

with $\psi \in (\pi/2, \pi)$ and $\epsilon > 0$. Then, we have for $0 < \alpha < 1$ and $x \in B_0 \cap B_1$

$$\begin{aligned}
\|A^\alpha T x\|_{L^p(\Omega)} = \|A^{-1+\alpha} A T x\|_{L^p(\Omega)} &\leq \frac{1}{2\pi} \left\| \int_\Gamma \lambda^{-1+\alpha} A R_\lambda T x \mathrm{d}\lambda \right\|_{L^p(\Omega)} \\
&\leq \frac{1}{2\pi} \left\| \int_{\Gamma_1} \lambda^{-1+\alpha} R_\lambda A T x \mathrm{d}\lambda + \int_{\Gamma_3} \lambda^{-1+\alpha} R_\lambda A T x \mathrm{d}\lambda + \int_{\Gamma_2} \lambda^{\alpha} R_\lambda T x \mathrm{d}\lambda \right\|_{L^p(\Omega)} \\
&\leq \frac{C}{2\pi} \left(2 \int_\epsilon^\infty r^{-2+\alpha} \mathrm{d}r \|A T x\|_{L^p(\Omega)} + \int_{-\psi}^{\psi} \epsilon^{-1+\alpha} \mathrm{d}\phi \|T x\|_{L^p(\Omega)} \right) \\
&= \frac{C}{2\pi} \left(\epsilon^{-1+\alpha} \|A T x\|_{L^p(\Omega)} + \epsilon^{-1+\alpha} \|T x\|_{L^p(\Omega)} \right).
\end{aligned}$$

Now, we choose $\epsilon = \|ATx\|_{L^p(\Omega)} / \|Tx\|_{L^p(\Omega)}$ and use $\|Tx\|_{L^p(\Omega)} = \|A^{-1}ATx\|_{L^p(\Omega)} \leq C\|ATx\|_{L^p(\Omega)}$ to obtain

$$\begin{aligned}
\|A^\alpha T x\|_{L^p(\Omega)} &\leq C \|A T x\|^\alpha_{L^p(\Omega)} \|T x\|^{1-\alpha}_{L^p(\Omega)} \\
&\leq C \|T x\|^\alpha_{W^2_p(\Omega)} \|T x\|^{1-\alpha}_{L^p(\Omega)}.
\end{aligned}$$

Finally, since $x \in B_0 \cap B_1$, it follows that

$$\|T\|_{L(B, W^\alpha_p(\Omega))} \leq C \|T\|^\alpha_{L(B_1, W^2_p(\Omega))} \|T\|^{1-\alpha}_{L(B_0, L^p(\Omega))}.$$

□

So far, we defined fractional powers of operators that led us to fractional derivatives if we consider the operator $A = \mathrm{d}_x^2$. With the resulting fractional order Sobolev spaces, we are able to fill the gap between Lesbegue and Sobolev spaces in a natural and elegant way. Consequently, regarding Sobolev embeddings, how are fractional order Sobolev spaces embedded into the space of continuous functions? Or equivalently, what is the necessary fractional derivative of L^p functions to be continuous? Here, we did not establish the techniques to answer this question and just mention the result. In [DNPV12], the authors derived $W^s_p(\Omega) \hookrightarrow C^{0,\alpha}(\Omega)$ with $sp > 1$ and $\alpha = (sp-1)/p$ for the one dimensional case. As an example and simply formulated, a function from $L^2(\Omega)$ needs at least more than a half derivative in $L^2(\Omega)$ to be continuous.

The fractional order Sobolev spaces offer a variety of function spaces to choose appropriate ones for our given system of PDEs. During the next chapter we introduce a method to prove the existence of a solution, which uses the same differential operator as for the definition of fractional order Sobolev spaces.

2.3 Semigroups

The usage of semigroups became an important tool in the analysis of PDEs. They allow a straightforward formulation of solutions to a variety of problems. Furthermore, they have interesting properties, that assist in the regularity analysis of solutions. The whole topic of the application of semigroup theory to PDEs will not be covered in this work. We refer to [Lun12, EN00, Ren04, Bre13].

We want to start this section with an example. Consider the differential equation

$$\mathrm{d}_t u(t) = \lambda u(t),$$

with initial condition $u(0) = u_0$. Immediately we obtain the solution

$$u(t) = \mathrm{e}^{\lambda t} u_0.$$

Now, if the constant λ where to be an operator, e.g. the Laplace operator, the question arises whether a similar solution exists. Let us have a look at the following problem

$$\partial_t u(t, x) = A u(t, x),$$

where the operator A may be given by $A = \mathrm{d}_x^2$. Again we have some initial condition $u(0, x) = u_0(x)$ and additionally some kind of boundary condition. Intuitively we expect the solution

$$u(t, x) = \mathrm{e}^{tA} u_0(x).$$

However, we need a meaningful definition of the exponential function with operators as argument and we have to understand the action of this exponential on functions like the initial condition. There are several possible definitions of e^A. If A is a bounded operator one could just use the series expansion of the exponential function or the sequence $(1 + A/n)^n$. Unfortunately, this is not possible with unbounded operators. For such operators we can use the inverse operator, if it exists, and utilize the sequence $(1 - A/n)^{-n}$. These approaches rely on powers of A or the corresponding resolvent operator. A more advanced defintion uses the Cauchy integral formula. Then, the drawback is the need to extend our calculations to the complex plane.

We begin with the basic idea of semigroups and their relation to operators. Then, we extend our considerations to the complex plane, which offers tools from complex analysis. Lastly, basic results are given that will be used to investigate the regularity of solutions to PDEs.

Definition 2.3.1. *Let X be a Banach space. A strongly continuous semigroup on X is a set of bounded linear operators $\{T(t)\}_{t \geq 0}$ with the following properties:*

1. $T(t + s) = T(t)T(s)$,
2. $T(0) = I$,
3. $\lim_{t \to 0}(T(t)x - x) = 0, \forall x \in X$.

Let us consider the following example. The translation operator defined by $T(h)u(t) = u(t{+}h)$ on a Banach space X forms a semigroup. Furthermore, we observe that $(T(h)u(t) - u(t))/h = (u(t+h) - u(t))/h$ is just the difference quotient. Indeed, there is a connection between certain operators and semigroups.

Definition 2.3.2. *Let X be a Banach space and $\{T(t)\}_{t\geq 0}$ a strongly continuous semigroup. The operator A given by*

$$Ax = \lim_{h\to 0_+} \frac{T(h)x - x}{h},$$

for all $x \in X$ such that the limit exists, is called infinitesimal generator of the semigroup.

Note, that every strongly continuous semigroup has a closed generator and the domain $\mathcal{D}(A)$ is dense, see [Ren04] for details. Now, we are able to calculate the generator of a given semigroup. In case of the translation semigroup we obtain the differential operator $Au(t) = d_t u(t) = \lim\limits_{h\to 0_+} (u(t+h) - u(t))/h$. However, in practical applications we often have an operator and we are interested in its properties, especially if the operator is the generator of a semigroup. This is achieved with the following theorem.

Theorem 2.3.1 (Hille-Yosida Theorem)**.** *Let A be a linear operator on the Banach space X, $\omega \in \mathbb{R}$ and $M > 0$. Then A is the infinitesimal generator of a strongly continuous semigroup $\{T(t)\}_{t\geq 0}$ with $\|T(t)\| \leq M e^{\omega t}$ if and only if*

1. *A is closed and $\mathcal{D}(A)$ is dense,*
2. *every real $\lambda > \omega$ is an element of the resolvent set of A and*

$$\|R(\lambda)^n\| \leq \frac{M}{(\lambda - \omega)^n}, \quad \forall n \in \mathbb{N}.$$

Proof. A complete proof can be found in [Ren04]. We just give the main ideas.

First, one shows the necessity of the conditions. Then, consider $U_n(t) = \left(I - \frac{t}{n}A\right)^{-n}$ and show sufficiency of the conditions. Finally, one proves convergence of U_n in the strong operator topology and verifies the semigroup properties of the limit. □

During the proof of the previous theorem, one finds a justification of the exponential of unbounded operators using the series $U_n(t) = \left(I - \frac{t}{n}A\right)^{-n}$. Now, we are closer to a meaningful definition of the expression e^{tA}, which suggests a relation between operator and semigroup anyways. There is another way to approach e^{tA}, similar to fractional powers of operators, but we have to extend the semigroup given by $T(t)$ with $t \in \mathbb{R}$ to a sector in the complex plane.

Definition 2.3.3. *Let $\{T(t)\}_{t\geq 0}$ be a strongly continuous semigroup. If the conditions*

1. *$T(t)$ can be extended to a sector $\Sigma_\theta = \{t \in \mathbb{C} : |\arg(t)| < \theta\} \cup \{0\}$ for $\theta \in (0, \pi/2)$, such that the semigroup properties are fulfilled for all $t \in \Sigma_\theta$,*

2. $T(t)$ is analytic in t for $t \in \Sigma_\theta \setminus \{0\}$ in the uniform operator topology,

hold, we call $T(t)$ analytic semigroup.

And again, we ask under which conditions an operator generates an analytic semigroup.

Theorem 2.3.2. *Let A be an operator in the Banach space X. Then, A is the generator of an analytic semigroup if and only if A is a sectorial operator of angle $\theta \in (\pi/2, \pi)$. Furthermore, the semigroup is given by*

$$\mathrm{e}^{tA} = \frac{1}{2\pi\mathrm{i}} \int_\Gamma \mathrm{e}^{t\lambda}(\lambda - A)^{-1}\mathrm{d}\lambda,$$

with Γ being a curve in the sector Σ_θ going from $\infty\mathrm{e}^{-\mathrm{i}\phi}$ to $\infty\mathrm{e}^{\mathrm{i}\phi}$, where $\pi/2 < \phi < \theta$.

Proof. We just give some ideas from the complete proof in [Ren04]. Assuming that e^{tA} is an analytic semigroup in some sector Σ_ψ with $\omega \in \mathbb{R}$, $0 < \psi < \pi/2$ and using $\|\mathrm{e}^{tA}\| \leq C\mathrm{e}^{\omega t}$ together with

$$R_\lambda = \int_0^\infty \mathrm{e}^{-\lambda t}\mathrm{e}^{tA}\mathrm{d}t,$$

for $\mathrm{Re}(\lambda) > \omega$, one obtains the desired estimate of the resolvent operator. Choosing λ such that $\lambda - \omega = R\mathrm{e}^{\mathrm{i}\theta}$ with $\theta \in (\pi/2, \pi)$ and some ϕ with $0 < \phi < \pi/2$, one uses

$$A - \lambda = A - \left(\omega + R\mathrm{e}^{\mathrm{i}\phi}\right) - R\left(\mathrm{e}^{\mathrm{i}\theta} - \mathrm{e}^{\mathrm{i}\phi}\right),$$

to calculate R_λ as a geometric series, if $\left|\mathrm{e}^{\mathrm{i}\theta} - \mathrm{e}^{\mathrm{i}\phi}\right| \leq C$. Thus, $\Sigma_\theta \subset \rho(A)$.

Next, given the sectorial operator A with the estimate $\|R_\lambda\| \leq C/|\lambda - \omega|$ with $\lambda \in \Sigma_\theta$, one verifies the semigroup properties of e^{tA}. □

Note, that for suitable complex functions $\phi : \mathbb{C} \to \mathbb{C}$ that are analytic in the complex plane but some subset D, we can always use Cauchy's integral formula $\phi(z) = (2\pi\mathrm{i})^{-1} \int_\Gamma \phi(\lambda)/(\lambda - z)\mathrm{d}\lambda$ with $\Gamma \subset \mathbb{C} \setminus D$ and z lies within the region enclosed by Γ. We used this to define fractional powers of operators and the exponential e^A. But even more functions are applicable and we could extend the previous considerations to some subset of the complex plane, e.g. complex powers of operators.

With our basic setup of semigroup theory we will now derive a property that we use extensively during the following chapter. Let us derive an upper bound for $\|A^\alpha \mathrm{e}^{tA}\|$.

Lemma 2.3.3. *Let A be a sectorial operator of angle $\theta \in (\pi/2, \pi)$ and generator of the analytic semigroup e^{tA}. Suppose there exists $\omega \in \mathbb{R}$, such that $\omega = \sup\{\mathrm{Re}(\lambda) : \lambda \in \sigma(A)\}$. Then, we have for $t > 0$ and $0 \leq \alpha \leq 1$ the estimate*

$$\|A^\alpha \mathrm{e}^{tA}\| \leq \frac{C}{t^\alpha}\mathrm{e}^{\omega t},$$

with a constant $C > 0$.

Proof. Let X be a Banach space and A has the aforementioned properties. Furthermore, let $n-1<\alpha<n$, $x\in X$ and Γ, Γ' be two curves in the resolvent set of A as before, such that Γ lies entirely to the left of Γ'. Applying the identity $AR_\mu=\mu R_\mu-1$ we calculate

$$\begin{aligned}
A^\alpha \mathrm{e}^{tA}x = A^n A^{\alpha-n}\mathrm{e}^{tA}x &= \frac{1}{(2\pi\mathrm{i})^2}\int_\Gamma\int_{\Gamma'}\lambda^{\alpha-n}\mathrm{e}^{t\mu}A^n R_\mu R_\lambda x\mathrm{d}\mu\mathrm{d}\lambda \\
&= \frac{A^{n-1}}{(2\pi\mathrm{i})^2}\left(\int_\Gamma\int_{\Gamma'}\lambda^{\alpha-n}\mathrm{e}^{t\mu}\mu R_\mu R_\lambda x\mathrm{d}\mu\mathrm{d}\lambda-\int_\Gamma\int_{\Gamma'}\lambda^{\alpha-n}\mathrm{e}^{t\mu}R_\lambda x\mathrm{d}\mu\mathrm{d}\lambda\right).
\end{aligned}$$

The second integral vanishes, since $\mathrm{e}^{t\mu}$ is holomorphic in the region encircled by Γ'. We continue our calculation and use the resolvent identity, $(\mu-\lambda)R_\mu R_\lambda=R_\lambda-R_\mu$, to obtain

$$\begin{aligned}
A^\alpha \mathrm{e}^{tA}x &= \frac{1}{(2\pi\mathrm{i})^2}\int_\Gamma\int_{\Gamma'}\lambda^{\alpha-n}\mathrm{e}^{t\mu}\mu^n\frac{R_\lambda x-R_\mu x}{\mu-\lambda}\mathrm{d}\mu\mathrm{d}\lambda \\
&= \frac{1}{(2\pi\mathrm{i})^2}\left(\int_\Gamma\int_{\Gamma'}\lambda^{\alpha-n}R_\lambda x\frac{\mathrm{e}^{t\mu}\mu^n}{\mu-\lambda}\mathrm{d}\mu\mathrm{d}\lambda-\int_\Gamma\int_{\Gamma'}\mathrm{e}^{t\mu}\mu^n R_\mu x\frac{\lambda^{\alpha-n}}{\mu-\lambda}\mathrm{d}\mu\mathrm{d}\lambda\right) \\
&= \frac{1}{2\pi\mathrm{i}}\int_\Gamma\lambda^\alpha\mathrm{e}^{t\lambda}R_\lambda x\mathrm{d}\lambda.
\end{aligned}$$

Once more, the second integral vanishes because the function $\lambda^{\alpha-n}$ is holomorphic in $\mathbb{C}\setminus(-\infty,0]$ and Γ lies to the left of Γ'.

Since A is a sectorial operator of angle $\theta\in(\pi/2,\pi)$ and the spectrum of A lies to the left of ω, we have the resolvent estimate $\|R_\lambda\|\le M/|\lambda-\omega|$, with $M>0$. Now, let $\epsilon>0$, $\psi\in(\pi/2,\theta)$ and Γ be the curve consisting of the three parts Γ_1, Γ_2, Γ_3 with

$$\begin{aligned}
\Gamma_1 &= \{\lambda\in\mathbb{C}:\lambda=\omega+r\mathrm{e}^{-\mathrm{i}\psi},\infty\ge r\ge\epsilon\},\\
\Gamma_2 &= \{\lambda\in\mathbb{C}:\lambda=\omega+\epsilon\mathrm{e}^{\mathrm{i}\phi},-\psi\le\phi\le\psi\},\\
\Gamma_3 &= \{\lambda\in\mathbb{C}:\lambda=\omega+r\mathrm{e}^{\mathrm{i}\psi},\epsilon\le r\le\infty\}.
\end{aligned}$$

Here, ϵ is chosen such that the curve Γ lies entirely in the resolvent set of A. Then, we obtain, after the transformations $r\to r/t$, $\epsilon\to\epsilon/t$, the estimate

$$\|A^\alpha\mathrm{e}^{tA}x\|\le\frac{M\mathrm{e}^{\omega t}}{2\pi}\left(2t^{-\alpha}\int_\epsilon^\infty r^{\alpha-1}\mathrm{e}^{r\cos(\psi)}\mathrm{d}r\|x\|+t^{-\alpha}\int_{-\psi}^{\psi}\epsilon^\alpha\mathrm{e}^{\epsilon\cos(\phi)}\mathrm{d}\phi\|x\|\right)$$

Let $R>\epsilon>0$, then we can split the first integral and find the following bound for $0<\alpha<1$

$$\begin{aligned}
\int_\epsilon^\infty r^{\alpha-1}\mathrm{e}^{r\cos(\psi)}\mathrm{d}r &= \int_\epsilon^R r^{\alpha-1}\mathrm{e}^{r\cos(\psi)}\mathrm{d}r+\int_R^\infty r^{\alpha-1}\mathrm{e}^{r\cos(\psi)}\mathrm{d}r\\
&\le \int_\epsilon^R r^{\alpha-1}\mathrm{d}r+R^{\alpha-1}\int_R^\infty\mathrm{e}^{r\cos(\psi)}\mathrm{d}r
\end{aligned}$$

$$= \frac{R^\alpha - \epsilon^\alpha}{\alpha} + R^{\alpha-1}\frac{\mathrm{e}^{R\cos(\psi)}}{-\cos(\psi)},$$

since $\cos(\psi) < 0$ with $\psi \in (\pi/2, \pi)$. For the case $\alpha = 0$ we have

$$\begin{aligned}
\int_\epsilon^\infty r^{-1}\mathrm{e}^{r\cos(\psi)}\mathrm{d}r &= \int_\epsilon^R r^{-1}\mathrm{e}^{r\cos(\psi)}\mathrm{d}r + \int_R^\infty r^{-1}\mathrm{e}^{r\cos(\psi)}\mathrm{d}r \\
&\leq \int_\epsilon^R r^{-1}\mathrm{d}r + R^{-1}\int_R^\infty \mathrm{e}^{r\cos(\psi)}\mathrm{d}r \\
&= \ln(R) - \ln(\epsilon) + R^{-1}\frac{\mathrm{e}^{R\cos(\psi)}}{-\cos(\psi)}.
\end{aligned}$$

Hence, we have the estimate

$$\|A^\alpha \mathrm{e}^{tA}x\| \leq \frac{C\mathrm{e}^{\omega t}}{t^\alpha}.$$

□

We observe that R_λ and A^α commute. Therefore, if an operator A is the generator of an analytic semigroup on $L^p(\Omega)$ it also generates an analytic semigroup on $W_p^\alpha(\Omega)$.

The application of functional calculus allowed us to define fractional powers of operators and semigroups. Furthermore, this formalism led to some important properties and estimates. On the downside, we have no method to actually calculate the fractional derivative of a given function or the action of the semigroup on a function at this moment. In case of fractional derivatives we would have to dive further into fractional calculus, studying Sobolev-Slobodeckji spaces, Besov spaces etc. In [Lun12], the equivalence of interpolation spaces by the K-method w.r.t. the operator A and interpolation spaces based on fractional powers of A was shown.

Concerning the semigroup e^{tA}, we give a short introduction into integral kernels in the next section. This allows the calculation of the action of e^{tA} on some function from the underlying Banach space.

2.4 Heat kernel

This section briefly covers the concept of heat kernels. Again, we begin with a basic example of the heat equation

$$\partial_t u - \partial_x^2 u = 0, \quad \forall x \in \mathbb{R},$$

with initial condition $u(0, x) = u_0(x)$. There are several ways to solve this problem, e.g. separation of variables or Fourier transformation. Then, one obtains the solution

$$\begin{aligned}
u(t,x) &= \int_{\mathbb{R}} H(t, x-y)u_0(y)\mathrm{d}y, \\
H(t, x-y) &= \mathrm{e}^{-\frac{(x-y)^2}{4t}},
\end{aligned}$$

where H is called fundamental solution or heat kernel. In case of an inhomogeneous equation with the inhomogeneity $f(t,x)$ one similarly has

$$u(t,x) = (H(t) * u_0(t))(x) + \int_0^t (H(t-s) * f(s))(x)\mathrm{d}s,$$

with the convolution $(u(t) * v(t))(x) = \int_{\mathbb{R}} u(t,x-y)v(t,y)\mathrm{d}y$. We observe that the heat kernel allows a closed representation of the solution to the heat equation. Also, this will be used when the inhomogeneity depends on the solution itself or if the heat kernel may only be given in terms of a series. Since we consider an inhomogeneous heat equation with nonlinearities on the bounded domain $\Omega = (0,1)$ later in this work, let us derive the corresponding heat kernel. The problem is stated for $\nu > 0$ as follows

$$\left.\begin{aligned} \partial_t K(t,x,y) - \nu\partial_x^2 K(t,x,y) &= 0, && x,y \in \Omega, t > 0,\\ \lim_{t\to 0} K(t,x,y) &= \delta(x-y), && x,y \in \Omega,\\ \partial_x K(t,x,y)|_{\partial\Omega} &= 0, && t > 0. \end{aligned}\right\} \tag{2.4.1}$$

By separation of variables we obtain

$$\begin{aligned} K(t,x,y) &= 1 + \sum_{n=1}^{\infty} (\cos(n\pi(x-y)) + \cos(n\pi(x+y)))\mathrm{e}^{-\nu n^2\pi^2 t}\\ &= \frac{1}{2}\left(\theta_3\left(\frac{\pi(x-y)}{2}, \mathrm{e}^{-\nu\pi^2 t}\right) + \theta_3\left(\frac{\pi(x+y)}{2}, \mathrm{e}^{-\nu\pi^2 t}\right)\right), \end{aligned}$$

with the theta function $\theta_3(z,q) = 1 + 2\sum\limits_{n=1}^{\infty}\cos(2nz)q^{n^2}$, see e.g. [WW96]. Note, that for $x,y \in \Omega$ we have

$$\lim_{t\to 0} K(t,x,y) = \delta(x-y),$$

in the sense of distributions. Furthermore, we can write $(Tf)(t,x) = (K * f)(t,x)$ with the integral operator T. The operator T also forms a semigroup generated by the operator $A = \nu\mathrm{d}_x^2$. Thus, we now have an integral representation of the action of the heat semigroup on a given function. This can be used for specific calculations or numerical schemes. However, convolutions involving the theta function θ_3 may be quite difficult to compute.

So far, we gave a brief introduction into functional analysis. The fractional and negative order Sobolev spaces allow a purposeful choice of function spaces that are well suited to the forthcoming system of PDEs. Additionally, we are able to calculate estimates in such spaces. We use these methods in the next chapter to analyze the full viscous quantum hydrodynamic model and prove existence of a solution.

Chapter 3

The full viscous quantum hydrodynamic model

This chapter covers the analysis of the full viscous quantum hydrodynamic model. We give a brief summary of its derivation. For details and further information on semiconductor models, especially a hierarchy of these models, we refer to [Jün09, DC11]. An extensive introduction to quantum mechanics and semiconductor physics is given in [Bre99]. In [BS02], an introduction to semiconductor physics and the Boltzmann equation is given. In this chapter, we proof the existence of a solution to the full viscous quantum hydrodynamic model and study its properties by use of the previously introduced semigroup methods. Additionally, we analyze the linearized version of the full viscous quantum hydrodynamic model.

First, let us motivate the importance of the full viscous quantum hydrodynamic model. We begin with the many particle Schrödinger equation for M particles in a domain $\Omega \subset \mathbb{R}^d$, given by

$$\left.\begin{aligned} \mathrm{i}\hbar\partial_t\psi(t,x) &= -\tfrac{\hbar^2}{2m}\sum_{j=1}^{M}\Delta_j\psi(t,x) + V[\psi(x,t)], \\ \psi(0,x) &= \psi_0(x), \end{aligned}\right\} \tag{3.0.1}$$

where $\Delta_j = \Delta_{x_j}^2$, $(t,x) \in \mathbb{R}_+ \times \Omega^M$, and $V[\psi]$ is a potential, that may depend on the wave function ψ itself. Considering electrons, the potential V takes electron-electron interactions and an external potential into account. Further interactions like electron-phonon scattering can also be included in the potential. In principle, the complete description of the quantum mechanical system is given by the Schrödinger equation. However, there are several aspects that render this equation not usefull in practical applications. First of all, the particle number M can be large, that is $M \gg 1$, and a numerical approach would need a lot of computational resources. Also, the wave function ψ contains information about the probability to find the j-th particle at a specific time in a specific region of the domain. But one is not interested in single particles in general, but especially in the particle density or current density. Lastly, the wave function ψ is complex valued in general, while the measure of physical quantities is real valued. In conclusion, using a statistical and fluid dynamical approach seems reasonable.

After transforming the many particle system into a representation in the phase space of position and momentum, some physical assumptions are applied. First, the potential can be split into an external and internal part, describing particle interactions. Then, the Hartree ansatz is applied to the internal potential and one shifts the complete discription of particle interactions to an effective potential. For deatils of the Hartree ansatz we refer to [Har28]. A detailed explanation and pracitcal application is given in [SO89]. Finally, particle interactions, besides electron electron interaction, can be described via an additional collision operator. For a detailed derivation and additional information concerning collision models we refer to [CEFM00]. Using the Focker-Planck collision operator leads to the full viscous quantum hydrodynamic model. Other collision operators are given by the relaxation time model [BGK54] and Caldeira-Leggett operator [CL83].

Rescaling of the physical constants gives the full viscious quantum hydrodynamic system

$$\left.\begin{aligned}
\partial_t n - \nu\Delta n &= -\mathrm{div} J,\\
\partial_t J - \nu\Delta J &= -\mathrm{div}\left(\frac{J\otimes J}{n}\right) - \nabla(Tn) + \frac{\epsilon^2}{2} n\nabla\left(\frac{\Delta\sqrt{n}}{\sqrt{n}}\right) - \frac{J}{\tau}\\
&\quad - \mu\nabla n + n\nabla(V+V_B),\\
\partial_t(ne) - \nu\Delta(ne) &= -\mathrm{div}\left(\frac{J}{n}(ne\mathbf{1}_d + P)\right) + J\nabla(V+V_B)\\
&\quad - \mu\mathrm{div} J - \frac{2}{\tau}\left(ne - \frac{dn}{2}\right),\\
\lambda^2\Delta V &= n - C(x).
\end{aligned}\right\} \tag{3.0.2}$$

For details about the scaling we refer to [Jün09]. The pressure tensor P and energy density ne are given by

$$P = Tn\mathbf{1}_d - \frac{\epsilon^2}{4} n(\nabla\otimes\nabla)\ln n, \tag{3.0.3}$$

$$ne = \frac{|J|^2}{2n} + \frac{d}{2}Tn - \frac{\epsilon^2}{8} n\Delta \ln n. \tag{3.0.4}$$

Also, we added a barrier potential V_B. The isothermal case, T being constant, was studied in [DS16]. Utilizing several simplifications one can derive the quantum drift diffusion model, considered in [Sel84, MR90] and also investigated in [DC11]. Neglecting quantum and electrostatic effects one obtains the classical Euler equations.

Now, we transform the full viscous quantum hydrodynamic model once more and have the new variable ni, the internal energy density. Note, that in classical gas dynamics, especially in case of the ideal gas, the internal energy is proportional to the temperature. Let $ne = E_{\mathrm{kin}} + ni$ with the kinetic energy density $E_{\mathrm{kin}} = |J|^2/2n$. One can calculate that the kinetic energy fulfills

$$\partial_t E_{\text{kin}} + \operatorname{div}(uE_{\text{kin}}) = \nu\Delta E_{\text{kin}} - \nu n \sum_k |\nabla u_k|^2 - \nabla u : (P + \mu n \mathbf{1}_d) - \frac{2}{\tau}\left(ni - \frac{n}{2}\right),$$

where $u = J/n$ and $a : b = \sum_{j,k} a_{jk} b_{jk}$ is the matrix scalar product. Subtracting this equation from the third one of (3.0.2) we obtain

$$\partial_t(ni) + \operatorname{div}\left(\frac{J}{n} ni\right) = \nu\Delta(ni) + \nu \sum_k |\nabla u_k|^2 - \nabla u : (P + \mu n \mathbf{1}_d) - \frac{2}{\tau}\left(ni - \frac{n}{2}\right). \quad (3.0.5)$$

Now, the full viscous quantum hydrodynamic system with the unknowns n, J, ni, V is given by

$$\left.\begin{aligned}
\partial_t n - \nu\Delta n &= -\operatorname{div} J, \\
\partial_t J - \nu\Delta J &= -\operatorname{div}\left(\frac{J \otimes J}{n}\right) - \nabla(Tn) + \frac{\epsilon^2}{2} n \nabla\left(\frac{\Delta\sqrt{n}}{\sqrt{n}}\right) - \frac{J}{\tau} \\
&\quad - \mu\nabla n + n\nabla(V + V_B), \\
\partial_t(ni) - \nu\Delta(ni) &= -\operatorname{div}\left(\frac{Jni}{n}\right) + \nu n \sum_k \left|\nabla\left(\frac{J_k}{n}\right)\right|^2 - \nabla u : (P + \mu n \mathbf{1}_d) \\
&\quad - \frac{2}{\tau}\left(ni - \frac{n}{2}\right), \\
\lambda^2 \Delta V &= n - C(x).
\end{aligned}\right\} \quad (3.0.6)$$

There are several possible approaches to the full viscous quantum hydrodynamic model concerning the variables, e.g. the temperature T or velocity density u. We use the internal energy density from now on and consider only the 1 dimensional case. Then, the pressure tensor is a scalar with $P = 2ni$ and the system is much easier to handle.

During the subsequent sections, we formulate the given problem with differential and boundary operators, prove existence of a mild solution, where we utilize the previously introduced methods, and study the regularity of the solution. Furthermore, we investigate the stability of stationary solutions after linearizing the full system.

3.1 Formulation of the problem

In this section, we reformulate problem (3.0.6) and write the system of PDEs in a more abstract way. By analysis of the resulting operators and nonlinear functions we will be able to apply the techniques from chapter 2 and proof the existence of a solution.

The one dimensional formulation of the full viscous quantum hydrodynamic model

(3.0.6) is given by

$$\left.\begin{aligned}
\partial_t n - \nu\partial_x^2(n) &= -\partial_x(J), \\
\partial_t J - \nu\partial_x^2 J &= -\partial_x\left(\frac{J^2}{n}\right) - \partial_x(2ni + \mu n) - \frac{J}{\tau} + n\partial_x(V + V_B), \\
\partial_t(ni) - \nu\partial_x^2(ni) &= -\partial_x\left(\frac{Jni}{n}\right) + \nu n\left(\partial_x\left(\frac{J}{n}\right)\right)^2 \\
&\quad - \left(\partial_x\left(\frac{J}{n}\right)\right)(2ni + \mu n) - \frac{2}{\tau}\left(ni - \frac{n}{2}\right), \\
\lambda^2\partial_x^2 V &= n - C_0(x),
\end{aligned}\right\} \tag{3.1.1}$$

with $(x,t) \in \Omega \times (0,\infty)$. In this case, the quantum Bohm potential does not appear in the equations. Hence, there are no third order spatial derivatives and the system has diagonal form. Additionally, we have the following boundary conditions for $t \geq 0$

$$\partial_x n = 0, \quad \partial_x J = 0, \quad \partial_x ni = 0, \quad \text{at } x = 0, 1 \tag{3.1.2}$$

$$V(0) = 0, \quad V(1) = V_0, \tag{3.1.3}$$

and the initial conditions for $x \in \Omega$

$$n(0,x) = n_0(x), \quad J(0,x) = J_0(x), \quad ni(0,x) = ni_0(x). \tag{3.1.4}$$

Since we are only interested in solutions with $\inf_{x\in\Omega}(n) > 0$ for all $t \geq 0$, we use the substitution $n(t,x) = \mathrm{e}^{w(t,x)}$. Then, the partial derivatives give

$$\partial_t n = \mathrm{e}^w \partial_t w, \tag{3.1.5}$$

$$\partial_x n = \mathrm{e}^w \partial_x w, \tag{3.1.6}$$

$$\partial_x^2 n = \mathrm{e}^w\left(\partial_x^2 w + (\partial_x w)^2\right), \tag{3.1.7}$$

and the first equation of 3.1.1, after multiplication by e^{-w}, becomes

$$\partial_t w - \nu\partial_x^2 w = \nu(\partial_x w)^2 - \mathrm{e}^{-w}\partial_x J. \tag{3.1.8}$$

Due to the appearance of $n^{-1} = \mathrm{e}^{-w}$ in the second and third equation of (3.1.1), we substitute $\tilde{J} = \mathrm{e}^{-w}J$ and $\widetilde{ni} = \mathrm{e}^{-w}ni$. Using the following identities

$$\mathrm{e}^{-w}\partial_t u = \partial_t\tilde{u} + \tilde{u}\partial_x w, \tag{3.1.9}$$

$$\mathrm{e}^{-w}\partial_x\left(\mathrm{e}^w\tilde{u}\right) = \partial_x\tilde{u} + \tilde{u}\partial_x w, \tag{3.1.10}$$

(3.1.11)

with $u = J$ or $u = ni$, we obtain the system of PDEs

$$\begin{aligned} \partial_t w - \nu\partial_x^2 w &= \nu\left(\partial_x w\right)^2 - \partial_x \tilde{J} - \tilde{J}\partial_x w, \\ \partial_t \tilde{J} - \nu\partial_x^2 \tilde{J} &= -\frac{1}{2}\partial_x\left(\tilde{J}^2\right) + 2\nu\partial_x\tilde{J}\partial_x w - 2\partial_x\widetilde{ni} - 2ni\partial_x w - \mu\partial_x w \\ &\quad - \frac{\tilde{J}}{\tau} + \partial_x(V + V_B), \\ \partial_t\widetilde{ni} - \nu\partial_x^2\widetilde{ni} &= 2\nu\partial_x\widetilde{ni}\partial_x w - \tilde{J}\partial_x\widetilde{ni} + \nu\left(\partial_x\tilde{J}\right)^2 - \partial_x\tilde{J}(2\widetilde{ni} + \mu) - \frac{2}{\tau}\widetilde{ni} + \frac{1}{\tau}. \end{aligned} \tag{3.1.12}$$

Additionally, we have the boundary conditions

$$\partial_x w = 0, \quad \partial_x\tilde{J} = 0, \quad \partial_x\widetilde{ni} = 0, \quad \text{at } x = 0, 1, \tag{3.1.13}$$

and initial conditions

$$w(0, x) = \ln n_0(x), \quad \tilde{J}(0, x) = \mathrm{e}^{-w(0,x)}J_0(x), \quad \widetilde{ni}(0, x) = \mathrm{e}^{-w(0,x)}ni_0(x). \tag{3.1.14}$$

Since we only use the unknowns $(w, \tilde{J}, \widetilde{ni}, V)$ in the forthcoming calculations, we omit the tilde. Let us now formulate problem (3.1.12) in the following way

$$\left.\begin{aligned} \partial_t U - AU &= F(U, \partial_x U), \\ BU|_{x=0,1} &= 0, \quad U(0, x) = U_0, \end{aligned}\right\} \tag{3.1.15}$$

$$\left.\begin{aligned} \lambda^2\partial_x^2 V &= \mathrm{e}^{U_1} - C_0(x), \\ V(0) &= 0, \quad V(1) = V_0, \end{aligned}\right\} \tag{3.1.16}$$

with $A = \mathbf{1}_3\nu\partial_x^2$ and boundary operator $B = \mathbf{1}_3\partial_x$, where $\mathbf{1}_3$ is the three dimensional identity matrix. Furthermore, $U = (U_1, U_2, U_3)$ is an element of a suitable function space and $F = (F_1, F_2, F_3)$ is given by (3.1.12), also handling the coupling to the Poisson equation. Note, that the barrier potential V_B may not be differentiable for all $x \in \Omega$, i.e. admitting jump-discontinuities and $\partial_x V_B \propto \delta$, where δ is the Dirac delta distribution, for some $x \in \Omega$.

3.2 Existence, uniqueness and regularity of the solution

This section is structured as follows. First, we study the spatial regularity of the right hand side of the one dimensional full viscous quantum hydrodynamic model. This allows us to choose a suitable function space E_1 for the subsequent considerations. Then, we give the solution to problem (3.1.16) and show that F is indeed bounded for all elements of a subset $M \subset E_1$. After the preliminaries, we prove that A is the generator of an analytic semigroup on E_1 and define the term *mild solution*. The existence of a mild solution is prooven by application of the Picard-Lindelöf scheme. Finally, we investigate the spatial regularity of the mild solution and give a result for a special case of initial conditions.

Let us analyze the given problem first. The system (3.1.15) is a parabolic evolution problem with Neumann boundary conditions coupled to the Poisson equation (3.1.16). We observe two difficult terms. As mentioned before, the barrier potential is not continuous in general. Thus, F_2 has to be understood in the sense of distributions and we need negative fractional order Sobolev spaces to achieve meaningful estimates. Let us determine suitable function spaces. Using Plancherel's theorem and Bessel potential spaces one can show that $\delta \in H^{-(1/2+\epsilon)}(\Omega)$ for some $\epsilon > 0$, also see [Ren04]. Additionally, the terms $(\partial_x w)^2$ and $(\partial_x J)^2$ require an appropriate choice of the Sobolev space $W_p^s(\Omega)$. If we demand ni to be an L^2-function, and therefore $F_3 \in L^2(\Omega)$, w and J need to be elements of the fractional Sobolev space $H^{1+1/4}(\Omega)$, due to the embedding $H^{1/4}(\Omega) \hookrightarrow L^4(\Omega)$.

Now, let $t > 0$ and let us fix $\Omega = (0,1)$, $R > 0$. Consider the Banach space $E_1 = H^{1+1/4}(\Omega) \times H^{1+1/4}(\Omega) \times H^{1+1/4}(\Omega)$ and for $U_0 \in E_1$ the following set

$$M := \{U(t) = (U_1, U_2, U_3) \in E_1 : \|U - U_0\| \leq R\}, \tag{3.2.1}$$

and the norm given by

$$\|U\| = \sup_{t' \in [0,t]} \left(\left\|U_1(t')\right\|_{H^{1+1/4}(\Omega)} + \left\|U_2(t')\right\|_{H^{1+1/4}(\Omega)} + \left\|U_3(t')\right\|_{H^{1+1/4}(\Omega)} \right). \tag{3.2.2}$$

With this setup, we first show that problem (3.1.1) is equivalent to problem (3.1.12) and (3.1.16).

Proposition 3.2.1. *There exist functions* $(n, J, ni, V) \in E_1$ *fulfilling problem* (3.1.1) *with* $\inf_{x\in\Omega}(n) > 0$ *for all* $t > 0$*, given that* $\inf_{x\in\Omega}(n_0) > 0$*, iff there exists functions* $(w, \tilde{J}, \widetilde{ni}, V) \in E_1$ *fulfilling problem* (3.1.12) *and* (3.1.16)*, with* w *being bounded in* $\bar{\Omega}$ *for all* $t \geq 0$.

Proof. Suppose $\inf_{x\in\Omega} n_0 > 0$, (n, J, ni, V) satisfy (3.1.1) and $\inf_{x\in\Omega} n > 0$. Set $w = \ln n$, $\tilde{J} = \mathrm{e}^{-w} J$, $\widetilde{ni} = \mathrm{e}^{-w} ni$. Then $(w, \tilde{J}, \widetilde{ni}, V)$ fulfill (3.1.12) and (3.1.16), as we have seen in the derivation of (3.1.12). Since $H^{1+1/4}(\Omega) \hookrightarrow C(\Omega)$ and $\partial_x w = 0$ for $x = 0, 1$, we obtain $w \in C(\bar{\Omega})$, hence w is bounded for all $t \geq 0$.

Now suppose $(w, \tilde{J}, \widetilde{ni}, V)$ solves (3.1.12) and (3.1.16) with w being bounded in $\bar{\Omega}$ for $t \geq 0$. Setting $n = \mathrm{e}^w$, $J = \mathrm{e}^w \tilde{J}$ and $ni = \mathrm{e}^w \widetilde{ni}$ gives a solution to problem (3.1.1). Since w is bounded in $\bar{\Omega}$, we have $\inf_{x\in\Omega} n > 0$ for all $t \geq 0$. □

Note, that the function F depends on the first derivative of the potential V, which is given by the solution of problem (3.1.16).

Theorem 3.2.2. *Let* $U \in E_1$*,* $C_0 \in L^\infty(\Omega)$*,* $V_0 \geq 0$ *and* $\lambda > 0$*. Then, the solution of*

(3.1.16) *is given by*

$$\begin{aligned}\lambda^2 V(x) = &\int_0^x \int_0^y \left(\mathrm{e}^{U_1(z)} - C_0(z)\right) \mathrm{d}z\mathrm{d}y \\ &+ x\left(\lambda^2 V_0 - \int_0^1 \int_0^y \left(\mathrm{e}^{U_1(z)} - C_0(z)\right) \mathrm{d}z\mathrm{d}y\right).\end{aligned} \tag{3.2.3}$$

Furthermore, we have $V \in H^2(\Omega)$ and

i) $\lambda^2 \|\partial_x (V - V')\|_{L^2(\Omega)} \leq C\|U - U'\|_{E_1}$,

ii) $\|V\|_{L^2(\Omega)} \leq \|\partial_x V\|_{L^2(\Omega)}$,

iii) $\lambda^2 \|\partial_x V\|_{L^2(\Omega)} \leq 2\mathrm{e}^{R+\|U_0\|} + 2\|C_0\|_{L^\infty(\Omega)} + \lambda^2 V_0$.

with $U, U' \in E_1$.

Proof. Let $U \in E_1$, $C_0 \in L^\infty(\Omega)$, $\lambda > 0$ and $V_0 \geq 0$ be given. Then, (3.1.16) is a linear ODE w.r.t. the spatial coordinate and Dirichlet boundary conditions

$$\begin{aligned}\lambda^2 \mathrm{d}_x^2 V(x) &= \mathrm{e}^{U_1(x)} - C(x), \\ V(0) = 0, &\quad V(1) = V_0,\end{aligned}$$

that can be solved by integration over the spatial domain. We obtain

$$\lambda^2 V(x) = \int_0^x \int_0^y \left(\mathrm{e}^{U_1(z)} - C(z)\right) \mathrm{d}z\mathrm{d}y + xK_1 + K_2.$$

Applying the boundary conditions we calculate

$$\begin{aligned}K_2 &= 0, \\ K_1 &= \lambda^2 V_0 - \int_0^1 \int_0^y \left(\mathrm{e}_1^U(z) - C(z)\right) \mathrm{d}z\mathrm{d}y.\end{aligned}$$

Next, we have, using the scalar product $(.,.)$ in $L^2(\Omega)$, the estimate

$$\begin{aligned}\lambda^4 \|\partial_x^2 V\|_{L^2(\Omega)}^2 &= \lambda^4 (\partial_x^2 V, \partial_x^2 V) = \lambda^2 \left(\mathrm{e}^{U_1} - C, \partial_x^2 V\right) \\ &\leq \lambda^2 \left\|\mathrm{e}^{U_1} - C\right\|_{L^2(\Omega)} \|\partial_x^2 V\|_{L^2(\Omega)} \leq \frac{1}{2}\left\|\mathrm{e}^{U_1} - C\right\|_{L^2(\Omega)}^2 + \frac{\lambda^4}{2}\|\partial_x^2 V\|_{L^2(\Omega)}^2,\end{aligned}$$

and therefore $V \in H^2(\Omega)$. Additionally, using the embedding $H^1(\Omega) \hookrightarrow L^\infty(\Omega)$ and

$$\|U_1\|_{L^\infty(\Omega)} \leq C\|U_1\|_{H^1(\Omega)} \leq C(R + \|U_0\|)$$

we obtain the estimate

$$
\begin{aligned}
\partial_x(V-V') &= \frac{1}{\lambda^2}\int_0^x \left(\mathrm{e}^{U_1(y)} - \mathrm{e}^{U_1'(y)}\right)\mathrm{d}y \\
&\le \frac{1}{\lambda^2}\int_0^1 \mathrm{e}^{U_1(y)}\left|1-\mathrm{e}^{U_1'(y)-U_1(y)}\right|\mathrm{d}y \\
&\le \frac{1}{\lambda^2}\int_0^1 \mathrm{e}^{U_1(y)}\mathrm{e}^{|U_1(y)-U_1'(y)|}\left|U_1(y)-U_1'(y)\right|\mathrm{d}y \\
&\le \frac{1}{\lambda^2}\left\|\mathrm{e}^{U_1}\right\|_{L^\infty(\Omega)}\left\|\mathrm{e}^{|U_1-U_1'|}\right\|_{L^\infty(\Omega)}\left\|U_1-U_1'\right\|_{L^1(\Omega)} \\
&\le K\left\|U_1-U_1'\right\|_{H^{1+1/4}(\Omega)},
\end{aligned}
$$

with the constant $K = \mathrm{e}^{C(R+\|U_0\|)}/\lambda^2$ and $U, U' \in E_1$. Finally, we calculate

$$
\begin{aligned}
\left\|V\right\|^2_{L^2(\Omega)} &= \int_0^1 (V(x))^2\mathrm{d}x = \int_0^1 \left|\int_0^x \partial_y V(y)\mathrm{d}y\right|^2 \mathrm{d}x \le \int_0^1 \left(\int_0^1 |\partial_y V(y)|\mathrm{d}y\right)^2 \mathrm{d}x \\
&= \|\partial_x V\|^2_{L^1(\Omega)} \le \left\|\partial_x V\right\|^2_{L^2(\Omega)}, \\
\lambda^2\left\|\partial_x V\right\|_{L^2(\Omega)} &\le \left\|\int_0^x \left(\mathrm{e}^{U_1(y)} - C_0(y)\right)\mathrm{d}y\right\|_{L^2(\Omega)} + \lambda^2 V_0 + \int_0^1\int_0^y \left|\mathrm{e}^{U_1(z)} - C_0(z)\right|\mathrm{d}z\mathrm{d}y \\
&\le \left(\int_0^1 \left(\int_0^1 \left|\mathrm{e}^{U_1(y)} - C_0(y)\right|\mathrm{d}y\right)^2 \mathrm{d}x\right)^{\frac{1}{2}} \\
&\quad + \lambda^2 V_0 + \int_0^1\int_0^1 \left|\mathrm{e}^{U_1(z)} - C_0(z)\right|\mathrm{d}z\mathrm{d}y \\
&\le \left\|\mathrm{e}^{U_1} - C_0\right\|_{L^1(\Omega)} + \lambda^2 V_0 + \left\|\mathrm{e}^{U_1} - C_0\right\|_{L^1(\Omega)} \\
&\le 2\left\|\mathrm{e}^{U_1}\right\|_{L^\infty(\Omega)} + 2\left\|C_0\right\|_{L^\infty(\Omega)} + \lambda^2 V_0 \\
&\le 2\mathrm{e}^{\|U_1\|_{L^\infty(\Omega)}} + 2\left\|C_0\right\|_{L^\infty(\Omega)} + \lambda^2 V_0.
\end{aligned}
$$

□

Given the set M, choose $\epsilon > 0$ arbitrarily small, fix $s = 1/2 + \epsilon$ and let us study the properties of the right hand side $F(U)$ with $U \in M$.

Theorem 3.2.3. *Let $U \in M$. Then, $F \in L^2(\Omega) \times H^{-s}(\Omega) \times L^2(\Omega)$ with the estimates*

$$
\begin{aligned}
\|F_1(U)\|_{L^2(\Omega)} &\le C_1\left(\|U_1\|_{H^{1+1/4}(\Omega)} + \nu\|U_1\|^2_{H^{1+1/4}(\Omega)} + \left\|U_2\right\|_{H^{1+1/4}(\Omega)} + \left\|U_2\right\|^2_{H^{1+1/4}(\Omega)}\right), \\
\|F_2(U)\|_{H^{-s}(\Omega)} &\le C_2\Bigg(1 + \mu\left\|U_1\right\|_{H^{1+1/4}(\Omega)} + (1+\nu)\left\|U_1\right\|^2_{H^{1+1/4}(\Omega)} + \frac{1}{\tau}\left\|U_2\right\|_{H^{1+1/4}(\Omega)} \\
&\quad + (1+\nu)\left\|U_2\right\|^2_{H^{1+1/4}(\Omega)} + \left\|U_3\right\|_{H^{1+1/4}(\Omega)} + \left\|U_3\right\|^2_{H^{1+1/4}(\Omega)}\Bigg),
\end{aligned}
$$

$$
\left\|F_3(U)\right\|_{L^2(\Omega)} \le C_3\Bigg(\frac{1}{\tau} + \nu\left\|U_1\right\|^2_{H^{1+1/4}(\Omega)} + \mu\left\|U_2\right\|_{H^{1+1/4}(\Omega)} + (1+\nu)\left\|U_2\right\|^2_{H^{1+1/4}(\Omega)}
$$

$$+\frac{2}{\tau}\|U_3\|_{H^{1+1/4}(\Omega)} + (1+\nu)\|U_3\|^2_{H^{1+1/4}(\Omega)}\Big).$$

Proof. First, using the embedding $H^{1/4}(\Omega) \hookrightarrow L^4(\Omega)$, Hölder's inequality and Young's inequality, we derive

$$\begin{aligned}
\|F_1(U)\|_{L^2(\Omega)} &\le \nu\|(\partial_x U_1)^2\|_{L^2(\Omega)} + \|\partial_x U_2\|_{L^2(\Omega)} + \|U_2\partial_x U_1\|_{L^2(\Omega)} \\
&\le \nu\|\partial_x U_1\|^2_{L^4(\Omega)} + \|\partial_x U_2\|_{L^2(\Omega)} + \frac{1}{2}\|U_2\|^2_{L^4(\Omega)} + \frac{1}{2}\|\partial_x U_1\|^2_{L^4(\Omega)} \\
&\le C\left(\|U_1\|_{H^{1+1/4}(\Omega)} + \nu\|U_1\|^2_{H^{1+1/4}(\Omega)} + \|U_2\|_{H^{1+1/4}(\Omega)} + \|U_2\|_{H^{1+1/4}(\Omega)^2}\right)
\end{aligned}$$

Repeating these steps we obtain in a similar way for F_2 and F_3 the estimates

$$\begin{aligned}
\|F_2(U)\|_{H^{-s}(\Omega)} \le C\bigg(&\left(\nu+\frac{1}{2}\right)\|U_2\|^2_{H^{1+1/4}(\Omega)} + \frac{1}{\tau}\|U_2\|_{H^{1+1/4}(\Omega)} \\
&+ \mu\|U_1\|_{H^{1+1/4}(\Omega)} + (\nu+1)\|U_1\|^2_{H^{1+1/4}(\Omega)} + 2\|U_3\|_{H^{1+1/4}(\Omega)} \\
&+ \|U_3\|^2_{H^{1+1/4}(\Omega)} + \|V_B\|_{H^{-s}(\Omega)} + \|\partial_x V\|_{L^2(\Omega)}\bigg), \\
\|F_3(U)\|_{L^2(\Omega)} \le C\bigg(&\frac{1}{\tau} + \frac{2}{\tau}\|U_3\|_{H^{1+1/4}(\Omega)} + \left(\nu+\frac{3}{2}\right)\|U_3\|^2_{H^{1+1/4}(\Omega)} \\
&+ \mu\|U_2\|_{H^{1+1/4}(\Omega)} + \left(\nu+\frac{3}{2}\right)\|U_2\|^2_{H^{1+1/4}(\Omega)} \\
&+ \nu\|U_1\|^2_{H^{1+1/4}(\Omega)}\bigg).
\end{aligned}$$

□

The regularity of F, and therefore the solution, is dominated by the barrier potential V_B and we allow V_B to be discontinuous.

Up to this point we prepared the theory to solve PDEs with the use of advanced analytical methods and studied some properties of the nonlinear perturbation. Now, we define a solution in a rather general sense, give a construction algorithm and investigate its regularity.

Theorem 3.2.4. *The operator* $\mathbf{A} = \nu\partial_x^2\mathbf{1}_3$ *with* $D(\mathbf{A}) = \{U \in W_p^{2+\alpha}(\Omega) \times W_q^{2+\beta}(\Omega) \times W_r^{2+\gamma}(\Omega) : BU\big|_{\partial\Omega} = 0\}$ *generates an analytic semigroup* $\{\mathrm{e}^{tA}\}_{t\ge 0}$ *on* $W_p^{\alpha}(\Omega) \times W_q^{\beta}(\Omega) \times W_r^{\gamma}(\Omega)$*, with* $0 < \alpha,\ \beta,\ \gamma < 1$.

Proof. It suffices to prove that the operator $A = \nu\partial_x^2$ with the domain $D(A) = \{u \in W_p^2(\Omega) : \partial_x u|_{\partial\Omega} = 0\}$ is a sectorial operator of angle $\theta \in (\pi/2, \pi)$. We follow the proof in seminar notes [LLMP05].

Since A is self adjoint its spectrum is real and its eigenvalues are given by $-\nu n^2\pi^2$, $n \in \mathbb{N}$ and $n \ge 0$. Now, fix $\lambda \in \mathbb{C} \setminus (-\infty, 0]$. The only solution to the equation $\lambda u - \nu u'' = 0$, that fulfills the boundary conditions, is $u \equiv 0$, hence $\lambda - A$ is injective. Let us consider the problem $\lambda u - \nu u'' = f$, with $f \in L^p(\Omega)$. We extend the function f to $\tilde{f}$ with $\tilde{f}|_\Omega = f$ and $\tilde{f} = 0$ for $x \notin \Omega$. Then, the solution of $\lambda\tilde{u} - \nu\tilde{u}'' = \tilde{f}$ on $\mathbb{R}$ is given by

$$\tilde{u}(x) = \frac{1}{2\sqrt{\nu\lambda}}\left(\int_{-\infty}^{x} \mathrm{e}^{-\sqrt{\frac{\lambda}{\nu}}(x-y)}\tilde{f}(y)\mathrm{d}y + \int_{x}^{\infty} \mathrm{e}^{\sqrt{\frac{\lambda}{\nu}}(x-y)}\tilde{f}(y)\mathrm{d}y\right) = (h * \tilde{f})(x),$$

with $h(x) = \mathrm{e}^{-\sqrt{\lambda/\nu}|x|}/(2\sqrt{\nu\lambda})$. The restricted function $\tilde{u}|_\Omega$ solves the respective differential equation on Ω. In order to satisfy the boundary conditions we add the solutions of the homogeneous problem, $u_1 = \mathrm{e}^{-\sqrt{\lambda/\nu}x}$ and $u_2 = \mathrm{e}^{\sqrt{\lambda/\nu}x}$. Then, the solution to the inhomogenous problem is

$$u(x) = \tilde{u}(x) + c_1 u_1(x) + c_2 u_2(x).$$

The boundary conditions $u'(0) = 0$ and $u'(1) = 0$ determine the constants c_1 and c_2. By calculation we have

$$c_1 = \sqrt{\frac{\nu}{\lambda}}\frac{\tilde{u}'(0)\mathrm{e}^{\sqrt{\frac{\lambda}{\nu}}} - \tilde{u}'(1)}{\mathrm{e}^{\sqrt{\frac{\lambda}{\nu}}} - \mathrm{e}^{\sqrt{\frac{\lambda}{\nu}}}}, \qquad c_2 = \sqrt{\frac{\nu}{\lambda}}\frac{\tilde{u}'(0)\mathrm{e}^{-\sqrt{\frac{\lambda}{\nu}}} - \tilde{u}'(1)}{\mathrm{e}^{\sqrt{\frac{\lambda}{\nu}}} - \mathrm{e}^{\sqrt{\frac{\lambda}{\nu}}}}.$$

From Young's inequality for convolutions we know

$$\|\tilde{u}\|_{L^p(\Omega)} \leq \|\tilde{u}\|_{L^p(\mathbb{R})} = \|h * \tilde{f}\|_{L^p(\mathbb{R})} \leq \|f\|_{L^p(\Omega)}\|h\|_{L^1(\mathbb{R})} \leq \frac{\|f\|_{L^p(\Omega)}}{|\lambda|\cos(\frac{\phi}{2})},$$

where $\arg(\lambda) = \phi$. Now, since the smooth functions are dense in $W_p^1(\mathbb{R})$, one can approximate $\tilde{f}$ by a sequence $(\tilde{f}_n)_{n\in\mathbb{N}} \subset C_0^\infty(\mathbb{R})$ and obtain an approximate solution $\tilde{u}_n$, that converges to $\tilde{u}$ in $L^p(\mathbb{R})$. Furthermore, $\tilde{u}_n'' = \lambda\tilde{u}_n - \tilde{f}_n$ converges in $L^P(\mathbb{R})$ to $\tilde{u}''$. Hence, $\tilde{u} \in W_p^2(\mathbb{R})$, $\tilde{u}|_\Omega \in W_p^2(\Omega)$ and $u \in D(A)$.

It remains to show the necessary estimate of the resolvent operator. This section of the proof consists of two parts. First, we show the estimate for sufficiently large $|\lambda|$. Then, due to $\lambda = 0$ being an eigenvalue, we calculate an estimate of the resolvent operator for λ being close to 0. By Hölder's inequality we have

$$\begin{aligned}
|\tilde{u}'(0)| &\leq \frac{1}{2\nu}\int_0^\infty \mathrm{e}^{-\sqrt{\frac{|\lambda|}{\nu}}\cos(\frac{\phi}{2})}|\tilde{f}(y) - \tilde{f}(-y)|\mathrm{d}y \\
&= \frac{1}{2\nu}\int_0^1 \mathrm{e}^{-\sqrt{\frac{|\lambda|}{\nu}}\cos(\frac{\phi}{2})}|\tilde{f}(y)|\mathrm{d}y \\
&\leq \frac{1}{2\nu}\left\|\mathrm{e}^{-\sqrt{\frac{|\lambda|}{\nu}}\cos(\frac{\phi}{2})}\right\|_{L^q(\Omega)}\|f\|_{L^p(\Omega)} \\
&\leq \frac{\|f\|_{L^p(\Omega)}}{2\nu\left(q\sqrt{\frac{|\lambda|}{\nu}}\cos(\frac{\phi}{2})\right)^{\frac{1}{q}}}.
\end{aligned}$$

The same estimate holds for $\tilde{u}'(1)$. As for the functions u_1 and u_2 we calculate

$$\begin{aligned}\left\| \mathrm{e}^{-\sqrt{\frac{\lambda}{\nu}}x} \right\|_{L^p(\Omega)}^p &= \int_0^1 \mathrm{e}^{-p\sqrt{\frac{|\lambda|}{\nu}}x\cos(\frac{\phi}{2})}\mathrm{d}x = \frac{1-\mathrm{e}^{-p\sqrt{\frac{|\lambda|}{\nu}}\cos(\frac{\phi}{2})}}{p\sqrt{\frac{|\lambda|}{\nu}}\cos(\frac{\phi}{2})} \\ &\leq \frac{1}{p\sqrt{\frac{|\lambda|}{\nu}}\cos(\frac{\phi}{2})}, \\ \left\| \mathrm{e}^{\sqrt{\frac{\lambda}{\nu}}x} \right\|_{L^p(\Omega)}^p &= \int_0^1 \mathrm{e}^{p\sqrt{\frac{|\lambda|}{\nu}}x\cos(\frac{\phi}{2})}\mathrm{d}x = \frac{\mathrm{e}^{p\sqrt{\frac{|\lambda|}{\nu}}\cos(\frac{\phi}{2})}-1}{p\sqrt{\frac{|\lambda|}{\nu}}\cos(\frac{\phi}{2})} \\ &\leq \frac{\mathrm{e}^{p\sqrt{\frac{|\lambda|}{\nu}}\cos(\frac{\phi}{2})}}{p\sqrt{\frac{|\lambda|}{\nu}}\cos(\frac{\phi}{2})}.\end{aligned}$$

Now, an estimate of $\left(\mathrm{e}^{\sqrt{\lambda/\nu}} - \mathrm{e}^{-\sqrt{\lambda/\nu}}\right)^{-1}$ remains. Using the triangle inequality we have

$$\left|\mathrm{e}^{\sqrt{\frac{\lambda}{\nu}}} - \mathrm{e}^{-\sqrt{\frac{\lambda}{\nu}}}\right| \geq \mathrm{e}^{\sqrt{\frac{|\lambda|}{\nu}}\cos(\frac{\phi}{2})} - \mathrm{e}^{-\sqrt{\frac{|\lambda|}{\nu}}\cos(\frac{\phi}{2})} \geq C\mathrm{e}^{\sqrt{\frac{|\lambda|}{\nu}}\cos(\frac{\phi}{2})},$$

for some constant $C > 0$ and sufficiently large $|\lambda|$. Combining the previous results, we obtain for appropriate $|\lambda|$

$$\begin{aligned}\|u\|_{L^p(\Omega)} \leq \|\tilde{u}\|_{L^p(\Omega)} &+ \sqrt{\frac{\nu}{|\lambda|}}\frac{|\tilde{u}'(0)|\mathrm{e}^{\sqrt{\frac{|\lambda|}{\nu}}\cos(\frac{\phi}{2})} + |\tilde{u}'(1)|}{\left|\mathrm{e}^{\sqrt{\frac{\lambda}{\nu}}} - \mathrm{e}^{-\sqrt{\frac{\lambda}{\nu}}}\right|}\left\|\mathrm{e}^{-\sqrt{\frac{\lambda}{\nu}}x}\right\|_{L^p(\Omega)} \\ &+ \sqrt{\frac{\nu}{|\lambda|}}\frac{|\tilde{u}'(0)|\mathrm{e}^{-\sqrt{\frac{|\lambda|}{\nu}}\cos(\frac{\phi}{2})} + |\tilde{u}'(1)|}{\left|\mathrm{e}^{\sqrt{\frac{\lambda}{\nu}}} - \mathrm{e}^{-\sqrt{\frac{\lambda}{\nu}}}\right|}\left\|\mathrm{e}^{\sqrt{\frac{\lambda}{\nu}}x}\right\|_{L^p(\Omega)} \\ &\leq \frac{C}{|\lambda|}\|f\|_{L^p(\Omega)},\end{aligned}$$

where we used the lower bound $\cos(\phi/2) \geq \cos(\phi_0/2)$ for some $\phi_0 \in (\pi/2, \pi)$, such that $\phi < \phi_0$. The constant C only depends on the choice of ϕ_0, some choice of a constant $R > 0$, such that the previous estimates hold for $|\lambda| > R$ and p.

Now, we analyze the case when λ is close to 0. We use the series expansion of the exponential function and cut the sum after the first two terms. Then, if $|\lambda| < R$, there exists some positive constant, such that $\left|\mathrm{e}^{\sqrt{\lambda/\nu}y} + \mathrm{e}^{-\sqrt{\lambda/\nu}y}\right| \leq C$, for all $y \in [0, 1]$. Let us have another look at the constants c_1 and c_2 and calculate

$$\tilde{u}'(0)\mathrm{e}^{\sqrt{\frac{\lambda}{\nu}}} - \tilde{u}'(1) = \frac{1}{2\nu}\int_0^1 \left(\mathrm{e}^{\sqrt{\frac{\lambda}{\nu}}(1-y)} + \mathrm{e}^{-\sqrt{\frac{\lambda}{\nu}}(1-y)}\right) f(y)\mathrm{d}y.$$

Again, by Hölder's inequality, we obtain

$$\left|\tilde{u}'(0)\mathrm{e}^{\sqrt{\frac{\lambda}{\nu}}} - \tilde{u}'(1)\right| \leq \frac{1}{2\nu}\left[\int_0^1 \left|\mathrm{e}^{\sqrt{\frac{\lambda}{\nu}}(1-y)} + \mathrm{e}^{-\sqrt{\frac{\lambda}{\nu}}(1-y)}\right|^q \mathrm{d}y\right]^{\frac{1}{q}} \|f\|_{L^p(\Omega)} \leq \frac{C}{\nu}\|f\|_{L^p(\Omega)},$$

$$\begin{aligned}\left|\tilde{u}'(0)\mathrm{e}^{-\sqrt{\frac{\lambda}{\nu}}} - \tilde{u}'(1)\right| &\leq \frac{1}{2\nu}\left[\int_0^1 \left|\mathrm{e}^{-\sqrt{\frac{\lambda}{\nu}}(1+y)} + \mathrm{e}^{-\sqrt{\frac{\lambda}{\nu}}(1-y)}\right|^q \mathrm{d}y\right]^{\frac{1}{q}} \|f\|_{L^p(\Omega)} \\ &\leq \frac{C}{\nu}\mathrm{e}^{-\sqrt{\frac{|\lambda|}{\nu}}\cos(\frac{\phi}{2})}\|f\|_{L^p(\Omega)} \\ &\leq \frac{C}{\nu}\|f\|_{L^p(\Omega)}.\end{aligned}$$

The denominator of c_1 and c_2 can be estimated by

$$\left|\mathrm{e}^{\sqrt{\lambda/\nu}} - \mathrm{e}^{-\sqrt{\lambda/\nu}}\right|^{-1} \leq C\sqrt{\nu}/(\sqrt{|\lambda|}\cos(\phi/2)).$$

Lastly, the remaining estimates are

$$\begin{aligned}\left\|\mathrm{e}^{-\sqrt{\frac{\lambda}{\nu}}x}\right\|_{L^p(\Omega)}^p &= \int_0^1 \left|\mathrm{e}^{-p\sqrt{\frac{\lambda}{\nu}}x}\right| \mathrm{d}x \leq C\int_0^1 \left(1 - p\sqrt{\frac{|\lambda|}{\nu}}x\cos\left(\frac{\phi}{2}\right)\right)\mathrm{d}x \leq C, \\ \left\|\mathrm{e}^{-\sqrt{\frac{\lambda}{\nu}}x}\right\|_{L^p(\Omega)}^p &= \int_0^1 \left|\mathrm{e}^{-p\sqrt{\frac{\lambda}{\nu}}x}\right| \mathrm{d}x \leq C\int_0^1 \left(1 + p\sqrt{\frac{|\lambda|}{\nu}}x\cos\left(\frac{\phi}{2}\right)\right)\mathrm{d}x \leq C.\end{aligned}$$

Again, by combining the previous estimates for sufficiently small λ, we have

$$\|u\|_{L^p(\Omega)} \leq \frac{C}{|\lambda|}\|f\|_{L^p(\Omega)}.$$

The constant C only depends on $R > 0$, $\phi_0 \in (\pi/2, \pi)$ and p. Therefore, we have the desired resolvent estimate by defining $u = R_\lambda f$. Hence, A with the given domain is a sectorial operator of angle $\theta \in (\pi/2, \pi)$. From theorem (2.3.2) follows, that A is the generator of an analytic semigroup on $L^p(\Omega)$.

Now, let us consider $(A - \lambda)u = f$, with f, $u \in D(A)$. Then $Au \in D(A)$ and from the equation

$$(A - \lambda)(A - 1)u = (A - 1)f$$

we deduce, using the previous result, that

$$\|(A-1)u\|_{L^p(\Omega)} \leq \frac{C}{|\lambda|}\|(A-1)f\|_{L^p(\Omega)} \Rightarrow \|u\|_{W_p^2(\Omega)} \leq \frac{C}{|\lambda|}\|f\|_{W_p^2(\Omega)}.$$

Since $W_p^\alpha(\Omega)$ is an interpolation space w.r.t. $\left(L^p(\Omega), W_p^2(\Omega)\right)$ of exponent $\alpha/2$, we obtain the estimate

$$\|u\|_{W_p^\alpha(\Omega)} \leq \frac{C}{|\lambda|}\|f\|_{W_p^\alpha(\Omega)},$$

for $f \in D(A)$. Hence, A is the generator of an analytic semigroup on $W_p^\alpha(\Omega)$ with $0 < \alpha < 1$.

□

Definition 3.2.1. *Let $A = \nu\partial_x^2 \mathbf{1}_3$ as before, $U_0 \in E_1$, the set M be given by* (3.2.1) *and the norm given by* (3.2.2)*. Then, we call*

$$U_j = \mathrm{e}^{tA_{jj}} U_{0,j} + \int_0^t \mathrm{e}^{(t-t')A_{jj}} F_j(U(t'))\mathrm{d}t', \quad j = 1, 2, 3, \tag{3.2.4}$$

the mild solution of problem (3.1.15)*.*

Note, that we will use $A = \nu\partial_x^2$ instead of A_{jj} whenever we investigate only the j-th element of the solution vector U.

A mild solution of a differential equation or system of PDEs is the generalization of solutions in a classical sense to a wider range of vector spaces. Such mild solutions may only exist in a space of distributions. However, the idea is to prove existence of a mild solution and then study its regularity. Using embeddings of function spaces, e.g. Sobolev embeddings, one may show continuity or even continuous differentiability of the mild solution w.r.t. time.

In order to obtain a solution via an algorithm like the Picard-Lindelöf-Iteration, we need Lipschitz-continuity of the right hand side $F(U)$.

Lemma 3.2.5. *Let $U, U' \in M$. Then, F is locally Lipschitz continuous and it holds*

$$\big\|F(U) - F(U')\big\|_{L^2(\Omega)\times H^{-s}(\Omega)\times L^2(\Omega)} \le L\big\|U - U'\big\|, \tag{3.2.5}$$

with a constant $L > 0$, depending on R and $\big\|U_0\big\|$.

Proof. We have to consider two distinct nonlinear terms of the form u^2 and u_1u_2, with u, u_1, $u_2 \in M$. Using Hölder's inequality and the embeddings $H^{1/4}(\Omega) \hookrightarrow L^4(\Omega)$ and $H^1(\Omega) \hookrightarrow L^\infty(\Omega)$, we obtain

$$\begin{aligned}
\|u^2 - v^2\|_{L^2(\Omega)} &= \|(u+v)(u-v)\|_{L^2(\Omega)} = \|(u+v)^2(u-v)^2\|_{L^1(\Omega)}^{\frac{1}{2}} \\
&\le \|(u+v)^2\|_{L^2(\Omega)}^{\frac{1}{2}} \|(u-v)^2\|_{L^2(\Omega)}^{\frac{1}{2}} \\
&\le (\|u\|_{L^4(\Omega)} + \|v\|_{L^4(\Omega)})\|u - v\|_{L^4(\Omega)} \\
&\le 2C_1\left(R + \big\|U_0\big\|\right)\|u - v\|_{H^{1+1/4}(\Omega)}, \\
\|u_1u_2 - v_1v_2\|_{L^2(\Omega)} &= \|u_1u_2 - u_1v_2 + u_1v_2 - v_1v_2\|_{L^2(\Omega)} \\
&\le \|u_1(u_2 - v_2)\|_{L^2(\Omega)} + \|v_2(u_1 - v_1)\|_{L^2(\Omega)} \\
&\le \|u_1\|_{L^\infty(\Omega)}\|u_2 - v_2\|_{L^2(\Omega)} + \|v_2\|_{L^\infty(\Omega)}\|u_1 - v_1\|_{L^2(\Omega)} \\
&\le C_2\left(R + \big\|U_0\big\|\right)(\|u_1 - v_1\|_{H^{1+1/4}(\Omega)} + \|u_2 - v_2\|_{H^{1+1/4}(\Omega)}),
\end{aligned}$$

with some constants C_1, $C_2 > 0$ depending on Ω. Now, we can apply the previous inequalities and theorem (3.2.2) to the RHS F and calculate

$$\begin{aligned}
\left\|F_1(U) - F_1(W)\right\|_{L^2(\Omega)} &\leq C_1 \left(1 + 2(\nu+1)\left(R + \left\|U_0\right\|\right)\right) \left\|U - W\right\|, \\
\left\|F_2(U) - F_2(W)\right\|_{H^{-s}(\Omega)} &\leq C_2 \Bigg(2 + \mu + \frac{1}{\tau} + (5 + 4\nu)\left(R + \left\|U_0\right\|\right) \\
&\qquad + \mathrm{e}^{C_3\left(R + \left\|U_0\right\|\right)} \Bigg) \left\|U - W\right\|, \\
\left\|F_3(U) - F_3(W)\right\|_{L^2(\Omega)} &\leq C_4 \left(\frac{2}{\tau} + (6 + 4\nu + 2\mu)\left(R + \left\|U_0\right\|\right) \right) \left\|U - W\right\|,
\end{aligned}$$

with constants $C_j > 0$, $j = 1, 2, 3, 4$. □

At this point, we are able to construct a mild solution utilizing the Picard-Lindelöf-Iteration.

Theorem 3.2.6. *Let $U_0 \in E_1$ with $U_{0,1}$ being bounded in $\bar{\Omega}$. Additionally, let $C_0 \in L^\infty(\Omega)$, $V_0, \lambda \geq 0$, $\nu > 0$ and $A = \nu \partial_x^2 \mathbf{1}_3$.*

Then, there exists $T \in \mathbb{R}$, with $T > 0$, such that

$$U = \mathrm{e}^{tA} U_0 + \int_0^t \mathrm{e}^{(t-s)A} F(U(s)) \mathrm{d}s$$

is the unique mild solution to problem (3.1.15) for all $t \in [0, T]$. Furthermore, the potential V is given by the unique solution to problem (3.1.16).

Proof. Let us define the map $S : M \to E_1$ by

$$S_j(U) = \mathrm{e}^{tA} U_{0,j} + \int_0^t \mathrm{e}^{(t-t')A} F_j(U(t')) \mathrm{d}t', \quad j = 1, 2, 3.$$

with $U = (U_1, U_2, U_3) \in M$. Then, we define a sequence by $U^{(0)} = (U_{0,1}, U_{0,2}, U_{0,3})$, $U^{(n+1)} = S\left(U^{(n)}\right)$ and solve for each $U^{(n)}$ problem (3.1.16), which gives us a $V^{(n)}$. The previous iteration and potential $V^{(n)}$ are used to calculate $F\big(U^{(n)}(t)\big)$. Now, we have to show that $S\big(U^{(n)}\big) \in M$ and the map S is a contraction. Note, that we use the abbreviation $F^{(n)}(t) = F\big(U^{(n)}(t)\big)$.

In the following, we only show the complete calculation for one component, since the over two are handled analogously. We calculate the estimate

$$\begin{aligned}
\nu^{-\alpha} \left\| A^\alpha \left(U_1^{(n)} - U_{0,1} \right) \right\|_{L^2(\Omega)} &\leq \nu^{-\alpha} \left\| \left(\mathrm{e}^{tA} - 1\right) A^\alpha U_{0,1} \right\|_{L^2(\Omega)} \\
&\quad + \nu^{-\alpha} \left\| A^\alpha \int_0^t \mathrm{e}^{(t-s)A} F_1^{(n-1)}(s) \mathrm{d}s \right\|_{L^2(\Omega)} \\
&\leq \nu^{-\alpha} \left\| \left(\mathrm{e}^{tA} - 1\right) A^\alpha U_{0,1} \right\|_{L^2(\Omega)}
\end{aligned}$$

$$\begin{aligned}
&+\nu^{-\alpha}\int_0^t (t-s)^{-\alpha}\big\|F_1^{(n-1)}(s)\big\|_{L^2(\Omega)}\mathrm{d}s\\
\leq{}& \left\|\left(\mathrm{e}^{tA}-1\right)U_{0,1}\right\|_{H^{2\alpha}(\Omega)}\\
&+\nu^{-\alpha}\frac{1}{1-\alpha}t^{1-\alpha}\sup_{s\in[0,t]}\left\|F_1^{(n-1)}(s)\right\|_{L^2(\Omega)},
\end{aligned}$$

with $\alpha=\frac{5}{8}$. For $U_2^{(n)}$ and $U_3^{(n)}$ we have the estimates

$$\begin{aligned}
\nu^{-\frac{5}{8}}\left\|A^{\frac{5}{8}}\left(U_2^{(n)}-U_{0,2}\right)\right\|_{L^2(\Omega)} \leq{}& \big\|\left(\mathrm{e}^{tA}-1\right)U_{0,2}\big\|_{H^{1+1/4}(\Omega)}\\
&+\frac{8\nu^{-\frac{5+4s}{8}}}{3-4s}t^{\frac{3-4s}{8}}\sup_{t'\in[0,t]}\left\|F_2^{(n-1)}(t')\right\|_{H^{-s/2}(\Omega)}
\end{aligned}$$

$$\begin{aligned}
\nu^{-\frac{5}{8}}\left\|A^{\frac{5}{8}}\left(U_3^{(n)}-U_{0,3}\right)\right\|_{L^2(\Omega)} \leq{}& \left\|\left(\mathrm{e}^{tA}-1\right)U_{0,3}\right\|_{H^{1+1/4}(\Omega)}\\
&+2\nu^{-\frac{5}{8}}t^{\frac{3}{8}}\sup_{t'\in[0,t]}\left\|F_3^{(n-1)}(t')\right\|_{L^2(\Omega)}.
\end{aligned}$$

Since $\|\mathrm{e}^{tA}x-x\|_{L^p(\Omega)}\to 0$ for $x\in L^p(\Omega)$ and $t\to 0$, we can choose $t_1>0$ such that $\big\|\left(\mathrm{e}^{tA}-1\right)A^{5/8}U_{0,j}\big\|_{L^p(\Omega)}$ is sufficiently small. Therefore, we have $S\big(U^{(n)}\big)\in M$ if $U^{(n)}\in M$. Next, we show that the map S is a contraction on M for appropiate time t. Let $U,W\in M$, we calculate for $0\leq\alpha<1$

$$\begin{aligned}
\nu^{-\alpha}\left\|A^{\alpha}\left(S_1(U)-S_1(W)\right)\right\|_{L^2(\Omega)} &\leq \nu^{-\alpha}\left\|A^{\alpha}\int_0^t \mathrm{e}^{(t-s)A}\left(F_1(U(s))-F_1(W(s))\right)\mathrm{d}s\right\|_{L^2(\Omega)}\\
&\leq L_1\nu^{-\alpha}\int_0^t (t-s)^{-\alpha}\big\|U-W\big\|_{E_1}\mathrm{d}s\\
&= L_1\nu^{-\alpha}\frac{t^{1-\alpha}}{1-\alpha}\big\|U-W\big\|_{E_1}.
\end{aligned}$$

Combining the results for $\alpha=0$ and $\alpha=5/8$ gives

$$\big\|S_1(U)-S_1(W)\big\|_{H^{1+1/4}(\Omega)}\leq L_1\left(t+\frac{8}{3}\nu^{-\frac{5}{8}}t^{\frac{3}{8}}\right)\|U-W\|_{E_1}.$$

Analogously, we obtain for S_2 and S_3 the estimates

$$\begin{aligned}
\nu^{-\alpha}\big\|A^{\alpha}\left(S_2(U)-S_2(W)\right)\big\|_{L^2(\Omega)} &\leq \nu^{-\alpha+\frac{s}{2}}\frac{2L_2}{2-2\alpha-s}t^{1-\alpha-\frac{s}{2}}\|U-W\|_{E_1},\\
\nu^{-\alpha}\big\|A^{\alpha}\left(S_3(U)-S_3(W)\right)\big\|_{L^2(\Omega)} &\leq \nu^{-\alpha}\frac{L_3}{1-\alpha}t^{1-\alpha}\|U-W\|_{E_1},
\end{aligned}$$

where we apply $\alpha=0$ and $\alpha=5/8$ to each inequality, respectively. Then, we have the estimates

$$\begin{aligned}
\left\|S_2(U) - S_2(W)\right\|_{H^{1+1/4}(\Omega)} &\leq L_2 \left(\nu^{-\frac{s}{2}} \frac{2}{2-s} t^{1-\frac{s}{2}} + \nu^{-\frac{5+4s}{8}} \frac{8}{3-4s} t^{\frac{3-4s}{8}} \right) \|U - W\|_{E_1}, \\
\left\|S_3(U) - S_3(W)\right\|_{H^{1+1/4}(\Omega)} &\leq L_3 \left(t + \frac{8}{3} \nu^{-\frac{5}{8}} t^{\frac{3}{8}} \right) \|U - W\|_{E_1}.
\end{aligned}$$

Finally, by combining the previous results we deduce

$$\begin{aligned}
\|S(U) - S(W)\|_{E_1} \leq \Bigg(&(L_1 + L_3) \left(t + \frac{8}{3} \nu^{-\frac{5}{8}} t^{\frac{3}{8}} \right) \\
&+ L_2 \left(\nu^{-\frac{s}{2}} \frac{2}{2-s} t^{1-\frac{s}{2}} + \nu^{-\frac{5+4s}{8}} \frac{8}{3-4s} t^{\frac{3-4s}{8}} \right) \Bigg) \|U - W\|_{E_1} \\
= \; &k(t) \|U - W\|_{E_1}.
\end{aligned}$$

Since t can be chosen sufficiently small, we have for appropiate $t_2 > 0$ that $k(t_2) < 1$. Thus, the map S is a contraction on M. Now, set $T = \min(t_1, t_2)$. Then, due to the Banach fixed point theorem there exists a unique fixed point $U^* \in M$ with $S(U^*) = U^*$ and $U^{(n)} \to U^*$ strongly in $H^{1+1/4}(\Omega) \times H^{1+1/4}(\Omega) \times H^{1+1/4}(\Omega)$. Also, we have the strong convergence of $V^{(n)} \to V^*$ in H^2, since $\lambda^2 \left\|\partial_x^2 (V^{(n)} - V^*)\right\|_{L^2(\Omega)} \leq C \left\|U_1^{(n)} - U_1^*\right\|_{H^{1+1/4}(\Omega)}$. Next, we show that (U_1^*, U_2, U_3) solves (3.1.15). The potential V^* is given by theorem (3.2.2) for given U^* and we calculate for $t \in [0, T]$

$$\partial_t U^* = A e^{tA} U_0 + A \int_0^t e^{(t-t')A} F(U^*(t')) \mathrm{d}t' + F(U^*(t)) = AU^* + F(U^*).$$

Hence, we conclude the existence of a unique mild solution $(U_1^*, U_2^*, U_3^*) \in M$ to problem (3.1.15) and the respective potential is given by theorem (3.2.2) for U_1^*. □

Note, that the previous theorem only gives the existence of solutions for sufficiently small time. Existence on arbitrary bounded time intervals requires precise estimates and restrictions to the initial conditions. In [Lun12], semilinear and fully nonlinear problems are discussed and several general results are given. For example, consider the equations $u_1'(t) = u_1^2$ and $u_2'(t) = -u_2 + u_2^2$ for $t > 0$, with $u_1(0) = u_2(0) = u_0 > 0$. While u_1 always blows up in finite time, there are solutions u_2 existing for any time $t > 0$. Especially u_2 is sensitive to changes of the initial condition, i.e. $u_0 < 1$, $u_0 = 1$ and $u_0 > 1$ give very different results. We expect that restrictions of the initial conditions allow stronger existence results for the full viscous quantum hydrodynamic system. Furthermore, the linear part or the linearization of the nonlinear function is crucial for the existence of solutions to the time dependent problem and stability of stationary solutions. During the next section we study the linearized full viscous quantum hydrodynamic system, in particular we give stability results for stationary solutions, whose existence is reasonable in case of physically relevant initial conditions.

So far, we have a solution where e.g. $U_2 \in H^{1+1/4}(\Omega)$ and observe the following. The second derivative of U_2 w.r.t. the spatial coordinate may only exists in a distributional sense. However, we also have $F_2(U) \in H^{-s}(\Omega)$. Therefore, we expect the mild solution to have at least the spatial regularity with e.g. $U_2 \in W_4^{2-s}(\Omega)$. Obviously, the spatial regularity of the initial condition is important for our estimates. Now, we consider the Banach space $E_s = H^{3-s}(\Omega) \times H^{2-s}(\Omega) \times H^{3-s}(\Omega) \subset E_1$.

Theorem 3.2.7. *Let $U_0 \in E_s$ and $t > 0$ be sufficiently small. Then, the mild solution $U \in M$ of problem* (3.1.15) *has the regularity*

$$\begin{aligned} U_1 &\in C\left([0,t], H^{3-s}(\Omega)\right), \\ U_2 &\in C\left([0,t], H^{2-s}(\Omega)\right), \\ U_3 &\in C\left([0,t], H^{3-s}(\Omega)\right). \end{aligned}$$

Proof. Let $U_0 \in E_s$. By theorem (3.2.6), there exists a unique mild solution $(w, \tilde{J}, \widetilde{ni}) \in M$ to problem (3.1.12). Due to proposition (3.2.1), there exists a unique mild solution $(U_1, U_2, U_3) \in M$ to problem (3.1.1), given by

$$U = \mathrm{e}^{tA} U_0 + \int_0^t \mathrm{e}^{(t-t')} F(U(t'))\mathrm{d}t'.$$

First, we will show, that the mild solution is Hölder continuous w.r.t. time in $H^1(\Omega) \times H^1(\Omega) \times H^1(\Omega)$. Then, we use this result to proof that the mild solution is bounded in E_s. Let w.l.o.g. $t \geq t' \geq 0$. We calculate the following

$$\begin{aligned} \left\| A^{\frac{1}{2}} \left(U_1(t) - U_1(t')\right) \right\|_{L^2(\Omega)} \leq& \left\| \left(\mathrm{e}^{tA} - \mathrm{e}^{t'A}\right) A^{\frac{1}{2}} U_{0,1} \right\|_{L^2(\Omega)} \\ &+ \left\| A^{\frac{1}{2}} \int_0^t \mathrm{e}^{(t-t'')A} F_1(t'')\mathrm{d}t'' - A^{\frac{1}{2}} \int_0^{t'} \mathrm{e}^{(t'-t'')A} F_1(t'')\mathrm{d}t'' \right\|_{L^2(\Omega)} \\ =& \left\| A \int_{t'}^t \mathrm{e}^{t''A} A^{\frac{1}{2}} U_{0,1} \mathrm{d}t'' \right\|_{L^2(\Omega)} \\ &+ \left\| A^{\frac{1}{2}} \int_{t'}^t \mathrm{e}^{(t-t'')A} F_1(t'')\mathrm{d}t'' \right. \\ &\left. + A^{\frac{3}{2}} \int_0^{t'} \int_{t'-t''}^{t-t''} \mathrm{e}^{rA} F_1(t'')\mathrm{d}r\mathrm{d}t'' \right\|_{L^2(\Omega)} \\ \leq& \left\| A^{\frac{s}{2}} \int_{t'}^t \mathrm{e}^{t''A} A^{\frac{3-s}{2}} U_{0,1} \right\|_{L^2(\Omega)} + \int_{t'}^t (t-t'')^{-\frac{1}{2}} \|F_1(t'')\|_{L^2(\Omega)} \mathrm{d}t'' \\ &+ \int_0^{t'} \int_{t'-t''}^{t-t''} r^{-\frac{3}{2}} \|F_1(t'')\|_{L^2(\Omega)} \mathrm{d}r\mathrm{d}t'' \\ \leq& \int_{t'}^t t''^{-\frac{s}{2}} \mathrm{d}t'' \|A^{\frac{3-s}{2}} U_{0,1}\|_{L^2(\Omega)} + 2(t-t')^{\frac{1}{2}} \sup_{t'' \in [t',t]} \left(\|F_1(t'')\|_{L^2(\Omega)} \right) \\ &+ 4\left((t-t')^{\frac{1}{2}} - \left(t^{\frac{1}{2}} - t'^{\frac{1}{2}}\right)\right) \sup_{t'' \in [0,t']} \left(\|F_1(t'')\|_{L^2(\Omega)} \right) \end{aligned}$$

$$
\begin{aligned}
&\le \nu^{-\frac{3-s}{2}} \frac{2}{2-s}\left(t^{1-\frac{s}{2}} - t'^{1-\frac{s}{2}}\right) \left\|U_{0,1}\right\|_{H^{3-s}(\Omega)} \\
&\quad + 6(t-t')^{\frac{1}{2}} \sup_{t''\in[0,t]} \left(\|F_1(t'')\|_{L^2(\Omega)}\right) \\
&\le \nu^{-\frac{3-s}{2}} \frac{2}{2-s}(t-t')^{1-\frac{s}{2}} \left\|U_{0,1}\right\|_{H^{3-s}(\Omega)} \\
&\quad + 6(t-t')^{\frac{1}{2}} \sup_{t''\in[0,t]} \left(\|F_1(t'')\|_{L^2(\Omega)}\right)
\end{aligned}
$$

We repeat this calculation with U_2 and U_3 to obtain

$$
\begin{aligned}
\left\|A^{\frac{1}{2}}\left(U_2(t) - U_2(t')\right)\right\|_{L^2(\Omega)} \le \Bigg(& \nu^{-(1-\frac{s}{2})} \frac{2}{1-s} \|U_{0,2}\|_{H^{2-s}(\Omega)} \\
& + \nu^{\frac{s}{2}} \frac{4}{1-s^2} \sup_{t''\in[0,t]} \left(\|F_2(t'')\|_{H^{-s}(\Omega)}\right) \Bigg) (t-t')^{\frac{1-s}{2}},
\end{aligned}
$$

$$
\begin{aligned}
\left\|A^{\frac{1}{2}}\left(U_3(t) - U_3(t')\right)\right\|_{L^2(\Omega)} \le\ & \nu^{-\frac{3-s}{2}} \frac{2}{2-s}(t-t')^{1-\frac{s}{2}} \|U_{0,3}\|_{H^{3-s}(\Omega)} \\
& + 6(t-t')^{\frac{1}{2}} \sup_{t''\in[0,t]} \left(\|F_3(t'')\|_{L^2(\Omega)}\right).
\end{aligned}
$$

Now, we are able to prove the assertion. We begin with U_2 and obtain

$$
\begin{aligned}
\left\|A^{\frac{2-s}{2}} U_2\right\|_{L^2(\Omega)} \le \left\|A^{\frac{2-s}{2}} U_{0,2}\right\|_{L^2(\Omega)} &+ C\int_0^t \left((t-t')^{-\frac{1+s}{2}} + \sqrt{t-t'} + (t-t')^{1-\frac{s}{2}}\right) \mathrm{d}t' \\
&+ \left\|\left(\mathrm{e}^{tA} - 1\right) A^{-\frac{s}{2}} F_2(t)\right\|_{L^2(\Omega)} < \infty.
\end{aligned}
$$

The continuity follows from the continuity of the analytic semigroup $\left\{\mathrm{e}^{tA}\right\}_{t\ge0}$. Therefore,

$$
U_2 \in C([0,t], H^{2-s}(\Omega)).
$$

It follows that $F_1(U) \in H^{1-s}(\Omega)$ for all $U_2 \in H^{2-s}(\Omega)$ and we use this result to investigate the spatial regularity of U_1. We begin with

$$
\begin{aligned}
\left\|A^{\frac{3-s}{2}} U_1\right\|_{L^2(\Omega)} \le \left\|A^{\frac{3-s}{2}} U_{0,1}\right\|_{L^2(\Omega)} &+ \int_0^t (t-t')^{-1} \left\|A^{\frac{2-s}{2}}\left(U_2(t) - U_2(t')\right)\right\|_{L^2(\Omega)} \mathrm{d}t' \\
&+ \left\|\left(\mathrm{e}^{tA} - 1\right) A^{\frac{1-s}{2}} F_1(t)\right\|_{L^2(\Omega)}.
\end{aligned}
$$

The question arises whether the remaining integral is finite since $1/(t-t')$ has a singularity at $t' = t$ and clearly F_1 is not Hölder continuous in $H^{1-s}(\Omega)$. Let again w.l.o.g. $t \ge t' \ge 0$.

By calculation we obtain

$$\begin{aligned}\left\|A^{\frac{2-s}{2}}\left(U_2(t)-U_2(t')\right)\right\|_{L^2(\Omega)} \leq{}& \left\|\left(\mathrm{e}^{tA}-\mathrm{e}^{t'A}\right)A^{\frac{2-s}{2}}U_{0,2}\right\|_{L^2(\Omega)} \\ &+\int_{t'}^{t}\left(t-t''\right)^{-1}\left\|A^{-\frac{s}{2}}\left(F_2(t)-F_2(t'')\right)\right\|_{L^2(\Omega)}\mathrm{d}t'' \\ &+2\left\|A^{-\frac{2}{s}}\left(F_2(t)-F_2(t')\right)\right\|_{L^2(\Omega)} \\ &+\left\|\left(\mathrm{e}^{tA}-\mathrm{e}^{t'A}\right)A^{-\frac{s}{2}}F_2(t')\right\|_{L^2(\Omega)} \\ &+\int_0^{t'}\frac{t-t'}{(t'-t'')(t-t'')}\left\|A^{-\frac{s}{2}}\left(F_2(t')-F_2(t'')\right)\right\|_{L^2(\Omega)}\mathrm{d}t''.\end{aligned}$$

Using $\|\left(\mathrm{e}^{tA}-1\right)x/t-Ax\|_{L^2(\Omega)}\to 0$ as $t\to 0$ for all $x\in D(A)$ and $\mathrm{e}^{tA}x\in D(A)$ for $t>0$, we observe that the first term leads to $\left\|A\mathrm{e}^{tA}A^{(2-s)/2}U_{0,2}\right\|_{L^2(\Omega)}$ for $t'\to t$, which is bounded for $t>0$. We can use the same calculation for the fourth term. The first integral gives the term $(t-t')^\alpha$ with $\alpha>0$ due to the Lipschitz continuity of F_2 and the Hölder continuity of U w.r.t. time. This holds for the third term as well. Finally, we have to investigate the following integral for $\alpha>0$

$$\begin{aligned}\int_0^t\int_0^{t'}(t'-t'')^{\alpha-1}(t-t'')^{-1}\mathrm{d}t''\mathrm{d}t' &= t^\alpha\int_0^1\int_0^1 y^\alpha(1-x)^{\alpha-1}(1-yx)^{-1}\mathrm{d}x\mathrm{d}y \\ &= \frac{t^\alpha}{\alpha}\int_0^1 {}_2F_1(1,1,1+\alpha,y)y^\alpha\mathrm{d}y=\frac{t^\alpha}{\alpha^2},\end{aligned}$$

where we used the hypergeometric function ${}_pF_q(a_1,\dots,a_p;b_1,\dots,b_q;z)$, see e.g. [AAR99]. We conclude that $\left\|A^{(2-s)/2}(U_2(t)-U_2(t'))\right\|_{L^2(\Omega)}/(t-t')$ is bounded for $t'\in[0,t]$. Since $\left\|tA\mathrm{e}^{tA}x\right\|_{L^2(\Omega)}\leq\|x\|_{L^2(\Omega)}$, we have $U_1\in H^{3-s}(\Omega)$ for all $t\geq 0$ and by continuity of the analytic semigroup $U_1\in C([0,t],H^{3-s}(\Omega))$. Using the Lipschitz continuity of F_3 w.r.t. U and Hölder continuity of U w.r.t. time we can show $U_3\in H^2(\Omega)$. Immediately, we have $F_3\in H^{1-s}(\Omega)$ which gives together with the previous results the Hölder continuity of U_1 and U_3 w.r.t. time, especially $U_1\in C^{1/2}([0,t],H^{2-s}(\Omega))$ and $U_3\in C^{1/2}([0,t],H^{2-s}(\Omega))$. At last, we obtain $U_3\in C([0,t],H^{3-s}(\Omega))$, where the calculations are analogously to the proof for U_1 and additional use of the Lipschitz continuity of F_3. □

Lastly, we want to give a result for a special case of initial conditions. We set $J_0=0$ while initial density and internal energy density can be rather arbitrary. This setting corresponds to switching on a device.

Theorem 3.2.8. *Let $U_{0,1}\in L^\infty(\Omega)$, $U_{0,2}=0$ and $U_{0,3}\in L^\infty(\Omega)$. Then, there exists a mild solution to problem* (3.1.15) *with the regularity*

$$U_1\in C\left((0,t],H^{3-s}(\Omega)\right),$$

$$U_2 \in C\left((0,t], H^{2-s}(\Omega)\right),$$
$$U_3 \in C\left((0,t], H^{3-s}(\Omega)\right).$$

Furthermore, the potential V is given by the unique solution to problem (3.1.16).

Proof. Let us calculate $F(U^{(0)})$. We obtain

$$\begin{aligned}
F_1^{(0)} &= 0, \\
F_2^{(0)} &= -\partial_x(2U_{0,3} + \mu U_{0,1}) + U_{0,1}\partial_x(V^{(0)} + V_B), \\
F_3^{(0)} &= -\frac{2}{\tau}\left(U_{0,3} - \frac{U_{0,1}}{2}\right).
\end{aligned}$$

Thus, we have $F_1^{(0)} \in L^2(\Omega)$, $F_2^{(0)} \in H^{-s}(\Omega)$ and $F_3^{(0)} \in L^2(\Omega)$. Furthermore, the first iteration gives

$$U_1^{(1)} = \mathrm{e}^{tA}U_{0,1}.$$

Now, from $\inf_{x\in\Omega}(U_{0,1}) \geq \delta$, with $\delta > 0$, and positivity of the heat semigroup follows

$$\inf_{x\in\Omega}\left(U_1^{(1)}\right) \geq \delta.$$

Existence of a mild solution is shown analogously to the proof of theorem (3.2.6). The analysis of the regularity is analogous to the previous proof. However, with $U_{0,1}$, $U_{0,3} \in L^\infty(\Omega)$ we only have Hölder regularity for $t > 0$ in $H^1(\Omega)$. This affects the estimates in $H^{3-s}(\Omega)$ and $H^{2-s}(\Omega)$, which only hold for $t > 0$ now. □

So far, we presented the full viscous quantum hydrodynamic model with an additional barrier potential in one space dimension. We observed the disappearence of the quantum Bohm potential and the necessity to use negative order Sobolev spaces, since the barrier potential may be discontinuous and its derivative is proportional to the δ-distribution. In order to preserve the positivity of the electron density, we used the substitution $n = \exp(w)$ with a suitable function w. We showed, if a set of functions w, $\tilde{J}$, $\widetilde{ni}$ and V exists, solving the corresponding system of PDEs with w being bounded in $\bar{\Omega}$, then there exists a solution to the original system with positive electron density. Then, we chose the function space $E = H^{1+1/4}(\Omega)\times H^{1+1/4}(\Omega)\times H^{1+1/4}(\Omega)$ and obtained $F \in L^2(\Omega)\times H^{-s}(\Omega)\times L^2(\Omega)$ for the inhomogeneity F. In order to apply the Picard-Lindelöf algorithm we calculated the solution to the Poisson equation of the full viscous quantum hydrodynamic system and showed local Lipschitz continuity of the function F. The unique mild solution w, $\tilde{J}$, $\widetilde{ni}$ and V to the modified system then gave us the unique mild solution n, J, ni and V to the original one. Finally, we derived the regularity of the mild solution for intial conditions from E_s and $L^\infty(\Omega) \times \{0\} \times L^\infty(\Omega)$.

Due to the substitution, positivity of the electron density was guaranteed. However, the exponential growth bound on the potential V only allows a solution for short time intervals. For a given time interval $[0,T]$, there may only exist a mild solution up to some time $t < T$. This issue may be resolved by restrictions to the initial conditions or precise upper bounds for the inhomogeneity of the full viscous quantum hydrodynamic system. The latter case requires an alternative proof for the positivity of the electron density.

In the following section, we give the linearized version of the full viscous quantum hydrodynamic system. This allows us the analysis of the stability of stationary solutions. Additionally, we calculate values for the current density, dependent on the electron density and internal energy density, such that the stability possibly changes.

3.3 Linearized full viscous quantum hydrodynamic system

Let us now investigate the linearized version of system 3.1.1 in order to study the stability of stationary solutions, whose existence we assume at this point. In [CCGJ95, JT06], hysteresis effects in the current-voltage characteristics have been observed, hence the stationary problem admits atleast two solutions for certain voltages.

Our considerations follow [Hen81, MV11]. First, suppose there exists at least one stationary solution $(n(t,x), J(t,x), ni(t,x), V(t,x))$ to the viscous quantum hydrodynamic system, such that $\partial_t(n, J, ni, V) = 0$, i.e. $-\nu(n, J, ni, V)'' = F(n, J, ni, V)$. Now, considering variations of such a stationary solution, $(n + u_1, J + u_2, ni + u_3, V + u_4)$, with a sufficiently small disturbation $U = (u_1, u_2, u_3, u_4)$, whereby $u_j'(0) = u_j'(1) = 0$ for all $j = 1, 2, 3$, and $u_4(0) = 0$, $u_4(1) = \epsilon$, we encounter nonlinear terms $(n + u_1)^{-k}$, with $k = 1, 2, 3$. Assuming u_1 has nice properties, such that a Taylor series expansion can be justified, we have

$$\frac{1}{(n+u_1)^k} = \frac{1}{n^k} - \frac{k}{n^{k+1}} u_1 + o(u_1^2). \tag{3.3.1}$$

We obtain the following lemma.

Lemma 3.3.1. *Suppose there exists a stationary solution to the full viscous quantum hydrodynamic system (n, J, ni, V). Then the linearization around this stationary solution is given by*

$$\partial_t u_1 - \nu \partial_x^2 u_1 = -\partial_x u_2, \tag{3.3.2}$$

$$\begin{aligned}\partial_t u_2 - \nu \partial_x^2 u_2 = &\left(\frac{J^2}{n^2} + V + V_B\right)' u_1 + \frac{\epsilon}{\lambda^2} n + \frac{\epsilon}{\lambda^2} u_1 \\ &- 2\left(\frac{J}{n}\right)' u_2 - \frac{1}{\tau} u_2 + \left(\frac{J^2}{n^2} - \mu\right) \partial_x u_1 - 2\frac{J}{n} \partial_x u_2 - 2\partial_x u_3 \\ &+ \frac{n}{\lambda^2}\left(\int_0^x u_1(y)\mathrm{d}y - \int_0^1 (1-y) u_1(y)\mathrm{d}y\right) + f(u_1, u_2, u_3),\end{aligned} \tag{3.3.3}$$

$$\begin{aligned}\partial_t u_3 - \nu\partial_x^2 u_3 = &\left[3\frac{J'ni}{n^2} + \frac{Jni'}{n^2} - 6\frac{Jnin'}{n^3} + \nu\left(-\frac{J'^2}{n^2} + 4\frac{JJ'n'}{n^3} - 3\frac{J^2n'^2}{n^4}\right)\right.\\ &\left. - \mu\frac{Jn'}{n^2} + \frac{1}{\tau}\right]u_1\\ &+\left[-\frac{ni'}{n} + 3\frac{nin'}{n^2} + \nu\left(-2\frac{J'n'}{n^2} + 2\frac{Jn'^2}{n^3}\right) + \mu\frac{n'}{n}\right]u_2\\ &+\left[-3\frac{J'}{n} + 3\frac{Jn'}{n^2} - \frac{2}{\tau}\right]u_3\\ &+\left[3\frac{Jni}{n^2} + \nu\left(-2\frac{JJ'}{n^2} + 2\frac{J^2n'}{n^3}\right) + \mu\frac{J}{n}\right]\partial_x u_1\\ &+\left[-3\frac{ni}{n} + \nu\left(2\frac{J'}{n} - 2\frac{Jn'}{n^2}\right) - \mu\right]\partial_x u_2 - \frac{J}{n}\partial_x u_3 + g(u_1,u_2,u_3),\end{aligned} \tag{3.3.4}$$

where f and g contain higher order terms, such that $f(0,0,0) = 0$, $g(0,0,0) = 0$, $\mathrm{D}f(0,0,0) = 0$ and $\mathrm{D}g(0,0,0) = 0$.

Proof. Applying the previous considerations to the full viscous quantum hydrodynamic system gives the above equations. Alternatively, replacing n and $\partial_x n$ with the variables q_1 and p_1, and J, ni and V accordingly, we can differentiate the function $F(n, \partial_x n, J, \partial_x J, ni, \partial_x ni, \partial_x V)$ in (3.1.15) w.r.t. the new variables q_i and p_i to obtain the same result. $\square$

Now, we add a fourth equation $\partial_t \epsilon = 0$ for the constant parameter ϵ. Then, the term ϵn in 3.3.3 is linear in ϵ and furthermore ϵu_1 is nonlinear. We define $f_\epsilon(u_1, u_2, u_3) = \epsilon u_1 + f(u_1, u_2, u_3)$. Let $W = (u_1, u_2, u_3, \epsilon)$, then we write the resulting system in the following form

$$\partial_t W = (A + C)W + N(W), \tag{3.3.5}$$

with the linear differential matrix operator A, the linear operator C and the nonlinear function N. The action of the operator C is defined via the equations

$$[CW]_1 = 0, \tag{3.3.6}$$

$$[CW]_2 = \frac{n}{\lambda^2}\left(\int_0^x u_1(y)\mathrm{d}y - \int_0^1 (1-y)u_1(y)\mathrm{d}y\right), \tag{3.3.7}$$

$$[CW]_3 = 0, \tag{3.3.8}$$

$$[CW]_4 = 0 \tag{3.3.9}$$

Now, let $X = H^{1-s}(\Omega) \times H^{-s}(\Omega) \times H^{1-s}(\Omega) \times H^1(\Omega)$ and $X^{\frac{1}{2}} = H^{2-s}(\Omega) \times H^{1-s}(\Omega) \times H^{2-s}(\Omega) \times H^2(\Omega)$. Since $\nu\partial_x^2$ generates an analytic semigroup and the operator B, given by

$$B = A - \begin{bmatrix} \nu\partial_x^2 \mathbf{1}_3 & 0 \\ 0 & 0 \end{bmatrix}, \tag{3.3.10}$$

is a linear bounded operator from $X^{\frac{1}{2}}$ to X, A is the generator of an analytic semigroup as well, see e.g. [Ren04]. Using lemma 2.3.3, the semigroup generated by $A+C$ has the upper bound $\|\mathrm{e}^{t(A+C)}\| \leq C\mathrm{e}^{\omega t}$, with $\omega = \sup\{\mathrm{Re}(\lambda) : \lambda \in \sigma(A+C)\}$. Hence, the homogeneous parabolic problem $\partial_t W - (A+C)W = 0$ has the solution $W(t) = \mathrm{e}^{t(A+C)}W_0$ with the estimate $\|W\| \leq C\mathrm{e}^{\omega t}\|W_0\|$. If $\omega < 0$, then $W \to 0$ for $t \to \infty$. Thus, every small initial perturbation to the stationary state converges exponentially fast to zero and the stationary state is stable. On the other hand, if $w > 0$, then we have instability of the stationary state. The case $\omega = 0$ is inconclusive and further study of the nonlinear terms becomes necessary.

The study of the spectrum of matrix differential operators with non-constant entries is very extensive. There are several results concerning perturbations of self-adjoint operators and compact perturbations. A comprehensive introduction into the perturbation of linear operators is found in [Kat66]. For further information regarding compact perturbations we refer to [Hen81, Lun12].

In order to characterize the spectrum of the linear operator $T = A + C$, we use the following result, which allows us to study the limit operators T_- and T_+ for $x \to -\infty$ and $x \to \infty$, respectively.

Theorem 3.3.2. *Let $T(x, \partial_x)$ be a $N \times N$ matrix-differential operator acting on $L^2\left(\mathbb{R}^n, \mathbb{C}^N\right)$, with $N \in \mathbb{N}$, and $p(x,\xi)$ be its pseudo-differential symbol. Furthermore, for $R > 0$ and $|x| \geq R$ it holds that $p(x,\xi) = p_0(\xi)$, with $p_0(\xi)$ being the pseudo-differential symbol of the operator $T_0(\partial_x)$, not depending on x . Let $\xi_0 \in \mathbb{R}^n$, with $\xi_0 \neq 0$, and $\lambda_0 \in \mathbb{C}$ be an eigenvalue of $p_0(\xi_0)$. Then $\lambda_0 \in \sigma_{\mathrm{app}}(T)$, where $\sigma_{\mathrm{app}}(T)$ is the approximate spectrum of T.*

Proof. Let $u_0 \in \mathbb{C}^N$ be the eigenvector corresponding to λ_0, that is

$$p_0(\xi_0)u_0 = \lambda_0 u_0.$$

Choose $x_0 \in \mathbb{R}^n$, such that $|x_0| \geq k^2$, for some $k \in \mathbb{N}$ with $k \gg 1$, and the function $\phi : \mathbb{R}^n \to \mathbb{C}^N$, given by

$$\phi(x) = \frac{1}{|u_0|}\left(\frac{1}{k}\sqrt{\frac{2}{\pi}}\right)^{\frac{n}{2}} u_0 \mathrm{e}^{-\frac{|x-x_0|^2}{k^2}} \mathrm{e}^{\mathrm{i}\xi_0 x},$$

such that $\|\phi\|_{L^2} = 1$. The Fourier transform of ϕ is given by

$$\hat{\phi}(\xi) = \frac{1}{|u_0|}\left(\frac{k}{\sqrt{2\pi}}\right)^{\frac{n}{2}} u_0 \mathrm{e}^{-k^2\frac{|\xi-\xi_0|^2}{4}} \mathrm{e}^{-\mathrm{i}(\xi-\xi_0)x_0},$$

with $\|\hat{\phi}\|_{L^2} = 1$. We deduce, that

$$\|T_0\phi - \lambda_0\phi\|_{L^2} = \|(p_0 - \lambda_0)\hat{\phi}\|_{L^2} \to 0, \text{ for } k \to \infty,$$

since $\hat{\phi}$ is a Gaussian function centered at ξ_0 and $(p(\xi_0) - \lambda_0)\hat{\phi}(\xi_0) = 0$. With ϕ being a Gaussian function centered at x_0, with $|x_0| \geq k^2 \gg R$, and $T = T_0$ for $|x| \geq R$ we obtain $\|(T - T_0)\phi\|_{L^2} \to 0$ as $k \to \infty$. Hence, it follows

$$\|(T - \lambda_0)\phi\|_{L^2} \leq \|(T - T_0)\phi\|_{L^2} + \|(T_0 - \lambda_0)\phi\|_{L^2} \to 0,$$

for $k \to \infty$. □

Since $\sigma_p(T_\pm) \subset \sigma_{\mathrm{app}}(A + C)$, the spectrum of $A + C$, except for some potentially existing eigenvalues of $A + C$, can be studied by calculating the eigenvalues of the limit operators $T_\pm$.

Let us assume, for simplicity, that $n(0) = n(1)$, $J(0) = J(1)$, $ni(0) = ni(1)$ and $V'(0) = V'(1) = 0$, which simplifies the forthcoming calculations and is also physically reasonable. At the boundary, i.e. the contact points of the device, we expect no charging of the diode, the current is identical at both ends of the device and the temperature should be equal at both ends, especially constant over time, such that there is no heating. Hence, the electric potential should be constant near the boundary. Furthermore, we assume that n, J, ni and V remain constant for $x < 0$ and $x > 1$, and especially are equal to the corresponding boundary values for $x = 0$ and $x = 1$. This assumption is reasonable, since we do not expect any changes outside of the device.

Then, we have to analyze the spectrum of the matrix

$$\tilde{\Lambda}_\xi = \begin{pmatrix} -\nu\xi^2 & -\mathrm{i}\xi & 0 & 0 \\ \mathrm{i}\xi\left(\frac{J^2}{n^2} - \mu\right) + \frac{n}{i\lambda^2\xi} & -\nu\xi^2 - 2\mathrm{i}\xi\frac{J}{n} - \frac{1}{\tau} & -2\mathrm{i}\xi & n \\ \mathrm{i}\xi\frac{J}{n}\left(3\frac{ni}{n} + \mu\right) + \frac{1}{\tau} & -\mathrm{i}\xi\left(3\frac{ni}{n} + \mu\right) & -\nu\xi^2 - \mathrm{i}\xi\frac{J}{n} - \frac{2}{\tau} & 0 \\ 0 & 0 & 0 & 0 \end{pmatrix}, \tag{3.3.11}$$

which is the pseudodifferential symbol of the limit operators T_- and T_+. Note, that $\det(\tilde{\Lambda}_\xi - \lambda\mathbf{1}_4) = -\lambda\det(\Lambda_\xi - \lambda\mathbf{1}_3)$, whereby Λ_ξ is the upper left 3×3 matrix of $\tilde{\Lambda}_\xi$. Thus, we only study the spectrum of Λ_ξ in the following.

Our first result concerns the behavior of the spectrum of Λ_ξ for large $|\xi|$.

Lemma 3.3.3. *The spectrum of the matrix Λ_ξ asymptotically approaches the parabola $\gamma = -\nu\xi^2 + \mathcal{O}(|\xi|)$ for $|\xi| \to \infty$.*

Proof. Using Geršgorin's circle theorem, see [Ger31], we have the circles $B(a_{ii}, R_i)$, with middle point a_{ii} and radius R_i, given by

$$\begin{aligned} a_{11} &= -\nu\xi^2, \quad R_1 = |\xi|, \\ a_{22} &= -\nu\xi^2 - \frac{1}{\tau}, \quad R_2 = 2|\xi| + 2\left|\frac{n}{\xi\lambda^2} + \xi\left(\frac{J^2}{n^2} - \mu\right)\right|, \\ a_{33} &= -\nu\xi^2 - \frac{2}{\tau}, \quad R_3 = |\xi|\left(3\frac{ni}{n} + \mu\right) + \left|\frac{1}{\tau} + \xi\frac{J}{n}\left(3\frac{ni}{n} + \mu\right)\right|, \end{aligned}$$

such that the eigenvalues of Λ_ξ are inside these circles. For $|\xi| \to \infty$ we have $a_{ii} = -\nu\xi^2 + \mathcal{O}(1)$ and $R_i = |\xi| + \mathcal{O}(1)$, since $|\xi|^{-1} \to 0$. Thus, the eigenvalues are enclosed by the parabola $\gamma = -\nu\xi^2 + \mathcal{O}(|\xi|)$, for $|\xi| \to \infty$. □

The complete description of $\sigma(\Lambda_\xi)$ is rather complicated, although the roots of the characteristic polynomial are given by the formula for the roots of a third order polynomial. Therefore, let us study the complex function

$$G(\gamma,\xi) = \gamma^3 + A_2\gamma^2 + A_1\gamma + A_0 = 0, \tag{3.3.12}$$

with the coefficients given by

$$A_2 = 3\left(\nu\xi^2 + \mathrm{i}\xi\frac{J}{n} + \frac{1}{\tau}\right), \tag{3.3.13}$$

$$A_1 = 3\nu^2\xi^4 + 3\left[2\frac{\nu}{\tau} - \frac{J^2}{n^2} + 2\frac{ni}{n} + \mu\right]\xi^2 + \frac{2}{\tau^2} + \frac{n}{\lambda^2} + \mathrm{i}\left[6\nu\xi^3\frac{J}{n} + \frac{5}{\tau}\frac{J}{n}\xi\right], \tag{3.3.14}$$

$$\begin{aligned} A_0 = {} & \nu^3\xi^6 + 3\nu\left[\frac{\nu}{\tau} - \frac{J^2}{n^2} + 2\frac{ni}{n} + \mu\right]\xi^4 + \left[2\frac{\nu}{\tau^2} + \frac{\nu n}{\lambda^2} - \frac{2}{\tau}\left(\frac{J^2}{n^2} - \mu\right) + \frac{2}{\tau}\right]\xi^2 \\ & + \frac{2n}{\tau\lambda^2} + \mathrm{i}\left[3\nu^2\xi^5\frac{J}{n} + \left(5\frac{\nu}{\tau}\frac{J}{n} - \frac{J}{n}\left(\frac{J^2}{n^2} - \mu\right) + 2\frac{J}{n}\left(3\frac{ni}{n} + \mu\right)\right)\xi^3 + \xi\frac{J}{\lambda^2}\right]. \end{aligned} \tag{3.3.15}$$

Note, that n, J, and ni are constant, as we consider only the limit operator for either $x \to -\infty$ or $x \to \infty$, that is $n = n(0) = n(1)$, $J = J(0) = J(1)$ and $ni = ni(0) = ni(1)$, by our assumptions. We observe the following.

Lemma 3.3.4. *Let $\gamma_1(\xi) = \gamma_{1,R}(\xi) + \mathrm{i}\gamma_{1,I}(\xi)$ be a solution of $G(\gamma,\xi) = 0$, with $\gamma_{1,R} =$ $\mathrm{Re}(\gamma_1)$ and $\gamma_{1,I} = \mathrm{Im}(\gamma_1)$. Then $\gamma_2(\xi) = \gamma_{1,R}(-\xi) - \mathrm{i}\gamma_{1,I}(-\xi)$ is another solution to $G(\gamma,\xi) = 0$.*

Proof. Let γ_1 be a solution to $G(\gamma,\xi) = 0$ for all $\xi \in \mathbb{R}$, as stated above. Then, for $\xi \in \mathbb{R}$, $\gamma_1(-\xi)$ is a solution to $G(\gamma,-\xi) = 0$. Additionally, we have

$$A_j(-\xi) = \overline{A_j(\xi)}.$$

Define $\gamma_2(\xi) = \gamma_{1,R}(-\xi) - \mathrm{i}\gamma_{1,I}(-\xi)$. It follows

$$\begin{aligned} \overline{G(\gamma_2,\xi)} &= \overline{\gamma_2(\xi)}^3 + \overline{A_2(\xi)}\,\overline{\gamma_2(\xi)}^2 + \overline{A_1(\xi)}\,\overline{\gamma_2(\xi)} + \overline{A_0(\xi)} \\ &= \gamma_1(-\xi)^3 + A_2(-\xi)\gamma_1(-\xi)^2 + A_1(-\xi)\gamma_1(-\xi) + A_0(-\xi) \\ &= G(\gamma_1,-\xi) = 0, \end{aligned}$$

since $\overline{\gamma_2(\xi)} = \gamma_{1,R}(-\xi) + \mathrm{i}\gamma_{1,I}(-\xi) = \gamma_1(-\xi)$. □

Due to the previous lemma, there are three solutions of $G(\gamma,\xi) = 0$, γ_0, γ_1 and γ_2, such that γ_0 is symmetrical w.r.t. the real line and γ_2 is identical to γ_1 mirrored at the real line.

In fig. 3.1, we present the real parts of these three curves for $n = 1$, $J = 0$ and $ni = T_0/2$, with the inital temperature $T_0 = 1.00585$. Furthermore, we use the following values for the scaled constants $\nu = 9.935 \cdot 10^{-4}$, $\mu = 1.014 \cdot 10^{-2}$, $\tau = 0.5654$ and $\lambda^2 = 3.032 \cdot 10^{-4}$, which were also used in [JT06]. The question arises, whether there are values for the

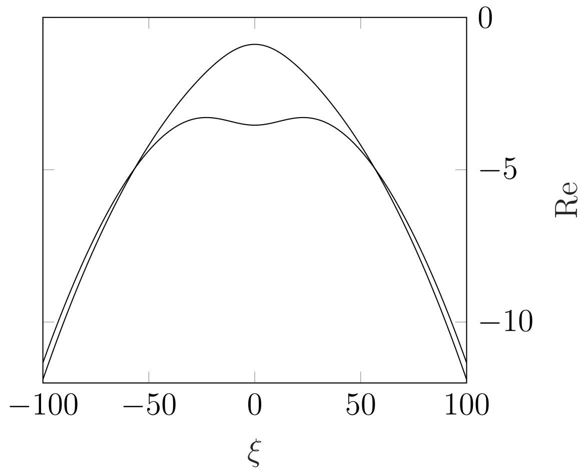

Figure 3.1: The approximate spectrum of the linearized full viscous quantum hydrodynamic system for $n = 1$, $J = 0$ and $ni = T_0/2$ with initial temperature $T_0 = 1.00585$.

density n, current density J and internal energy density ni, such that the eigenvalues of the limit operators $T_\pm$ have positive real part. In such a case, the linearized system would be unstable. However, the curves γ_0 and γ_1 are some algebraic functions depending on ξ, n, J and ni and any further analytical investigation would require unreasonable effort. Applying a generalized Routh-Hurwitz criterion, see [HM23], results in extensive polynomials and it remains to analyze, whether these become negative for some values of ξ, n, J and ni.

Instead, we give examples for the values of n, J and ni, such that we observe eigenvalues with positive real part, see fig. 3.2. In comparison to numerical solutions of the isothermal and full viscous quantum hydrodynamic system, where the density is usually $n = 1$ and the temperature of the contact points remains constant, i.e. $ni = T_0/2$, we vary the current density and observe significant changes of the eigenvalues of $T_\pm$. These changes occur for current densities $J > 6$, which is a much larger value for the current density compared to numerical results, where this values is around 0-0.02. Furthermore, we observe, that decreasing the density or the internal energy density increases the real part of the eigenvalues. In conclusion, stationary solutions of the full viscous quantum hydrodynamic system with barrier potential are unstable for large current densities. However, we did not cover the complete spectrum of the matrix differential operator, but a subset of its approximate spectrum, and there may exist eigenvalues those real part is positive for smaller values of the current density.

At this point we end the analytical study of the full viscous quantum hydrodynamic system and continue with our numerical approach.

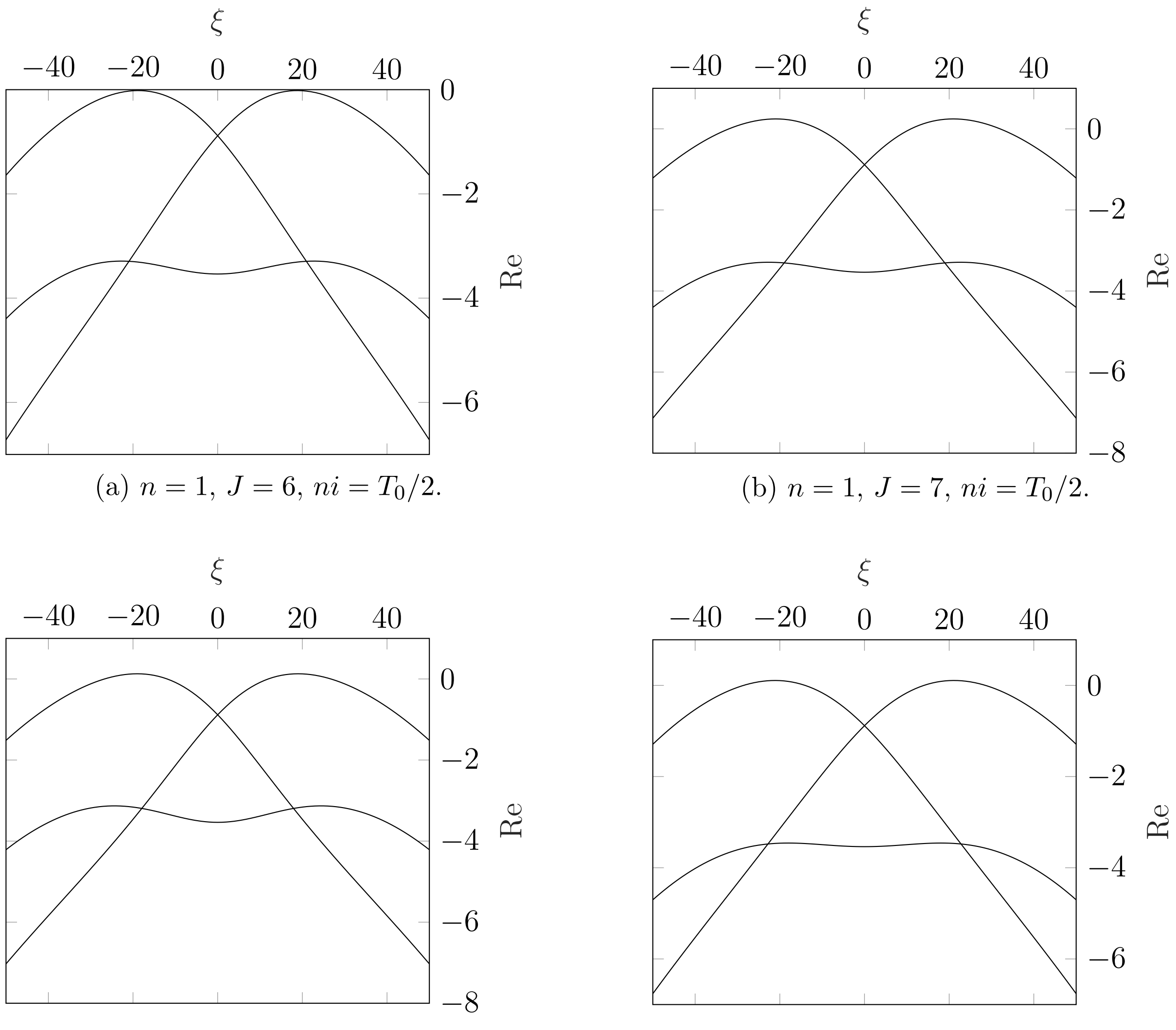

(a) $n = 1$, $J = 6$, $ni = T_0/2$.

(b) $n = 1$, $J = 7$, $ni = T_0/2$.

(c) $n = 0.9$, $J = 6$, $ni = T_0/2$.

(d) $n = 1$, $J = 6$, $ni = T_0/2 - 0.1$.

Figure 3.2: Real parts of the eigenvalues of the limit operators $T_\pm$ for different values of the density n, current density J and internal energy density ni.

Chapter 4

Simulation of a Resonant Tunneling Diode

In this chapter, we describe numerical schemes to solve problem (3.1.1). First, we describe spatial discretization and mention different approaches to handle a discrete spatial mesh in 4.1. Thereafter, we describe the continuation method in 4.2, which allows us to follow a solution curve, e.g. resulting from a root finding problem, from a given starting point. In 4.3, we give our algorithm to solve the time dependent viscous quantum hydrodynamic equations, using the continuation method, and present our results for the applied voltage of $0V$. This solution can be used to calculate subsequent solutions for different voltages via the continuation method. We solve the time independent system by tracking the solution curve from $0V$ up to 0.48V in 4.4. In order to validate our algorithm, we apply our method to the viscous quantum hydrodynamic model from [JT06].

4.1 Spatial discretization

There are several methods for the discretization of derivatives, e.g. forward, backward and central finite differences, with different error behavior and precision. We give a short introduction to the central finite difference scheme, that we will use later on.

Let $\Omega = [0, 1]$ be divided into N intervals $[x_i, x_{i+1}]$ with $x_i < x_{i+1}$ for $i = 0, \ldots, N-1$, where the spatial grid points x_i are not equidistributed in general. Additionally, the grid points may adopt to the problem dynamically, resulting in an adaptive grid. Then, the central finite difference schemes for the first and second order derivatives are given by

$$\Delta_x u = \frac{u_{i+1} - u_{i-1}}{x_{i+1} - x_{i-1}},$$
$$\Delta_x^2 u = \frac{\frac{u_{i+1}-u_i}{x_{i+1}-x_i} - \frac{u_i-u_{i-1}}{x_i-x_{i-1}}}{\frac{1}{2}(x_{i+1} - x_{i-1})},$$

and we replace the spatial derivatives with these approximations. This approach introduces no artificial damping compared to an upwind scheme but may lead to oscillations in the data. In [LTWZ09, Dor16], the error behavior of the central finite difference scheme is analyzed.

Depending on the underlying phenomenon, which the system of partial differential equations describe, one may have different unknown functions, describing different physical properties, like position, density, momentum or temperature. When discretizing the system of PDEs, one has to guarantee consistency of the resulting system of ODEs or algebraic equations. For example, the flux between adjacent cells of the discrete spatial grid should be consistent, such that no artifical sources or sinks are introduced. Hence, we approximate the current density in the viscous quantum hydrodynamic system at the mid points between two grid points. An introduction into numerics of hydrodynamic equations can be found in [Pat80], where also discretization methods, the numerical treatment of heat transfer, convection and diffusion are covered in depth.

Besides the consistent approximation of the unknown functions, one has to choose an appropriate grid, which allows computations in a reasonable time and also a sufficiently good approximation. For example, the error of the central finite difference approximation to the first order derivative is proportional to Δx^2 for equidistributed grid points, where Δx is the distance of adjacent grid points. Thus, increasing the number of grid points would increase the accuracy of our calculation. However, the computation becomes more expensive, especially if we have to solve a system of equations. Furthermore, we have to consider the efficiency of the grid point distribution. Regions, where the function is almost constant, need considerably less grid points compared to regions where the function admits steep slopes.

One possible approach to achieve an optimal grid point distribution is the equidistribution principle, such that each interval (x_i, x_{i+1}) admits the same error, as discussed in [FVZ90]. This idea can be stated as follows

$$(x_{i+1} - x_i)\omega_i = \text{const}, \tag{4.1.1}$$

where ω_i is a weightfunction evaluated at x_i. Although this approach allows to solve problems, where thin layers appear, it also introduces nonlinear algebraic differential equations, which are then coupled to the system of ordinary differential equations. This increases the overall computational costs compared to constant grid methods. Additionally, this algorithm is only applicable to continuous functions, since jump discontinuities always have a minimum jump height, indepent of the grid point position.

Another approach is the mesh refinement. In this case, one solves the problem on a coarse grid and improves this solution on a finer grid. For details we refer to [LW93], where also a time step control was implemented. The downside of this method is the necessary interpolation of the data for each new grid.

For further reading and several applications regarding spatial discretization we refer to [VBSS89, FVZ90, BLdP96].

After spatial discretization of the time dependet system, we obtain a system of nonlinear first order differential equations coupled to a system of algebraic equations, resulting from the discretization of the Laplace equation. This system has to be solved by numerical time integration, for example forward or backward Euler, Crank-Nicolson or Runge-Kutta method. Then, we obtain a system of equations, which can be stated as

$$F(t, x) = 0.$$

Note, that after spatial discretization using an equidistant grid of $N+1$ grid points, we actually have to solve a system of $4N+5$ equations in case of the viscous quantum hydrodynamic equations. We solve this root finding problem with the continuation method. In case of the time dependent system, we use some initial conditions and the time as free parameter. The stationary system is solved by tracking the solution curve starting from the solution for $0V$ applied voltage and the voltage is the free parameter. We describe this procedure, the continuation method, in the next section.

4.2 Continuation Method

Consider a root finding problem, given in the following form

$$F(x, \epsilon) = 0, \tag{4.2.1}$$

with the free parameter ϵ. Alternatively, we can include the free parameter ϵ and obtain an underdetermined set of equations $F(y) = 0$, with $y = (x, \epsilon)$. If we assume sufficient regularity of F, existence of atleast one solution y_0 with $F(y_0) = 0$ and that the Jacobian $DF(y_0) = (D_x F(y_0), D_\epsilon F(y_0))$ has maximum rank, then one can show existence of a curve Γ, such that there exist solutions y along this curve with $F(y) = 0$.

Given a starting point y_0, we have to calculate another point on the solution curve, which can be carried out by a predictor-corrector scheme. From a given point x_{j-1} on the curve we predict a new point, say x^P, and then approximate a point on the curve, named x_j, with a corrector process. For example, using a tangent predictor, the predictor point is given by

$$x^P = x_{j-1} + h \cdot x'_{j-1},$$

where x'_{j-1} is the tanget at the previously calculated solution x_{j-1}, normalized with $|x'_{j-1}| = 1$ and h is the stepsize, such that $\epsilon_j = \epsilon_{j-1} + h$. Then, a Newton corrector scheme is given by

$$x_j^{(k)} = x_j^{(k-1)} - \left[D_x F\left(x_j^{(k-1)}, \epsilon_j \right) \right]^{-1} F(x_j^{(k-1)}, \epsilon_j), \quad k \geq 1,$$

with $x_j^{(0)} = x^P$. As long as $D_x F\left(x_j^{(k-1)}, \epsilon_j \right)$ is regular, this algorithm calculates subsequent points on the curve. However, there are several scenarios, such that the Jacobian of F becomes singular, for example at turning points or crossings of at least two solution branches. Especially in case of turning points, it is apparent that this algorithm will likely fail, since the stepsize has to decrease, approaching 0, when the previous point is close to such a turning point, see fig. 4.1. This issue can be resolved by using the arclength of

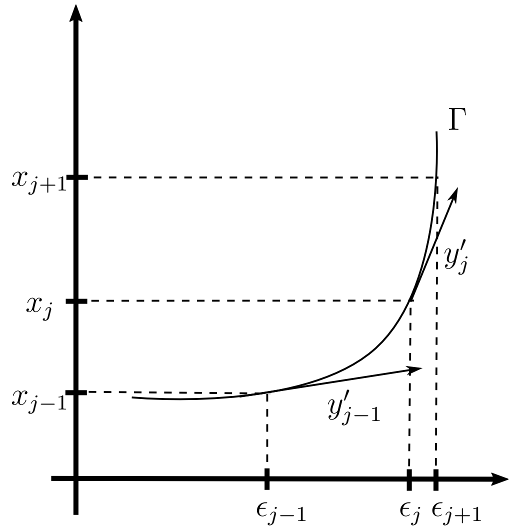

Figure 4.1: Subsequent approximtion of points on the solution curve Γ using the natural parametrization by ϵ and tangent predictor with length $|y'_{j-1}| = 1$.

the curve as parametrization, that is $x = x(s)$ and $\epsilon = \epsilon(s)$ or $y = y(s)$, with arclength s. Furthermore, one approximates the next point on the curve by approching the curve on a plane in the predictor point, perpendicular to the tangent vector of the previous point, see fig. 4.2. This introduces an additional equation and one has to solve the system

$$\begin{pmatrix} F(y(s_j)) \\ (y(s_j) - y(s_{j-1})) \cdot y'(s_{j-1}) - h \end{pmatrix} = 0, \tag{4.2.2}$$

for $y(s_j)$. This can be done with the tangent predictor $y^P = y_{j-1} + h_{j-1}y'_{j-1}$ and the Newton corrector given by

$$y_j^{(k)} = y_j^{(k-1)} - A^{-1}\left(F\left(y_j^{(k-1)}\right)^T, (y_j^{(k-1)} - y_{j-1})) \cdot y'_{j-1} - h\right)^T, \quad k \geq 1,$$

with $y_j^0 = y^P$ and $A = \left[DF\left(y_j^{(k-1)}\right)^T, y'^T_{j-1}\right]^T$. The tangent vector y'_{j-1} is calculated by QR decomposition of the transposed Jacobian, $DF(y_{j-1})^T$, and taking the last column of the resulting Q-matrix as tangent vector, which is then normalized, such that $|y'_{j-1}| = 1$. In order to preserve orientation we compare the current tangent vector with the previous one by calculation of their scalar product. If this product is negative we invert the direction of the current tangent vector. Our approach requires the calculation of the Jacobian DF. For further reading about predictor-corrector methods, continuation methods, numerics of systems of equations and especially numerics of differential equations we refer to [Gov00, AG03].

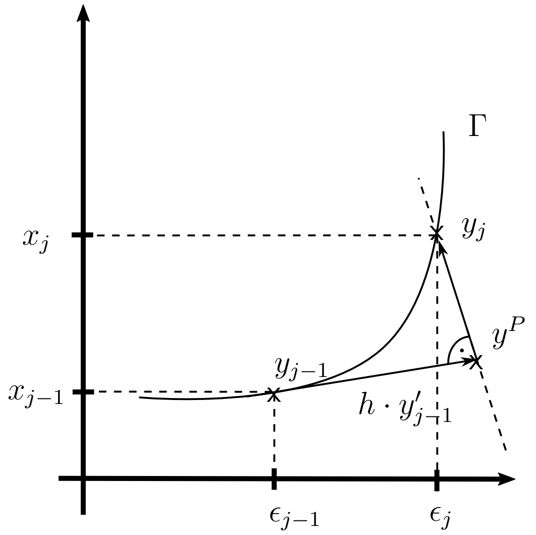

Figure 4.2: Subsequent approximation of points on the solution curve Γ using the arclength parametrization and tangent predictor with length $|y'_{j-1}| = 1$.

So far we explained our methods to solve the time dependent viscous quantum hydrodynamic system and the static system. During the following sections we present the implementation of these algorithms and some results. The complete Matlab code is given in the appendix B.

4.3 The time dependent system

In this section, we present our algorithm to solve the time dependent viscous quantum hydrodynamic system with central finite differences, backward Euler method and continuation method. Furthermore, we give results concerning different parameter values.

We choose an equidistant grid with $N+1$ grid points, with $x_0 = 0$, $x_N = 1$ and $h = x_{i+1} - x_i = 1/N$. The functions n, ni and V are approximated at the grid points x_i, while the current density J is approximated at the points $x_{i-\frac{1}{2}}$ with $J_{i-\frac{1}{2}} = (J_i + J_{i-1})/2$. The discretized system is given by

$$F_{1,i} = \frac{\nu}{h^2}(n_{i+1} - 2n_i + n_{i-1}) - \frac{1}{h}(J_{i+\frac{1}{2}} - J_{i-\frac{1}{2}}), \tag{4.3.1}$$

$$\begin{aligned} F_{2,i-\frac{1}{2}} = {} & \frac{\nu}{h^2}(J_{i+\frac{1}{2}} - 2J_{i-\frac{1}{2}} + J_{i-\frac{3}{2}}) - \frac{1}{4h}\left(\frac{(J_{i+\frac{1}{2}} + J_{i-\frac{1}{2}})^2}{n_i} - \frac{(J_{i-\frac{1}{2}} + J_{i-\frac{3}{2}})^2}{n_{i-1}}\right) \\ & - \frac{2}{h}(ni_i - ni_{i-1}) - \frac{\mu}{h}(n_i - n_{i-1}) - \frac{J_{i-\frac{1}{2}}}{\tau} \\ & + \frac{n_i + n_{i-1}}{2h}(V_i - V_{i-1} + V_{B,i} - V_{B,i-1}), \end{aligned} \tag{4.3.2}$$

$$\begin{aligned} F_{3,i} = {} & \frac{\nu}{h^2}(ni_{i+1} - 2ni_i + ni_{i-1}) \\ & - \frac{1}{4h}\left(\frac{(J_{i+\frac{3}{2}} + J_{i+\frac{1}{2}})ni_{i+1}}{n_{i+1}} - \frac{(J_{i-\frac{1}{2}} + J_{i-\frac{3}{2}})ni_{i-1}}{n_{i-1}}\right) \\ & + \frac{\nu}{16h^2}n_i\left(\frac{J_{i+\frac{3}{2}} + J_{i+\frac{1}{2}}}{n_{i+1}} - \frac{J_{i-\frac{1}{2}} + J_{i-\frac{3}{2}}}{n_{i-1}}\right)^2 \\ & - \frac{1}{4h}\left(\frac{J_{i+\frac{3}{2}} + J_{i+\frac{1}{2}}}{n_{i+1}} - \frac{J_{i-\frac{1}{2}} - J_{i-\frac{3}{2}}}{n_{i-1}}\right)(2ni_i + \mu n_i) - \frac{2}{\tau}ni_i - \frac{1}{\tau}n_i, \end{aligned} \tag{4.3.3}$$

for $i = 1, \ldots, N-1$. In the same way we discretize the Poisson equation and obtain

$$\lambda^2 \frac{V_{i+1} - 2V_i + V_{i-1}}{h^2} = n_i - C_i, \quad i = 1, \ldots, N-1. \tag{4.3.4}$$

Furthermore, we use the following boundary conditions

$$\left.\begin{aligned} n_1 - n_0 = 0, &\quad n_N - n_{N-1} = 0, \\ J_{-\frac{1}{2}} - J_{\frac{1}{2}} = 0, &\quad J_{N+\frac{1}{2}} - J_{N-\frac{1}{2}} = 0, \\ ni_1 - ni_0 = 0, &\quad ni_N - ni_{N-1} = 0, \\ V_0 = 0, &\quad V_N = U_0, \\ x_0 = 0, &\quad x_N = 1. \end{aligned}\right\} \tag{4.3.5}$$

The barrier potential and doping profile are approximated by the logistic function

$$f(x) = \frac{b-a}{2}(1 + \tanh(r(x - x_0))) + a, \tag{4.3.6}$$

where x_0 is the position of the jump discontinuity and r determines the slope of the approximation. If $a < b$, then f is monotone increasing with upper bound a and lower bound b. Then, the barrier potential and doping profile are given by

$$V_B(x) = \frac{\overline{V}_B}{2}(\tanh(r(x - 0.44)) - \tanh(r(x - 0.48)) \tag{4.3.7}$$

$$+ \tanh(r(x - 0.52)) - \tanh(r(x - 0.56))), \tag{4.3.8}$$

$$C(x) = 1 + \frac{1 - C_0}{2}\left(-\tanh(r(x - 0.4)) + \tanh(r(x - 0.6))\right), \tag{4.3.9}$$

with the barrier height $\overline{V}_B = -31.2435$, or equivalently without scaling $\overline{V} = -0.209\mathrm{V}$, and minimum doping $C_0 = 5 \cdot 10^{-3}$.

After the spatial discretization, we combine (4.3.1) to (4.3.3) and (4.3.4) with the boundary conditions (4.3.5) to obtain a system of time dependent DAEs. Applying the backward Euler method we have to solve a nonlinear system of equations, which can be stated as

$$u^{n+1} - u^n - (t_{n+1} - t_n)F\left(u^{n+1}\right) = 0,$$

$$B\left(u^{n+1}\right) = 0,$$
$$L\left(u^{n+1}\right) = 0,$$

with $u = (n, J, ni, V)$, where we omitted the lower index from spatial discretization, u^j is the approximation to $u(t)$ at $t = t_j$, B describes the boundary equations and L the Laplace equation. This problem can equivalently be stated as $H(u,t) = 0$, which we solve by the previously explained continuation method. The complete Matlab code is given in the app. B. The Jacobian matrix is given in the app. D. Let us briefly describe the algorithm:

1. Use the doping profile as initial electron density, set the current density to zero, internal energy density to half the initial temperature, $T_0/2$, multiplied by the electron density and the electric potential to zero, or use some given initial conditions.

2. Calculate the QR decomposition of the transposed Jacobian of $H(u, 0)$ w.r.t. u using the initial data.

3. Set the tangent vector to the last column of the resulting Q matrix. This includes a prediction of the next timestamp.

4. As long as no error occurs or a condition for termination is met, repeatedly calculate the tangent predictor with the current tangent and the current timestep size, and run the corrector loop for each predictor. The corrector loop calculates the Jacobian of $H(u,t)$ w.r.t. u using the predictor and solves the system (4.2.2), with the current predictor and tangent vector.

5. After each corrector loop, the timestep size is adjusted according to the performance of the corrector loop and a new tangent vector is calculated.

Using the initial conditions $n = C(x)$, $J = 0$, $ni = nT_0/2$, with initial temperature $T_0 = 1.00585$, and $V = 0$, we observe steep slopes around the regions, where the barrier potential and doping profile admit steep slopes. This results in a decrese of the time stepsize until the algorithm stops. Increasing the number of grid points does not solve this problem and we have to use a different set of initial conditions, see fig. 4.3 and 4.4. Setting the barrier potential height to 0 and using the same initial conditions as before, we obtain the results shown in fig. 4.5, with maximum time 100, which is approximately 92 ps and hence enough time to achieve static equilibirum. Then, we used this solution and subsequently increased the barrier potential height to $\overline{V}_B/10$, $\overline{V}_B/5$, $\overline{V}_B/2$ up to the full height $\overline{V}_B = -31.2435$. However, we had to increase the number of grid points from 500 to 1000, when we used $\overline{V}_B/2$ and $\overline{V}_B$ as barrier height. The result for the full barrier potential is shown in fig. 4.6. We observe a drastic change in the electron density, internal energy density and electric potential. The electron density develops two minima in the valleys of the barrier potential and the overall charge in the valley of the doping

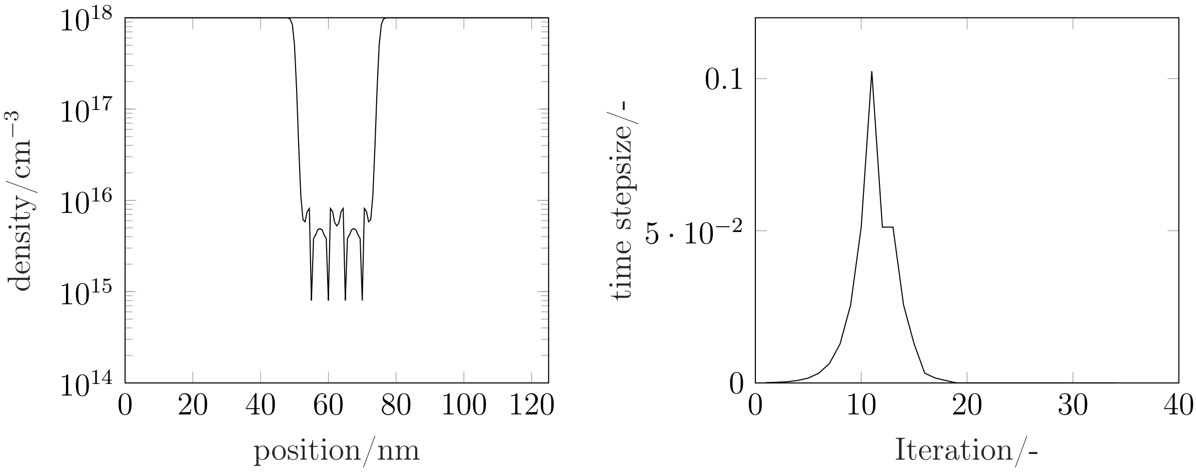

Figure 4.3: Numerical solution to the full viscous quantum hydrodynamic system with 200 grid points.

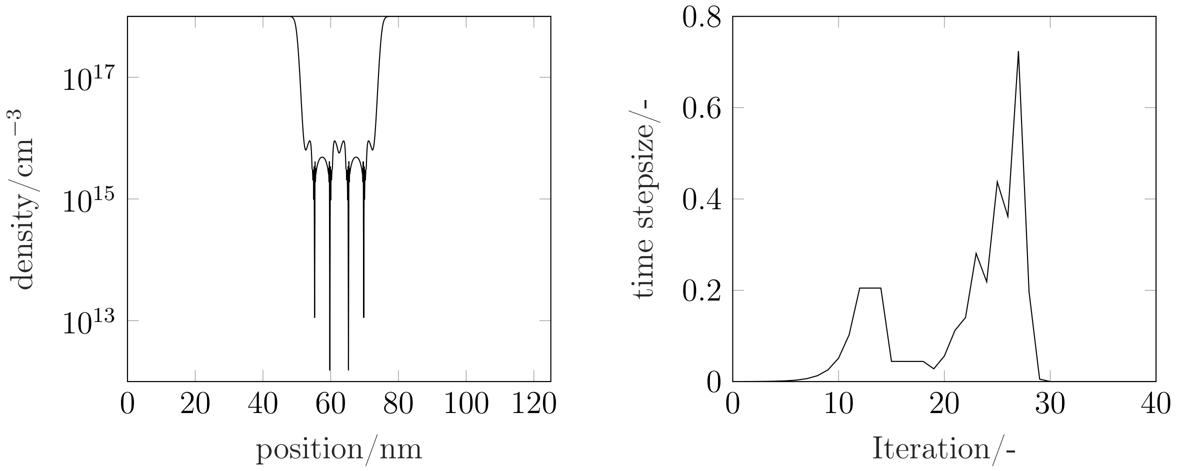

Figure 4.4: Numerical solution to the full viscous quantum hydrodynamic system with 1000 grid points.

profile increases. Corresponding to the density, the temperature, hence the internal energy density, increases before and after the barrier. Lastly, due to the charge build up inside the valley of the doping profile, before and after the potential barriers, we observe an increased electric potential. In fig. 4.7, we present the doping profile, electron density and barrier potential in the same figure.

We conclude, that appropriate initial conditions are crucial in order to obtain any meaningfull data with our numerical scheme. If such data is used, the system approaches a steady state over time. The results in this section are similar to other results but show some difference, especially in the region of the barrier potential. There, the electron density is not as smooth as in [DS16].

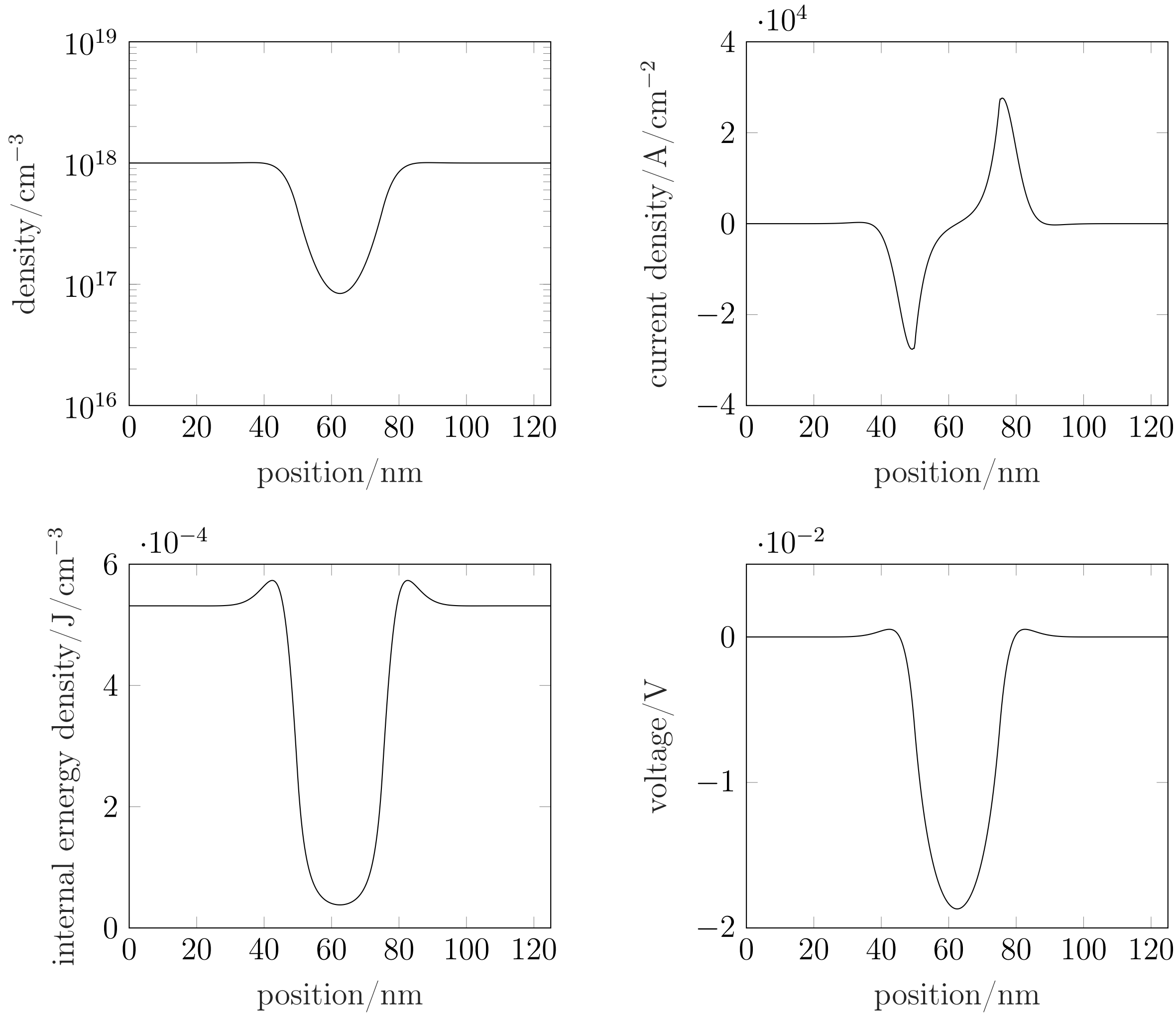

Figure 4.5: Numerical solution to the full viscous quantum hydrodynamic system with 500 grid points and no barrier potential.

4.4 Current-voltage characterstics

Here, we present our implementation of the continuation method for the stationary system. Additionally, we present the current-voltage characteristic of the modeled resonant tunneling diode. The complete MATLAB code is given in app. B and in app. C we present our results with our method applied to the isothermal model used in [JT06].

Note, that in the stationary case the system of equations after discretization has the form $H(u, U_0)$, with the applied voltage U_0 as free parameter. Hence, our algorithm described in 4.3 now increments the voltage. Starting from the solution for 0V, the tangent predictor predicts the next value for the applied voltage and the corrector loop approximates a solution for the stationary system. Since we require the continuity of the solution curve, defined by $H(u, U_0)$, our algorithm follows the solution curve through unstable branches and does not jump from one stable branch to the next one.

We use the same setting as before and set $\partial_t(n, J, ni, V) = 0$. After spatial discretiza-

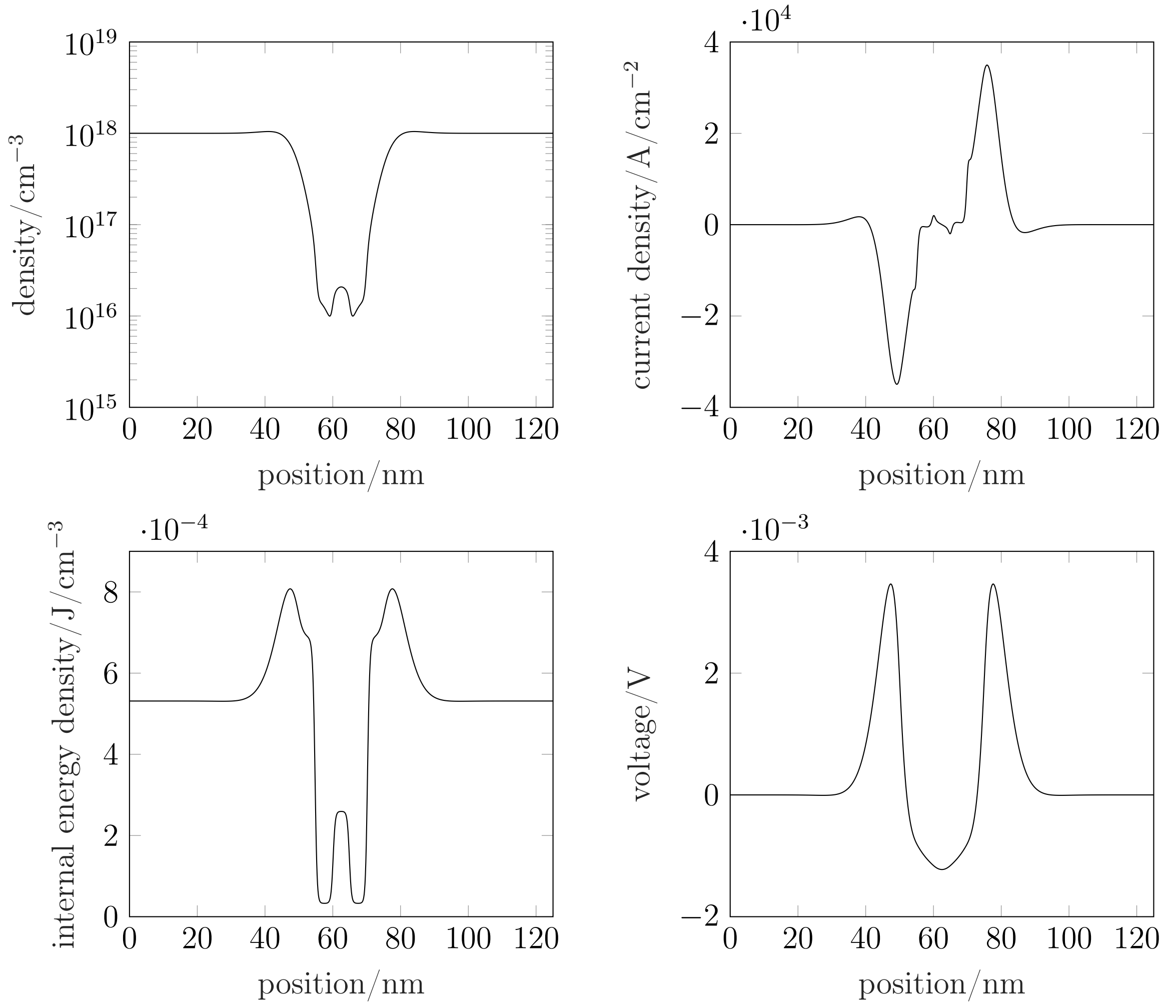

Figure 4.6: Numerical solution to the full viscous quantum hydrodynamic system with 1000 grid points and full barrier potential. The initial conditions were calculated with a smaller barrier potential.

tion, we obtain

$$F_{1,i} = \frac{\nu}{h^2}(n_{i+1} - 2n_i + n_{i-1}) - \frac{1}{h}(J_{i+\frac{1}{2}} - J_{i-\frac{1}{2}}), \tag{4.4.1}$$

$$\begin{aligned} F_{2,i-\frac{1}{2}} = {} & \frac{\nu}{h^2}(J_{i+\frac{1}{2}} - 2J_{i-\frac{1}{2}} + J_{i-\frac{3}{2}}) - \frac{1}{4h}\left(\frac{(J_{i+\frac{1}{2}} + J_{i-\frac{1}{2}})^2}{n_i} - \frac{(J_{i-\frac{1}{2}} + J_{i-\frac{3}{2}})^2}{n_{i-1}}\right) \\ & - \frac{2}{h}(ni_i - ni_{i-1}) - \frac{\mu}{h}(n_i - n_{i-1}) - \frac{J_{i-\frac{1}{2}}}{\tau} \\ & + \frac{n_i + n_{i-1}}{2h}(V_i - V_{i-1} + V_{B,i} - V_{B,i-1}), \end{aligned} \tag{4.4.2}$$

$$\begin{aligned} F_{3,i} = {} & \frac{\nu}{h^2}(ni_{i+1} - 2ni_i + ni_{i-1}) + \frac{\nu}{16h^2}n_i\left(\frac{J_{i+\frac{3}{2}} + J_{i+\frac{1}{2}}}{n_{i+1}} - \frac{J_{i-\frac{1}{2}} + J_{i-\frac{3}{2}}}{n_{i-1}}\right)^2 \\ & - \frac{1}{4h}\left(\frac{(J_{i+\frac{3}{2}} + J_{i+\frac{1}{2}})ni_{i+1}}{n_{i+1}} - \frac{(J_{i-\frac{1}{2}} + J_{i-\frac{3}{2}})ni_{i-1}}{n_{i-1}}\right) \\ & - \frac{1}{4h}\left(\frac{J_{i+\frac{3}{2}} + J_{i+\frac{1}{2}}}{n_{i+1}} - \frac{J_{i-\frac{1}{2}} - J_{i-\frac{3}{2}}}{n_{i-1}}\right)(2ni_i + \mu n_i) - \frac{2}{\tau}ni_i - \frac{1}{\tau}n_i, \end{aligned} \tag{4.4.3}$$

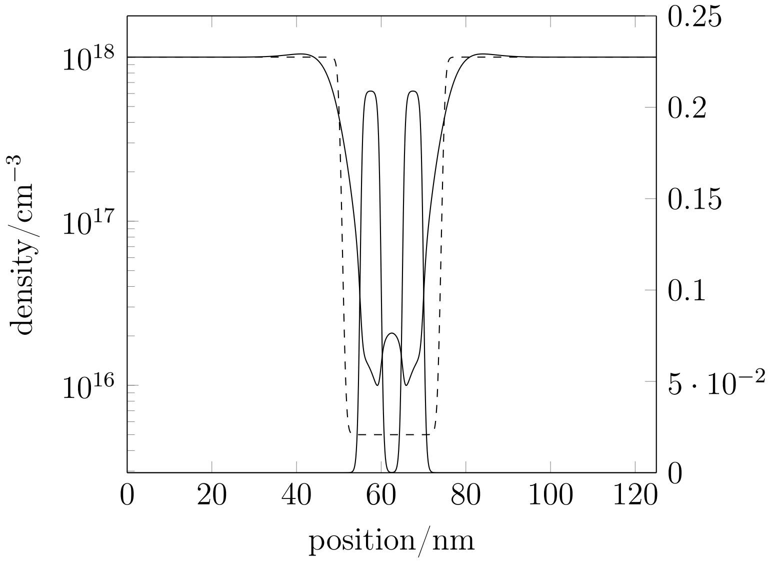

Figure 4.7: Doping profile, electron density and barrier potential, mirrored at the x-axis, of the full viscous quantum hydrodynamic system with 1000 grid points.

for $i = 1, \ldots, N-1$. The Poisson equation is discretized as before. Since the corresponding Jacobian matrix is rather extensive, we give its entries in the app. D. The boundary conditions are given by

$$\left.\begin{aligned} n_1 - n_0 &= 0, \quad & n_N - n_{N-1} &= 0, \\ J_{-\frac{1}{2}} - J_{\frac{1}{2}} &= 0, \quad & J_{N+\frac{1}{2}} - J_{N-\frac{1}{2}} &= 0, \\ ni_1 - ni_0 &= 0, \quad & ni_N - ni_{N-1} &= 0, \\ V_0 &= 0, \quad & V_N &= U_0. \end{aligned}\right\} \tag{4.4.4}$$

The doping profile and barrier potential are approximated by the logistic function again.

In order to obtain the initial solution (n_0, J_0, ni_0, V_0), we use the the results from the time dependent system and interpolate, if the grid sizes are different. Alternatively, one can use the damped Newton algorithm with two different damping constants, namely 0.01 and 0.1. These values are chosen after some tests with different slope constants and number of grid points. Due to numerical instability, one has to calculate the initial solution for the applied voltage 0V for the doping profile with minimum scaled density of 0.1. Then, one calculates the initial solution with this one as initial guess for the minimum scaled density of 0.005.

In fig. 4.8, we present the electron density of the static viscous quantum hydrodynamic system for the applied voltage $V = 0.48$V, after continuation of the solution for 0V, obtained from the time dependen system for 1000 grid points. We observe two important features. First, the density developes a rather steep slope before the left side of the barrier, with additional oscillations. We expect, that these oscillations are due to numerical discretization and not a physical feature. Second, the density decreases drastically to the right of the barrier. From a physical point of view, a decrease in density, hence particle number, results from the difference of the source and sink for the electrons, where the sink dominates. Note, that the total charge, $\int_0^1 (n(x) - C(x))\mathrm{d}x$, is approximately $6.87 \cdot 10^{13}$. In fig. 4.9, we present the current voltage characteristics of the simulated

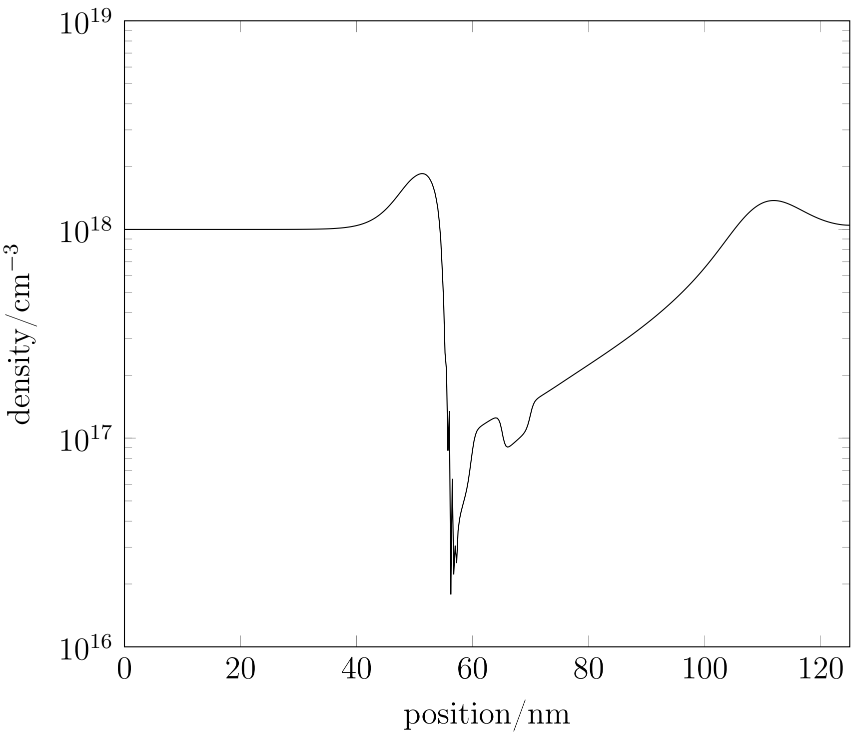

Figure 4.8: Electron density of the static viscous quantum hydrodynamic system for the applied voltage $V = 0.48$V with 500 grid points.

resonant tunneling diode. We observe, that the current increases with increasing voltage almost everywhere but a small region between 0.33V and 0.35V. In this region, the current voltage curve undergoes an "S" shaped curve, indicating hysteresis effect. However, repeating the calculation with 1000 grid points does not reproduce the same current voltage curve. Instead, the same behavior can be observed for higher voltages, e.g. between 0.4V and 0.54V. Hence, this is a numerical error.

In conclusion, the full viscous quantum hydrodynamic system with barrier potential in one space dimension, used in this work, may not be suited to model resonant tunneling diodes for larger values of the applied voltage, i.e. > 0.3V.

Note, that different coefficients were used in [JM07], albeit the equations are very similar. More precisely, in [JM07] the energy density is given by

$$ne = \frac{|J|^2}{2n} + \frac{3}{2}nT - \frac{\epsilon^2}{24}n\Delta \ln n,$$

hence the internal energy density would be

$$ni = \frac{3}{2}nT - \frac{\epsilon^2}{24}n\Delta \ln n$$

and we use the internal energy density

$$ni = \frac{d}{2}nT - \frac{\epsilon^2}{8}n\Delta \ln n,$$

with $d = 1$ in one space dimension.

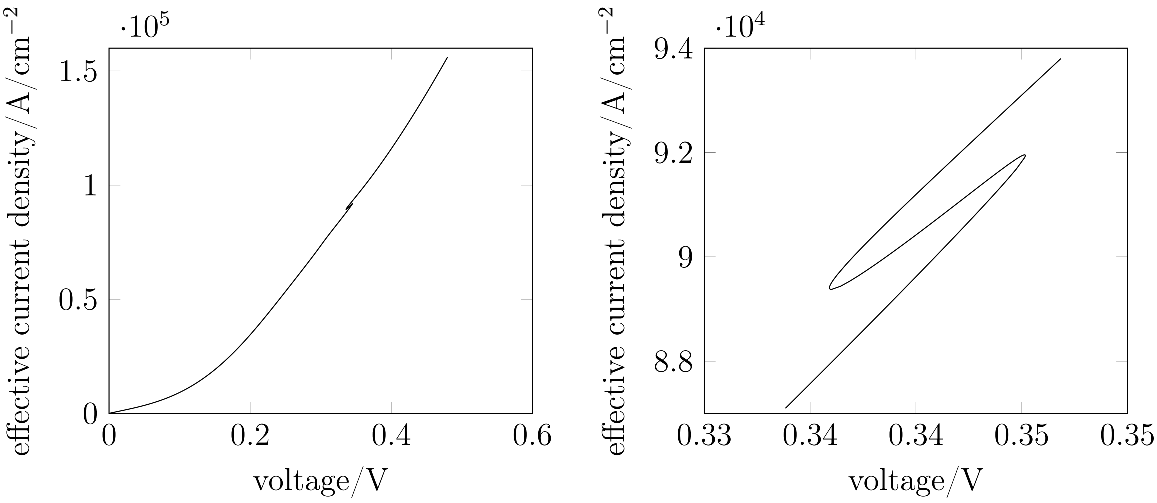

Figure 4.9: Current voltage characteristics of the simulated resonant tunneling diode with maximum voltage $V = 0.48$V for 500 grid points. The figure on the right side shows an area between 0.33V and 0.35V of the left plot.

Chapter 5

Summary

Let us recapitulate the results of this work and give some outlook for further investigations. In chapter 3, we showed that the principal part of the differential operator in the one dimensional full viscous quantum hydrodynamic system generates an analytic semigroup. However, due to the Neumann boundary conditions, we have to take care of 0 being an element of the spectrum of the principal part. An alternative approach is the use of lower order derivatives, including all linear terms and then show that the resulting operator generates an analytic semigroup. In [CD11], the authors studied the isothermal viscous quantum hydrodynamic system, where they have proven, that the principal part of the differential operator with some additional linear terms generates an analytic semigroup.

Furthermore, using the Picard-Lindelöf iteration, we showed existence of a solution for rather arbitrary initial conditions, and observed smoothing properties of the analytic semigroup. Due to the weak requirements on the initial conditions, existence can only be guaranteed for a sufficiently small time interval. The study of admissible initial conditions for the full viscous quantum hydrodynamic system is crucial for analytic proofs and numerical calculations.

We completed ch. 3 with the linearization of the full viscous quantum hydrodynamic system at a steady state, those existence we assumed at this point, and studied its stability. Considering the limit operator at the boundary, the linearized system becomes unstable for large current densities, being larger several orders of magnitude compared to the currents in numerical simulations.

The second part of this work, ch. 4, covered the numerical solution of the full viscous quantum hydrodynamic system. We applied the continuation method with a predictor-corrector scheme to the isothermal and nonisothermal viscous quantum hydrodynamic system. The current-voltage characteristic of the isothermal system shows qualitatively the same behaviour as in [JT06]. As mentioned before, using reasonable initial conditions can be a delicate task and we had to approximate our initial conditions after several iterations, starting from a hydrodynamic system without barrier potential. Also, the current-voltage characteristic of the nonisothermal showed unphysical hysteresis effects, that were altered by the grid resolution. As was also observed in [JM07], the current-voltage characteristic developed no local maxima and jumps afterwards, when neglecting the unphysical hysteresis.

Bibliography

[A$^+$19] Frank Arute et al. Quantum supremacy using a programmable superconducting processor. *Nature*, 574:505–510, 10 2019.

[AAR99] George E. Andrews, Richard Askey, and Ranjan Roy. *Special Functions*. Encyclopedia of Mathematics and its Applications. Cambridge University Press, 1999.

[AF03] Robert A. Adams and John J. F. Fournier. *Sobolev Spaces*. London: Academic Press, 2003.

[AG03] Eugene L. Allgower and Kurt Georg. *Introduction to Numerical Continuation Methods*. Society for Industrial and Applied Mathematics, 2003.

[AH96] David R. Adams and Lars I. Hedberg. *Function Spaces and Potential Theory*. Springer-Verlag Berlin Heidelberg, 1996.

[Ama95] Herbert Amann. *Linear and Quasilinear Parabolic Problems, Vol. I: Abstract Linear Theory*. Birkhäuser, Basel, 1995.

[AS16] Masahiro Asada and Safumi Suzuki. Room-temperature oscillation of resonant tunneling diodes close to 2 thz and their functions for various applications. *Journal of Infrared, Millimeter, and Terahertz Waves*, 37, 12 2016.

[BGK54] P. L. Bhatnagar, E. P. Gross, and M. Krook. A Model for Collision Processes in Gases. I. Small Amplitude Processes in Charged and Neutral One-Component Systems. *Phys. Rev.*, 94:511–525, May 1954.

[BLdP96] Pavel Bochev, Guojun Liao, and Gary dela Pena. Analysis and computation of adaptive moving grids by deformation. *Numerical Methods for Partial Differential Equations*, 12(4):489–506, 1996.

[BM18] Haïm Brezis and Petru Mironescu. Gagliardo-Nirenberg inequalities and non-inequalities: the full story. *Annales de l'Institut Henri Poincaré (C) Non Linear Analysis*, 35(5):1355–1376, 2018.

[Bre99] Kevin F. Brennan. *The Physics of Semiconductors: With Applications to Optoelectronic Devices*. Cambridge University Press, 1999.

[Bré11] H. Brézis. *Functional analysis, Sobolev spaces and partial differential equations.* Springer, New York London, 2011.

[Bre13] Alberto Bressan. *Lecture notes on functional analysis with applications to linear partial differential equations.* American Mathematical Society, Providence, Rhode Island, 2013.

[BS02] Fabian Bufler and Andreas Schenk. *Halbleitertransporttheorie und Monte-Carlo-Bauelementsimulation.* Lecture Notes. ETH Zürich, Switzerland, 2002.

[CCGJ95] Zhangxin Chen, Bernardo Cockburn, Carl L. Gardner, and Joseph W. Jerome. Quantum hydrodynamic simulation of hysteresis in the resonant tunneling diode. *Journal of Computational Physics*, 117(2):274 – 280, 1995.

[CD11] Li Chen and Michael Dreher. Viscous quantum hydrodynamics and parameter-elliptic systems. *Mathematical Methods in the Applied Sciences*, 34(5):520–531, 2011.

[CEFM00] F. Castella, L. Erdős, F. Frommlet, and P. A. Markowich. Fokker–Planck Equations as Scaling Limits of Reversible Quantum Systems. *Journal of Statistical Physics*, 100:543–601, 2000.

[CL83] A. O. Caldeira and A. J. Leggett. Path integral approach to quantum brownian motion. *Physica A: Statistical Mechanics and its Applications*, 121(3):587 – 616, 1983.

[DC11] Michael Dreher and Li Chen. Quantum Semiconductor Models. In *Partial Differential Equations and Spectral Theory*, number 211 in Operator Theory : Advances and Applications, pages 1–72. Springer, 2011.

[DNPV12] Eleonora Di Nezza, Giampiero Palatucci, and Enrico Valdinoci. Hitchhikers guide to the fractional sobolev spaces. *Bulletin des Sciences Mathématiques*, 136(5):521 – 573, 2012.

[Dor16] L. V. Dorodnitsyn. Grid oscillations in finite-difference scheme and a method for their approximate analysis. *Computational Mathematics and Modeling*, 27(4):472 – 488, 2016.

[DS16] Michael Dreher and Johannes Schnur. Large data solutions to the viscous quantum hydrodynamic model with barrier potential. *Mathematical Methods in the Applied Sciences*, 39(11):3016–3034, 2016.

[EN00] Klaus-Jochen Engel and Rainer Nagel. *One-Parameter Semigroups for Linear Evolution Equations.* Springer-Verlag New York, 2000.

[Eva10] Lawrence Evans. *Partial differential equations.* American Mathematical Society, Providence, R.I, 2010.

[Fei19] Michael Feiginov. Frequency limitations of resonant-tunnelling diodes in sub-thz and thz oscillators and detectors. *Journal of Infrared, Millimeter, and Terahertz Waves*, 40, 04 2019.

[FSCM12] M. Feiginov, C. Sydlo, O. Cojocari, and P. Meissner. Operation of resonant-tunnelling-diode oscillators beyond tunnel-lifetime limit at 564 GHz. *EPL (Europhysics Letters)*, 97(5):58006, mar 2012.

[FVZ90] R. M. Furzeland, J. G. Verwer, and P. A. Zegeling. A numerical study of three moving-grid methods for one-dimensional partial differential equations which are based on the method of lines. *Journal of Computational Physics*, 89(2):349 – 388, 1990.

[Ger31] S. Geršgorin. über die abgrenzung der eigenwerte einer matrix. *Bulletin de l'Académie des Sciences de l'URSS. Classe des sciences mathématiques et na*, 6:749 – 754, 1931.

[Gov00] Willy J. F. Govearts. *Numerical Methods for Bifurcations of Dynamical Equilibria.* Society for Industrial and Applied Mathematics, 2000.

[Har28] D. R. Hartree. The Wave Mechanics of an Atom with a Non-Coulomb Central Field. Part I. Theory and Methods. *Mathematical Proceedings of the Cambridge Philosophical Society*, 24(1):89–110, 1928.

[Hen81] Dan Henry. *Geometric Theory of Semilinear Parabolic Equations.* Springer-Verlag, Berlin, Heidelberg, 1981.

[HM23] Anthony Hastir and Riccardo Muolo. A generalized routh-hurwitz criterion for the stability analysis of polynomials with complex coefficients: application to the pi-control of vibrating structures, 2023.

[JM07] Ansgar Jüngel and Josipa Pina Milišić. Physical and numerical viscosity for quantum hydrodynamics. *Communications in Mathematical Sciences*, 5(2):447 – 471, 2007.

[JT06] Ansgar Jüngel and Shaoqiang Tang. Numerical approximation of the viscous quantum hydrodynamic model for semiconductors. *Applied Numerical Mathematics*, 56(7):899 – 915, 2006.

[Jün09] Ansgar Jüngel. *Transport Equations for Semiconductors.* Springer, Berlin, 2009.

[Kat66] Tosio Kato. *Perturbation theory for linear operators*. Springer Berlin, Heidelberg, 1966.

[KKFR89] N. C. Kluksdahl, A. M. Kriman, D. K. Ferry, and C. Ringhofer. Self-consistent study of the resonant-tunneling diode. *Phys. Rev. B*, 39:7720–7735, Apr 1989.

[LLMP05] Luca Lorenzi, Alessandra Lunardi, Giorgio Metafune, and Diego Pallara. Analytic semigroups and reaction-diffusion problems. "https://www.math.tecnico.ulisboa.pt/ czaja/ISEM/08internetseminar200405.pdf", 2005. Accessed: 11.01.2021.

[LTWZ09] Jiequan Li, Huazhong Tang, Gerald Warnecke, and Lumei Zhang. Local oscillations in finite difference solutions of hyperbolic conservation laws. *Math. Comput.*, 78:1997–2018, 10 2009.

[Lun12] Alessandra Lunardi. *Analytic semigroups and optimal regularity in parabolic problems*. Basel: Birkhäuser, reprint of the 1995 hardback ed. edition, 2012.

[LW93] Jens Lang and Artur Walter. An adaptive rothe method for nonlinear reaction-diffusion systems. *Applied Numerical Mathematics*, 13(1):135 – 146, 1993.

[MKSA16] Takeru Maekawa, Hidetoshi Kanaya, Safumi Suzuki, and Masahiro Asada. Oscillation up to 1.92 THz in resonant tunneling diode by reduced conduction loss. *Applied Physics Express*, 9(2):024101, jan 2016.

[MR90] P. A. Markowich and C. Ringhofer, C.and Schmeiser. *Semiconductor Equations*. Springer, 1990.

[MV11] Bernd Marx and Werner Vogt. *Dynamische Systeme - Theorie und Numerik*. Springer Spektrum, Berlin, Heidelberg, 2011.

[Pat80] S. Patankar. *Numerical Heat Transfer and Fluid Flow (1st ed.)*. CRC Press, 1980.

[Ren04] Michael Renardy. *An introduction to partial differential equations*. Springer, New York, 2004.

[Sch13] Ben Schweizer. *Partielle Differentialgleichungen Eine anwendungsorientierte Einführung*. Imprint Springer Spektrum, Berlin, Heidelberg, 2013.

[Sel84] Siegfried Selberherr. *Analysis and Simulation of Semiconductor Devices*. Springer-Verlag, Wien New York, 1984.

[SO89] Attila Bangha Szabo and Neil S. Ostlund. *Modern Quantum Chemistry: Introduction to Advanced Electronic Structure Theory*. McGraw-Hill, New York, 1989.

[VBSS89] J. G. Verwer, J. G. Blom, and J. M. Sanz-Serna. An adaptive moving grid method for one-dimensional systems of partial differential equations. *Journal of Computational Physics*, 82(2):454 – 486, 1989.

[WW96] E. T. Whittaker and G. N. Watson. *A Course of Modern Analysis*. Cambridge Mathematical Library. Cambridge University Press, 4 edition, 1996.

[XDZ12] Zhi Xiao, Shi-sen Du, and Chun-Xi Zhang. Revisiting 1-dimensional double-barrier tunneling in quantum mechanics. *arXiv*, 10 2012.

Appendix A

Transmission coefficient

This section covers the derivation of the transmission coefficient, discussed in the introduction. The solution to the Schrödinger equation of a single electron in vacuum with a rectangular potential barrier is given by

$$\psi(x) = \begin{cases} \mathrm{e}^{\mathrm{i}kx} + R\mathrm{e}^{-\mathrm{i}kx}, & x < a \\ c\mathrm{e}^{\alpha x} + d\mathrm{e}^{-\alpha x}, & a \leq x \leq b \\ T\mathrm{e}^{\mathrm{i}kx}, & x > b, \end{cases} , \tag{A.0.1}$$

with $\alpha^2 = U - E$ and $E = k^2$. Using the continuity conditions

$$\psi(a-0) = \psi(a+0), \tag{A.0.2}$$

$$\psi(b-0) = \psi(b+0), \tag{A.0.3}$$

$$\psi'(a-0) = \psi'(a+0), \tag{A.0.4}$$

$$\psi'(b-0) = \psi'(b+0), \tag{A.0.5}$$

we obtain a linear system of equations

$$\mathrm{e}^{\mathrm{i}ka} + R\mathrm{e}^{-\mathrm{i}ka} = c\mathrm{e}^{\alpha a} + d\mathrm{e}^{-\alpha a}, \tag{A.0.6}$$

$$T\mathrm{e}^{\mathrm{i}kb} = c\mathrm{e}^{\alpha b} + d\mathrm{e}^{-\alpha b}, \tag{A.0.7}$$

$$\mathrm{i}k\left(\mathrm{e}^{\mathrm{i}ka} - R\mathrm{e}^{-\mathrm{i}ka}\right) = \alpha\left(c\mathrm{e}^{\alpha a} - d\mathrm{e}^{-\alpha a}\right), \tag{A.0.8}$$

$$\mathrm{i}kT\mathrm{e}^{\mathrm{i}kb} = \alpha\left(c\mathrm{e}^{\alpha b} - d\mathrm{e}^{-\alpha b}\right), \tag{A.0.9}$$

which can be solved by elimination of variables or Gaussian elimination. Solving (A.0.6) for c gives us

$$c = \mathrm{e}^{-\alpha a}\left(\mathrm{e}^{\mathrm{i}ka} + R\mathrm{e}^{-\mathrm{i}ka} - d\mathrm{e}^{-\alpha a}\right). \tag{A.0.10}$$

After inserting the formular for c into (A.0.8) and solving for d, we have

$$d = \frac{\mathrm{e}^{\alpha a}}{2\alpha}\left(\mathrm{e}^{\mathrm{i}ka}(\alpha - \mathrm{i}k) + R\mathrm{e}^{-\mathrm{i}ka}(\alpha + \mathrm{i}k)\right). \tag{A.0.11}$$

Now we can replace d in (A.0.10) and get

$$c = \frac{\mathrm{e}^{-\alpha a}}{2\alpha}\left(\mathrm{e}^{\mathrm{i}ka}(\alpha + \mathrm{i}k) + R\mathrm{e}^{-\mathrm{i}ka}(\alpha - \mathrm{i}k)\right). \tag{A.0.12}$$

Replacing c and d in (A.0.7) and solving for R leads to

$$R = \mathrm{e}^{\mathrm{i}ka}\frac{2\alpha T\mathrm{e}^{\mathrm{i}kb} - \mathrm{e}^{\mathrm{i}ka}\left(\mathrm{e}^{\alpha D}(\alpha + \mathrm{i}k) + \mathrm{e}^{-\alpha D}(\alpha - \mathrm{i}k)\right)}{\mathrm{e}^{\alpha D}(\alpha - \mathrm{i}k) + \mathrm{e}^{-\alpha D}(\alpha + \mathrm{i}k)}, \tag{A.0.13}$$

with the barrier width $D = b - a$. Inserting (A.0.12), (A.0.11) and (A.0.13) in (A.0.9), we obtain, after some rearrangements, the equation

$$\begin{aligned}
\mathrm{i}kT\mathrm{e}^{\mathrm{i}kb} = \frac{\mathrm{e}^{\mathrm{i}ka}}{2}\Bigg(&\mathrm{e}^{\alpha D}\left(\alpha + \mathrm{i}k - (\alpha - \mathrm{i}k)\frac{\mathrm{e}^{\alpha D}(\alpha + \mathrm{i}k) + \mathrm{e}^{-\alpha D}(\alpha - \mathrm{i}k)}{\mathrm{e}^{\alpha D}(\alpha - \mathrm{i}k) + \mathrm{e}^{-\alpha D}(\alpha + \mathrm{i}k)}\right)\\
&- \mathrm{e}^{-\alpha D}\left(\alpha - \mathrm{i}k - (\alpha + \mathrm{i}k)\frac{\mathrm{e}^{\alpha D}(\alpha + \mathrm{i}k) + \mathrm{e}^{-\alpha D}(\alpha - \mathrm{i}k)}{\mathrm{e}^{\alpha D}(\alpha - \mathrm{i}k) + \mathrm{e}^{-\alpha D}(\alpha + \mathrm{i}k)}\right)\Bigg)\\
&+ \alpha T\mathrm{e}^{\mathrm{i}kb}\frac{\mathrm{e}^{\alpha D}(\alpha - \mathrm{i}k) - \mathrm{e}^{-\alpha D}(\alpha + \mathrm{i}k)}{\mathrm{e}^{\alpha D}(\alpha - \mathrm{i}k) + \mathrm{e}^{-\alpha D}(\alpha + \mathrm{i}k)}.
\end{aligned} \tag{A.0.14}$$

Using the identities

$$(\alpha + \mathrm{i}k)^2 - (\alpha - \mathrm{i}k)^2 = 4\mathrm{i}\alpha k, \tag{A.0.15}$$

$$\alpha\frac{\mathrm{e}^{\alpha D}(\alpha - \mathrm{i}k) - \mathrm{e}^{-\alpha D}(\alpha + \mathrm{i}k)}{\mathrm{e}^{\alpha D}(\alpha - \mathrm{i}k) + \mathrm{e}^{-\alpha D}(\alpha + \mathrm{i}k)} - \mathrm{i}k = \frac{\mathrm{e}^{\alpha D}(\alpha - \mathrm{i}k)^2 - \mathrm{e}^{-\alpha D}(\alpha + \mathrm{i}k)^2}{\mathrm{e}^{\alpha D}(\alpha - \mathrm{i}k) + \mathrm{e}^{-\alpha D}(\alpha + \mathrm{i}k)}, \tag{A.0.16}$$

and solving (A.0.14) for T gives us the formular of the transmission coefficient

$$T = \frac{2\alpha k\mathrm{e}^{-\mathrm{i}kD}}{2\alpha k\cosh(\alpha D) + \mathrm{i}(\alpha^2 - k^2)\sinh(\alpha D)}. \tag{A.0.17}$$

Then, the transmission probability is given by

$$|T|^2 = \frac{1}{1 + \frac{U^2}{4E(U-E)}\sinh^2(\alpha D)}. \tag{A.0.18}$$

Appendix B

MATLAB implementation

Here, we give the function that was used to calculate the data in the chapter 4. The physical constants are taken from [JT06, JM07]. We use the following designation: As input we have the number of grid points N, maximum time T, maximum Voltage $Vmax$, slope of the logistic function *slope*, the solver *stringSolver*, the maximu path length *smax*, the error tolerance *tol* and initial conditions or initial guess *stringLoadInit*. The data given by the string *stringLoadInit* has to be consistent with the chosen solver, that is data for the isothermal case has the format $X = (n, J, V)$ with the size $3N+6$ and data for the other models has the format $X = (n, J, ni, V)$ with the size $4N + 5$. The program returns the performed stepsizes with *Stepsizes*, the voltage and current in Y, in case of the isothermal or static solver, and the final solution X. Since no previous solutions are stored, solutions at specific voltages or timestamps can be obtained by appropriate choices of the maximum voltage or maximum time.

```
function [Stepsizes,Y,X]=vqhdsolver(N,slope,T,Vmax,stringSolver,
    smax,tol,stringLoadInit)
    close all
    warning('off','all')
    if ~exist('N','var')
        N=500;
    end
    if ~exist('slope','var')
        slope=200;
    end
    if ~exist('T','var')
        T=0;
    end
    if ~exist('Vmax','var')
        Vmax=0;
    end
    if ~exist('stringSolver','var')
```

```
        fprintf('Please specify the version of the viscous
           quantum hydrodynamic equations using "isotherm", "
           static" or "full"!\n');
        return
    end
    if ~exist('smax','var')
        smax=10^3;
    end
    if ~exist('tol','var')
        tol=10^(-6);
    end
    if ~exist('stringLoadInit','var')
        stringLoadInit='null';
    end
    if(sign(N)<0)
        fprintf('The number of grid points must be positive!\n')
           ;
        return
    end
    if(sign(slope)<0)
        fprintf('The slope must be positive!\n');
        return
    end
    if(sign(T)<0)
        fprintf('The maximal timestamp must be positive!\n');
        return
    end
    if(sign(smax)<0)
        smax=-smax;
    end
    if(sign(tol)<0)
        tol=-tol;
    end
    %Physical constants
    global nu mu lambda tau T0 epsilon VBmax Cmin
    nu=9.935*1E-4;
    mu=1.014*1E-2;
    lambda=3.032*1E-4;
    tau=0.5654;
    T0=1.00585;
```

```
epsilon=3.893*1E-3;
VBmax=-0.209*149.490238287;
Cmin=0.005;
%Numerical constants
grid=(0:1/N:1)';
switch stringSolver
    case 'isotherm'
        sizeX=3*N+6;
    case 'static'
        sizeX=4*N+5;
    case 'full'
        sizeX=4*N+5;
    otherwise
        fprintf('Please specify the version of the viscous
            quantum hydrodynamic equations using isotherm,
            static or full!\n');
        return
end
%Numerical variables
steps=0;
s=0;
t0=0;
t=0;
V=0;
hmax=1;
hmin=10^(-12);
anglemax=0.08;
distmax=1;
ratemax=1;
rho=1;
h=10^(-4);
k=0;
alphamax=0.1;
alpha=alphamax;
alphamin=0.001;
kopt=6;
eigsize=4;
Current=[];
Voltage=[];
Stepsizes=[];
```

```
    %Doping profile
    fC=@(x) 1+(1-Cmin)*(-tanh(slope*(x-0.4))+tanh(slope*(x-0.6)))/2;
    %Initial conditions
    if(~strcmp(stringLoadInit,'null'))
        S=load(stringLoadInit,'X');
        tmpX=S.X;
        if(strcmp(stringSolver,'isotherm'))
            tmpN=(length(tmpX)-6)/3;
            tmpgrid=(0:1/tmpN:1)';
            X(2:N+2)=interp1(tmpgrid,tmpX(1:tmpN+1),grid,'makima');
            X(1)=X(3);
            X(N+3)=X(N+1);
            X(N+4:2*N+4)=interp1(tmpgrid,(tmpX(tmpN+4:2*tmpN+4)+tmpX(tmpN+5:2*tmpN+5))/2,grid,'makima');
            X(N+5:2*N+4)=(X(N+4:2*N+3)+X(N+5:2*N+4))/2;
            X(N+4)=X(N+5);
            X(2*N+5)=X(2*N+4);
            X(2*N+6:3*N+6)=interp1(tmpgrid,tmpX(2*tmpN+6:3*tmpN+6),grid,'makima');
        else
            tmpN=(length(tmpX)-5)/4;
            tmpgrid=(0:1/tmpN:1)';
            X(1:N+1)=interp1(tmpgrid,tmpX(1:tmpN+1),grid,'makima');
            X(N+2:2*N+3)=interp1(-1/(2*tmpN):1/tmpN:1+1/(2*tmpN),tmpX(tmpN+2:2*tmpN+3),-1/(2*N):1/N:1+1/(2*N),'makima');
            X(2*N+4:3*N+4)=interp1(tmpgrid,tmpX(2*tmpN+4:3*tmpN+4),grid,'makima');
            X(3*N+5:4*N+5)=interp1(tmpgrid,tmpX(3*tmpN+5:4*tmpN+5),grid,'makima');
        end
    else
        if(strcmp(stringSolver,'isotherm'))
            X=zeros(3*N+6,1);
            X(2:N+2)=fC(grid);
            X(1)=X(3);
            X(N+3)=X(N+1);
```

```
            else
                X=zeros(sizeX,1);
                X(1:N+1)=fC(grid);
                X(2*N+4:3*N+4)=X(1:N+1)*T0/2;
            end
        end
        tmp=size(X);
        if(tmp(1)==1)
            X=X';
        end
        Y=[];
        if(~strcmp(stringSolver,'full'))
            while((norm(getF(t0,t,X,X,V,N,slope,stringSolver))>tol))
                A=sparse(getDF(t0,t,X,N,slope,stringSolver));
                A=A(:,1:sizeX);
                b=getF(t0,t,X,X,V,N,slope,stringSolver);
                Delta=-A\b;
                if(norm(b)<norm(getF(t0,t,X,X+alpha*Delta,V,N,slope,
                    stringSolver)))
                    alpha=alphamin;
                else
                    alpha=alphamax;
                end
                X=X+Delta*alpha;
                k=k+1;
                if(min(X(1:N+1))<0)
                    error('Negative density!\n');
                end
            end
            Y(steps+1,1)=V;
            Y(steps+1,2)=(X(2*N+2)+X(2*N+3))/2;
            Pmax=Vmax;
            rho=kopt/k;
            rho=min(rho,2);
            rho=max(rho,1/2);
            h=h*rho;
            if(h>hmax)
                h=hmax;
            end
        else
```

```
            Pmax=T;
        end
        H=sparse(getDF(t0,t,X,N,slope,stringSolver));
        [Q,R]=qr(H');
        tangent=Q(:,sizeX+1);
        tangent=tangent/norm(tangent);
        if(sign(tangent(sizeX+1))<0)
            tangent=-tangent;
        end
        traversing=true;
        while(traversing)
            steps=steps+1;
            s=s+h;
            if(strcmp(stringSolver,'full'))
                predictor=[X;t0]+h*tangent;
                tmpt=predictor(sizeX+1);
                tmpV=0;
                p0=t0;
            else
                predictor=[X;V]+h*tangent;
                tmpV=predictor(sizeX+1);
                tmpt=0;
                p0=V;
            end
            acceptpredictor=true;
            correctorloop=true;
            k=0;
            while(correctorloop)
                Hv=sparse(getDF(t0,tmpt,predictor(1:sizeX),N,slope,
                    stringSolver));
                Hfull=[Hv;tangent'];
                if(rcond(full(Hfull))<10^(-20))
                    acceptpredictor=false;
                    correctorloop=false;
                else
                    b=Hfull\[getF(t0,tmpt,X,predictor(1:sizeX),tmpV,
                        N,slope,stringSolver);tangent'*(predictor-[X;
                        p0])-h];
                    predictor=predictor-b;
                    if(strcmp(stringSolver,'full'))
```

```
                tmpt=predictor(sizeX+1);
            else
                tmpV=predictor(sizeX+1);
            end
            if(k==0)
                dist=norm(b);
                rhodist=sqrt(dist/distmax);
                rho=rhodist;
                rho=max(min(rho,2),1/2);
            end
            if(k==1)
                rate=norm(b)/dist;
                rhorate=sqrt(rate/ratemax);
                rhodist=sqrt(dist/distmax);
                rho=max([rhorate,rhodist]);
                rho=max(min(rho,2),1/2);
            end
            k=k+1;
            if(rho>=2)
                acceptpredictor=false;
                correctorloop=false;
                fprintf('Bad predictor!\n');
            end
            if(k>100)
                acceptpredictor=false;
                correctorloop=false;
                fprintf('Max iterations exceeded!\n');
            end
            if((norm(getF(t0,tmpt,X,predictor(1:sizeX),tmpV,
               N,slope,stringSolver))<tol))
                correctorloop=false;
            end
        end
    end
    if(strcmp(stringSolver,'isotherm'))
        if(any(isnan(predictor))||any(predictor(1:N+1)<0)||
           not(acceptpredictor))
            acceptpredictor=false;
            h=h/2;
            steps=steps-1;
```

```
                fprintf('Predictor not accepted!\n');
            end
        else
            if(any(isnan(predictor))||any(predictor(1:N+1)<0)||
              any(predictor(2*N+4:3*N+4)<0)||not(
              acceptpredictor))
                acceptpredictor=false;
                h=h/2;
                steps=steps-1;
                fprintf('Predictor not accepted!\n');
            end
        end

        if(acceptpredictor)
            X=predictor(1:sizeX);
            if(strcmp(stringSolver,'full'))
                t=predictor(sizeX+1);
                p0=t;
            else
                V=predictor(sizeX+1);
                p0=V;
                Y(steps+1,1)=V;
                Y(steps+1,2)=(X(2*N+2)+X(2*N+3))/2;
            end
            %Stepsize control
            Stepsizes(steps)=h;
            h=h/rho;
            if(abs(p0)>=abs(Pmax)||s>smax)
                traversing=false;
            end
            Hv=sparse(getDF(t0,t,X,N,slope,stringSolver));
            [Qv,Rv]=qr(Hv');
            tangentv=Qv(:,sizeX+1);
            tangentv=tangentv/norm(tangentv);
            if(~strcmp(stringSolver,'full'))
                %Test for Bifurcation
                eigs1=eigs([H;tangent'],eigsize,'SM');
                eigs2=eigs([Hv;tangentv'],eigsize,'SM');
                eigtest=1;
                for j=1:eigsize
```

```
                    eigtest=eigtest*sign(real(eigs1(j)))*sign(
                       real(eigs2(j)));
                end
                H=Hv;
                if(eigtest<0)
                    fprintf('Simple bifurcation point passed!\n'
                       );
                end
            else
                t0=t;
            end
            if(tangent'*tangentv<0)
                tangentv=-tangentv;
            end
            tangent=tangentv;
        end
        if(h>hmax)
            h=hmax;
        end
        if(h<10^(-5))
            fprintf('Warning! Small Stepsize!\n');
        end
        if(h<hmin)
            fprintf('Break! Stepsize too small!\n');
            break;
        end
    end
end
function F=getF(t0,t,X0,X,V,N,slope,stringSolver)
    %Physical constants
    global nu mu lambda tau T0 epsilon VBmax Cmin

    %Numerical constants
    dx=1/N;
    grid=(0:dx:1)';

    %Doping profile and barrier potential
    fC=@(x) 1+(1-Cmin)*(-tanh(slope*(x-0.4))+tanh(slope*(x-0.6))
        )/2;
```

```
    fVB=@(x) VBmax*(tanh(slope*(x-0.44))-tanh(slope*(x-0.48))+tanh(slope*(x-0.52))-tanh(slope*(x-0.56)))/2;

    VB=fVB(grid);
    C=fC(grid);
    switch stringSolver
        case 'isotherm'
            F1=@(n1,n2,n3,J1,J2) nu/dx^2*(n3-2*n2+n1)-(J2-J1)/dx;
            F2=@(n1,n2,n3,n4,J1,J2,J3,V1,V2,VB1,VB2) nu/dx^2*(J3-2*J2+J1)-J2/tau-((J3+J2).^2./(n3)-(J2+J1).^2./(n2))/(4*dx)-T0*(n3-n2)/dx+(n3+n2).*(V2-V1+VB2-VB1+epsilon.*(sqrt(n4./n3)+sqrt(n2./n3)-sqrt(n3./n2)-sqrt(n1./n2))./(2*dx^2))/(2*dx);
            F3=@(V1,V2,V3,n1,C0) lambda*(V3-2*V2+V1)/dx^2-n1+C0;

            funF=@(x,U) [x(1)-x(3);x(2)-C(1);F1(x(2:N),x(3:N+1),x(4:N+2),x(N+5:2*N+3),x(N+6:2*N+4));x(N+2)-C(N+1);x(N+3)-x(N+1);
              x(N+4)-x(N+5);F2(x(1:N),x(2:N+1),x(3:N+2),x(4:N+3),x(N+4:2*N+3),x(N+5:2*N+4),x(N+6:2*N+5),x(2*N+6:3*N+5),x(2*N+7:3*N+6),VB(1:N),VB(2:N+1));x(2*N+5)-x(2*N+4);
              x(2*N+6);F3(x(2*N+6:3*N+4),x(2*N+7:3*N+5),x(2*N+8:3*N+6),x(3:N+1),C(2:N));x(3*N+6)-U];
            F=funF(X,V);
        case 'static'
            F1=@(n1,n2,n3,J1,J2) nu/dx^2*(n3-2*n2+n1)-(J2-J1)/dx;
            F2=@(n1,n2,J1,J2,J3,ni1,ni2,VB1,VB2,V1,V2) nu/dx^2*(J3-2*J2+J1)-((J3+J2).^2./n2-(J2+J1).^2./n1)/(4*dx)-2*(ni2-ni1)/dx-mu*(n2-n1)/dx-J2/tau+(n2+n1).*((V2-V1)+VB2-VB1)/(2*dx);
            F3=@(n1,n2,n3,J1,J2,J3,J4,ni1,ni2,ni3) nu/dx^2*(ni3-2*ni2+ni1)-((J4+J3).*ni3./n3-(J2+J1).*ni1./n1)/(4*dx)+nu.*n2./(16*dx^2).*((J4+J3)./n3-(J2+J1)./n1).^2-((J4+J3)./n3-(J2+J1)./n1).*(2.*ni2+mu.*n2)/(4*dx)-2*ni2/tau+n2/tau;
            F4=@(n1,C0,V1,V2,V3) lambda*(V3-2*V2+V1)/dx^2-n1+C0;

```

```
        funF=@(x,U) [x(1)-x(2);F1(x(1:N-1),x(2:N),x(3:N+1),x(N+3:2*N+1),x(N+4:2*N+2));x(N+1)-x(N);
                x(N+2)-x(N+3);F2(x(1:N),x(2:N+1),x(N+2:2*N+1),x(N+3:2*N+2),x(N+4:2*N+3),x(2*N+4:3*N+3),x(2*N+5:3*N+4),VB(1:N),VB(2:N+1),x(3*N+5:4*N+4),x(3*N+6:4*N+5));x(2*N+3)-x(2*N+2);
                x(2*N+4)-x(2*N+5);F3(x(1:N-1),x(2:N),x(3:N+1),x(N+2:2*N),x(N+3:2*N+1),x(N+4:2*N+2),x(N+5:2*N+3),x(2*N+4:3*N+2),x(2*N+5:3*N+3),x(2*N+6:3*N+4));x(3*N+4)-x(3*N+3);
                x(3*N+5);F4(x(2:N),C(2:N),x(3*N+5:4*N+3),x(3*N+6:4*N+4),x(3*N+7:4*N+5));x(4*N+5)-U];

        F=funF(X,V);
    case 'full'
        F1=@(n1,n2,n3,J1,J2) nu/dx^2*(n3-2*n2+n1)-(J2-J1)/dx;
        F2=@(n1,n2,J1,J2,J3,ni1,ni2,VB1,VB2,V1,V2) nu/dx^2*(J3-2*J2+J1)-((J3+J2).^2./n2-(J2+J1).^2./n1)/(4*dx)-2*(ni2-ni1)/dx-mu*(n2-n1)/dx-J2/tau+(n2+n1).*((V2-V1)+VB2-VB1)/(2*dx);
        F3=@(n1,n2,n3,J1,J2,J3,J4,ni1,ni2,ni3) nu/dx^2*(ni3-2*ni2+ni1)-((J4+J3).*ni3./n3-(J2+J1).*ni1./n1)/(4*dx)+nu.*n2./(16*dx^2).*((J4+J3)./n3-(J2+J1)./n1).^2-((J4+J3)./n3-(J2+J1)./n1).*(2.*ni2+mu.*n2)/(4*dx)-2*ni2/tau+n2/tau;
        F4=@(n1,C0,V1,V2,V3) lambda*(V3-2*V2+V1)/dx^2-n1+C0;

        funF=@(x) [0;x(2:N)-X0(2:N)-(t-t0)*F1(x(1:N-1),x(2:N),x(3:N+1),x(N+3:2*N+1),x(N+4:2*N+2));0;
                0;x(N+3:2*N+2)-X0(N+3:2*N+2)-(t-t0)*F2(x(1:N),x(2:N+1),x(N+2:2*N+1),x(N+3:2*N+2),x(N+4:2*N+3),x(2*N+4:3*N+3),x(2*N+5:3*N+4),VB(1:N),VB(2:N+1),x(3*N+5:4*N+4),x(3*N+6:4*N+5));0;
                0;x(2*N+5:3*N+3)-X0(2*N+5:3*N+3)-(t-t0)*F3(x(1:N-1),x(2:N),x(3:N+1),x(N+2:2*N),x(N+3:2*N+1),x(N+4:2*N+2),x(N+5:2*N+3),x(2*N
```

```
                         +4:3*N+2),x(2*N+5:3*N+3),x(2*N+6:3*N+4))
                         ;0;
                      zeros(N+1,1)];
                funB=@(x) [x(1)-x(2);
                   zeros(N-1,1);
                   x(N+1)-x(N);
                   x(N+2)-x(N+3);
                   zeros(N,1);
                   x(2*N+3)-x(2*N+2);
                   x(2*N+4)-x(2*N+5);
                   zeros(N-1,1);
                   x(3*N+4)-x(3*N+3);
                   x(3*N+5);
                   F4(x(2:N),C(2:N),x(3*N+5:4*N+3),x(3*N+6:4*N+4),x
                     (3*N+7:4*N+5));
                   x(4*N+5)];
                F=funF(X)+funB(X);
        end
end

function DF=getDF(t0,t,X,N,slope,stringSolver)
    %Physical constants
    global nu mu lambda tau T0 epsilon VBmax

    %Numerical constants
    dx=1/N;
    grid=(0:dx:1)';

    %Doping profile
    fVB=@(x) VBmax*(tanh(slope*(x-0.44))-tanh(slope*(x-0.48))+
      tanh(slope*(x-0.52))-tanh(slope*(x-0.56)))/2;

    VB=fVB(grid);
    switch stringSolver
        case 'isotherm'
            funDF=@(x) [1 0 -1 zeros(1,3*N+3);0 1 zeros(1,3*N+4)
              ;[zeros(N-1,1) diag(nu/dx^2*ones(N-1,1)) zeros(N
              -1,4) diag(1/dx*ones(N-1,1)) zeros(N-1,N+3)]+[
              zeros(N-1,2) diag(-2*nu/dx^2*ones(N-1,1)) zeros(N
              -1,4) diag(-1/dx*ones(N-1,1)) zeros(N-1,N+2)]+[
```

```
        zeros(N-1,3) diag(nu/dx^2*ones(N-1,1)) zeros(N
        -1,2*N+4)]; zeros(1,N+1) 1 zeros(1,2*N+4); zeros(1,
        N) -1 0 1 zeros(1,2*N+3);
    zeros(1,N+3) 1 -1 zeros(1,2*N+1); [diag(-epsilon/(8*dx^3)
      *(x(3:N+2)+x(2:N+1))./sqrt(x(2:N+1).*x(1:N))) zeros(N
      ,3) diag(nu/dx^2+1/(2*dx)*(x(N+4:2*N+3)+x(N+5:2*N+4))
      ./(x(2:N+1))) zeros(N,2) diag(-(x(2:N+1)+x(3:N+2))
      /(2*dx)) zeros(N,1)]+[zeros(N,1) diag(-1/(4*dx)*(x(N
      +5:2*N+4)+x(N+4:2*N+3)).^2./(x(2:N+1)).^2+T0/dx+1/(2*
      dx)*(x(2*N+7:3*N+6)-x(2*N+6:3*N+5)+VB(2:N+1)-VB(1:N)+
      epsilon/(2*dx^2)*(sqrt(x(4:N+3)./x(3:N+2))+sqrt(x(2:N
      +1)./x(3:N+2))-sqrt(x(3:N+2)./x(2:N+1))-sqrt(x(1:N)./
      x(2:N+1))))+epsilon/(8*dx^3)*(x(3:N+2)+x(2:N+1))
      .*(1./sqrt(x(3:N+2).*x(2:N+1))+sqrt(x(3:N+2))./sqrt((
      x(2:N+1)).^(3))+sqrt(x(1:N))./sqrt((x(2:N+1)).^(3))))
       zeros(N,3) diag(-2*nu/dx^2-1/tau-1/(2*dx)*((x(N+6:2*
      N+5)+x(N+5:2*N+4))./(x(3:N+2))-(x(N+5:2*N+4)+x(N+4:2*
      N+3))./(x(2:N+1)))) zeros(N,2) diag((x(3:N+2)+x(2:N
      +1))/(2*dx))]+[zeros(N,2) diag(1/(4*dx)*(x(N+6:2*N+5)
      +x(N+5:2*N+4)).^2./(x(3:N+2)).^2-T0/dx+1/(2*dx)*(x(2*
      N+7:3*N+6)-x(2*N+6:3*N+5)+VB(2:N+1)-VB(1:N)+epsilon
      /(2*dx^2)*(sqrt(x(4:N+3)./x(3:N+2))+sqrt(x(2:N+1)./x
      (3:N+2))-sqrt(x(3:N+2)./x(2:N+1))-sqrt(x(1:N)./x(2:N
      +1))))-epsilon/(8*dx^3)*(x(3:N+2)+x(2:N+1)).*(sqrt(x
      (4:N+3))./sqrt((x(3:N+2)).^(3))+sqrt(x(2:N+1))./sqrt
      ((x(3:N+2)).^(3))+1./(sqrt(x(3:N+2).*x(2:N+1)))))
      zeros(N,3) diag(nu/dx^2-1/(2*dx)*(x(N+6:2*N+5)+x(N
      +5:2*N+4))./(x(3:N+2))) zeros(N,N+1)]+[zeros(N,3)
      diag(epsilon/(8*dx^3)*(x(3:N+2)+x(2:N+1))./sqrt(x(4:N
      +3).*x(3:N+2))) zeros(N,2*N+3)]; zeros(1,2*N+3) -1 1
      zeros(1,N+1);
    zeros(1,2*N+5) 1 zeros(1,N); [zeros(N-1,2) diag(-1*ones(N
      -1,1)) zeros(N-1,N+4) diag(lambda/dx^2*ones(N-1,1))
      zeros(N-1,2)]+[zeros(N-1,2*N+6) diag(-2*lambda/dx^2*
      ones(N-1,1)) zeros(N-1,1)]+[zeros(N-1,2*N+7) diag(
      lambda/dx^2*ones(N-1,1))]; zeros(1,3*N+5) 1];
      DF=[funDF(X) [zeros(3*N+5,1); -1]];
    case 'static'
      funDF=@(x) [1 -1 zeros(1,4*N+3); [diag(nu/dx^2*ones(N
        -1,1)) zeros(N-1,3) diag(1/dx*ones(N-1,1)) zeros(
```

```
    N-1,2*N+4)]+[zeros(N-1,1) diag(-2*nu/dx^2*ones(N
    -1,1)) zeros(N-1,3) diag(-1/dx*ones(N-1,1)) zeros
    (N-1,2*N+3)]+[zeros(N-1,2) diag(nu/dx^2*ones(N
    -1,1)) zeros(N-1,3*N+4)];zeros(1,N-1) -1 1 zeros
    (1,3*N+4);
zeros(1,N+1) 1 -1 zeros(1,3*N+2);[diag(mu/dx-1/(4*dx)*(x
  (N+3:2*N+2)+x(N+2:2*N+1)).^2./(x(1:N)).^2+1/(2*dx)*(x
  (3*N+6:4*N+5)-x(3*N+5:4*N+4)+VB(2:N+1)-VB(1:N)))
  zeros(N,1) diag(nu/dx^2+1/(2*dx)*(x(N+3:2*N+2)+x(N
  +2:2*N+1))./(x(1:N))) zeros(N,2) diag(2/(dx)*ones(N
  ,1)) zeros(N,1) diag(-1/(2*dx)*(x(2:N+1)+x(1:N)))
  zeros(N,1)]+[zeros(N,1) diag(-mu/dx+1/(4*dx)*(x(N
  +4:2*N+3)+x(N+3:2*N+2)).^2./(x(2:N+1)).^2+1/(2*dx)*(x
  (3*N+6:4*N+5)-x(3*N+5:4*N+4)+VB(2:N+1)-VB(1:N)))
  zeros(N,1) diag(-1/tau-2*nu/dx^2-1/(2*dx)*((x(N+4:2*N
  +3)+x(N+3:2*N+2))./(x(2:N+1))-(x(N+3:2*N+2)+x(N+2:2*N
  +1))./(x(1:N)))) zeros(N,2) diag(-2/(dx)*ones(N,1))
  zeros(N,1) diag(1/(2*dx)*(x(2:N+1)+x(1:N)))]+[zeros(N
  ,N+3) diag(nu/dx^2-1/(2*dx)*(x(N+4:2*N+3)+x(N+3:2*N
  +2))./(x(2:N+1))) zeros(N,2*N+2)];zeros(1,2*N+1) -1 1
   zeros(1,2*N+2);
zeros(1,2*N+3) 1 -1 zeros(1,2*N);[diag(-1/(4*dx)*(x(N
  +3:2*N+1)+x(N+2:2*N)).*x(2*N+4:3*N+2)./(x(1:N-1)).^2+
  nu/(8*dx^2)*(x(2:N)).*((x(N+5:2*N+3)+x(N+4:2*N+2))./(
  x(3:N+1))-(x(N+3:2*N+1)+x(N+2:2*N))./(x(1:N-1))).*(x(
  N+3:2*N+1)+x(N+2:2*N))./(x(1:N-1)).^2-1/(4*dx)*(x(N
  +3:2*N+1)+x(N+2:2*N)).*(2.*x(2*N+5:3*N+3)+mu.*x(2:N))
  ./(x(1:N-1)).^2) zeros(N-1,2) diag(1/(4*dx)*(x(2*N
  +4:3*N+2))./(x(1:N-1))-nu/(8*dx^2)*(x(2:N)).*((x(N
  +5:2*N+3)+x(N+4:2*N+2))./(x(3:N+1))-(x(N+3:2*N+1)+x(N
  +2:2*N))./(x(1:N-1)))./(x(1:N-1))+1/(4*dx)*(2*x(2*N
  +5:3*N+3)+mu*x(2:N))./(x(1:N-1))) zeros(N-1,3) diag(
  nu/dx^2+1/(4*dx)*(x(N+3:2*N+1)+x(N+2:2*N))./(x(1:N-1)
  )) zeros(N-1,N+3)]+[zeros(N-1,1) diag(nu/(16*dx^2)*((
  x(N+5:2*N+3)+x(N+4:2*N+2))./(x(3:N+1))-(x(N+3:2*N+1)+
  x(N+2:2*N))./(x(1:N-1))).^2-mu/(4*dx)*((x(N+5:2*N+3)+
  x(N+4:2*N+2))./(x(3:N+1))-(x(N+3:2*N+1)+x(N+2:2*N))
  ./(x(1:N-1)))+1/tau) zeros(N-1,2) diag(1/(4*dx)*(x(2*
  N+4:3*N+2))./(x(1:N-1))-nu/(8*dx^2)*x(2:N).*((x(N
  +5:2*N+3)+x(N+4:2*N+2))./(x(3:N+1))-(x(N+3:2*N+1)+x(N
```

```
        +2:2*N))./(x(1:N-1)))./(x(1:N-1))+1/(4*dx).*(2.*x(2*N
        +5:3*N+3)+mu.*x(2:N))./(x(1:N-1))) zeros(N-1,3) diag
        (-2*nu/dx^2-1/(2*dx)*((x(N+5:2*N+3)+x(N+4:2*N+2))./(x
        (3:N+1))-(x(N+3:2*N+1)+x(N+2:2*N))./(x(1:N-1)))-2/tau
        ) zeros(N-1,N+2)]+[zeros(N-1,2) diag(1/(4*dx)*(x(N
        +5:2*N+3)+x(N+4:2*N+2)).*x(2*N+6:3*N+4)./(x(3:N+1))
        .^2-nu/(8*dx^2)*(x(2:N)).*((x(N+5:2*N+3)+x(N+4:2*N+2)
        )./(x(3:N+1))-(x(N+3:2*N+1)+x(N+2:2*N))./(x(1:N-1)))
        .*(x(N+5:2*N+3)+x(N+4:2*N+2))./(x(3:N+1)).^2+1/(4*dx)
        *(x(N+5:2*N+3)+x(N+4:2*N+2)).*(2.*x(2*N+5:3*N+3)+mu.*
        x(2:N))./(x(3:N+1)).^2) zeros(N-1,2) diag(-1/(4*dx)*x
        (2*N+6:3*N+4)./(x(3:N+1))+nu/(8*dx^2)*(x(2:N)).*((x(N
        +5:2*N+3)+x(N+4:2*N+2))./(x(3:N+1))-(x(N+3:2*N+1)+x(N
        +2:2*N))./(x(1:N-1)))./(x(3:N+1))-1/(4*dx)*(2*x(2*N
        +5:3*N+3)+mu*x(2:N))./(x(3:N+1))) zeros(N-1,3) diag(
        nu/dx^2-1/(4*dx)*(x(N+5:2*N+3)+x(N+4:2*N+2))./(x(3:N
        +1))) zeros(N-1,N+1)]+[zeros(N-1,N+4) diag(-1/(4*dx)*
        x(2*N+6:3*N+4)./(x(3:N+1))+nu/(8*dx^2)*(x(2:N)).*((x(
        N+5:2*N+3)+x(N+4:2*N+2))./(x(3:N+1))-(x(N+3:2*N+1)+x(
        N+2:2*N))./(x(1:N-1)))./(x(3:N+1))-1/(4*dx)*(2*x(2*N
        +5:3*N+3)+mu*x(2:N))./(x(3:N+1))) zeros(N-1,2*N+2)];
        zeros(1,3*N+2) -1 1 zeros(1,N+1);
    zeros(1,3*N+4) 1 zeros(1,N);[zeros(N-1,1) diag(-1*ones(N
        -1,1)) zeros(N-1,2*N+4) diag(lambda/dx^2*ones(N-1,1))
         zeros(N-1,2)]+[zeros(N-1,3*N+5) diag(-2*lambda/dx^2*
        ones(N-1,1)) zeros(N-1,1)]+[zeros(N-1,3*N+6) diag(
        lambda/dx^2*ones(N-1,1))];zeros(1,4*N+4) 1];
        DF=[funDF(X) [zeros(4*N+4,1);-1]];
    case 'full'
        F1=@(n1,n2,n3,J1,J2) nu/dx^2*(n3-2*n2+n1)-(J2-J1)/dx
            ;
        F2=@(n1,n2,J1,J2,J3,ni1,ni2,VB1,VB2,V1,V2) nu/dx^2*(
            J3-2*J2+J1)-((J3+J2).^2./n2-(J2+J1).^2./n1)/(4*dx
            )-2*(ni2-ni1)/dx-mu*(n2-n1)/dx-J2/tau+(n2+n1).*((
            V2-V1)+VB2-VB1)/(2*dx);
        F3=@(n1,n2,n3,J1,J2,J3,J4,ni1,ni2,ni3) nu/dx^2*(ni3
            -2*ni2+ni1)-((J4+J3).*ni3./n3-(J2+J1).*ni1./n1)
            /(4*dx)+nu.*n2./(16*dx^2).*((J4+J3)./n3-(J2+J1)./
            n1).^2-((J4+J3)./n3-(J2+J1)./n1).*(2.*ni2+mu.*n2)
            /(4*dx)-2*ni2/tau+n2/tau;
```

```
        funF=@(x) [0;F1(x(1:N-1),x(2:N),x(3:N+1),x(N+3:2*N+1),x(N+4:2*N+2));0;
                0;F2(x(1:N),x(2:N+1),x(N+2:2*N+1),x(N+3:2*N+2),x(N+4:2*N+3),x(2*N+4:3*N+3),x(2*N+5:3*N+4),VB(1:N),VB(2:N+1),x(3*N+5:4*N+4),x(3*N+6:4*N+5));0;
                0;F3(x(1:N-1),x(2:N),x(3:N+1),x(N+2:2*N),x(N+3:2*N+1),x(N+4:2*N+2),x(N+5:2*N+3),x(2*N+4:3*N+2),x(2*N+5:3*N+3),x(2*N+6:3*N+4));0;
                zeros(N+1,1)];
        funDF=@(x) [0 0 zeros(1,4*N+3);[diag(nu/dx^2*ones(N-1,1)) zeros(N-1,3) diag(1/dx*ones(N-1,1)) zeros(N-1,2*N+4)]+[zeros(N-1,1) diag(-2*nu/dx^2*ones(N-1,1)) zeros(N-1,3) diag(-1/dx*ones(N-1,1)) zeros(N-1,2*N+3)]+[zeros(N-1,2) diag(nu/dx^2*ones(N-1,1)) zeros(N-1,3*N+4)];zeros(1,N-1) 0 0 zeros(1,3*N+4);
            zeros(1,N+1) 0 0 zeros(1,3*N+2);[diag(mu/dx-1/(4*dx)*(x(N+3:2*N+2)+x(N+2:2*N+1)).^2./(x(1:N)).^2+1/(2*dx)*(x(3*N+6:4*N+5)-x(3*N+5:4*N+4)+VB(2:N+1)-VB(1:N))) zeros(N,1) diag(nu/dx^2+1/(2*dx)*(x(N+3:2*N+2)+x(N+2:2*N+1))./(x(1:N))) zeros(N,2) diag(2/(dx)*ones(N,1)) zeros(N,1) diag(-1/(2*dx)*(x(2:N+1)+x(1:N))) zeros(N,1)]+[zeros(N,1) diag(-mu/dx+1/(4*dx)*(x(N+4:2*N+3)+x(N+3:2*N+2)).^2./(x(2:N+1)).^2+1/(2*dx)*(x(3*N+6:4*N+5)-x(3*N+5:4*N+4)+VB(2:N+1)-VB(1:N))) zeros(N,1) diag(-1/tau-2*nu/dx^2-1/(2*dx)*((x(N+4:2*N+3)+x(N+3:2*N+2))./(x(2:N+1))-(x(N+3:2*N+2)+x(N+2:2*N+1))./(x(1:N)))) zeros(N,2) diag(-2/(dx)*ones(N,1)) zeros(N,1) diag(1/(2*dx)*(x(2:N+1)+x(1:N)))]+[zeros(N,N+3) diag(nu/dx^2-1/(2*dx)*(x(N+4:2*N+3)+x(N+3:2*N+2))./(x(2:N+1))) zeros(N,2*N+2)];zeros(1,2*N+1) 0 0 zeros(1,2*N+2);
            zeros(1,2*N+3) 0 0 zeros(1,2*N);[diag(-1/(4*dx)*(x(N+3:2*N+1)+x(N+2:2*N)).*x(2*N+4:3*N+2)./(x(1:N-1)).^2+nu/(8*dx^2)*(x(2:N)).*((x(N+5:2*
```

```
N+3)+x(N+4:2*N+2))./(x(3:N+1))-(x(N+3:2*N+1)+
x(N+2:2*N))./(x(1:N-1))).*(x(N+3:2*N+1)+x(N
+2:2*N))./(x(1:N-1)).^2-1/(4*dx)*(x(N+3:2*N
+1)+x(N+2:2*N)).*(2.*x(2*N+5:3*N+3)+mu.*x(2:N
))./(x(1:N-1)).^2) zeros(N-1,2) diag(1/(4*dx)
*(x(2*N+4:3*N+2))./(x(1:N-1))-nu/(8*dx^2)*(x
(2:N)).*((x(N+5:2*N+3)+x(N+4:2*N+2))./(x(3:N
+1))-(x(N+3:2*N+1)+x(N+2:2*N))./(x(1:N-1)))
./(x(1:N-1))+1/(4*dx)*(2*x(2*N+5:3*N+3)+mu*x
(2:N))./(x(1:N-1))) zeros(N-1,3) diag(nu/dx
^2+1/(4*dx)*(x(N+3:2*N+1)+x(N+2:2*N))./(x(1:N
-1))) zeros(N-1,N+3)]+[zeros(N-1,1) diag(nu
/(16*dx^2)*((x(N+5:2*N+3)+x(N+4:2*N+2))./(x
(3:N+1))-(x(N+3:2*N+1)+x(N+2:2*N))./(x(1:N-1)
)).^2-mu/(4*dx)*((x(N+5:2*N+3)+x(N+4:2*N+2))
./(x(3:N+1))-(x(N+3:2*N+1)+x(N+2:2*N))./(x(1:
N-1)))+1/tau) zeros(N-1,2) diag(1/(4*dx)*(x
(2*N+4:3*N+2))./(x(1:N-1))-nu/(8*dx^2)*x(2:N)
.*((x(N+5:2*N+3)+x(N+4:2*N+2))./(x(3:N+1))-(x
(N+3:2*N+1)+x(N+2:2*N))./(x(1:N-1)))./(x(1:N
-1))+1/(4*dx).*(2.*x(2*N+5:3*N+3)+mu.*x(2:N))
./(x(1:N-1))) zeros(N-1,3) diag(-2*nu/dx
^2-1/(2*dx)*((x(N+5:2*N+3)+x(N+4:2*N+2))./(x
(3:N+1))-(x(N+3:2*N+1)+x(N+2:2*N))./(x(1:N-1)
))-2/tau) zeros(N-1,N+2)]+[zeros(N-1,2) diag
(1/(4*dx)*(x(N+5:2*N+3)+x(N+4:2*N+2)).*x(2*N
+6:3*N+4)./(x(3:N+1)).^2-nu/(8*dx^2)*(x(2:N))
.*((x(N+5:2*N+3)+x(N+4:2*N+2))./(x(3:N+1))-(x
(N+3:2*N+1)+x(N+2:2*N))./(x(1:N-1))).*(x(N
+5:2*N+3)+x(N+4:2*N+2))./(x(3:N+1)).^2+1/(4*
dx)*(x(N+5:2*N+3)+x(N+4:2*N+2)).*(2.*x(2*N
+5:3*N+3)+mu.*x(2:N))./(x(3:N+1)).^2) zeros(N
-1,2) diag(-1/(4*dx)*x(2*N+6:3*N+4)./(x(3:N
+1))+nu/(8*dx^2)*(x(2:N)).*((x(N+5:2*N+3)+x(N
+4:2*N+2))./(x(3:N+1))-(x(N+3:2*N+1)+x(N+2:2*
N))./(x(1:N-1)))./(x(3:N+1))-1/(4*dx)*(2*x(2*
N+5:3*N+3)+mu*x(2:N))./(x(3:N+1))) zeros(N
-1,3) diag(nu/dx^2-1/(4*dx)*(x(N+5:2*N+3)+x(N
+4:2*N+2))./(x(3:N+1))) zeros(N-1,N+1)]+[
zeros(N-1,N+4) diag(-1/(4*dx)*x(2*N+6:3*N+4)
```

```
./(x(3:N+1))+nu/(8*dx^2)*(x(2:N)).*((x(N+5:2*
N+3)+x(N+4:2*N+2))./(x(3:N+1))-(x(N+3:2*N+1)+
x(N+2:2*N))./(x(1:N-1)))./(x(3:N+1))-1/(4*dx)
*(2*x(2*N+5:3*N+3)+mu*x(2:N))./(x(3:N+1)))
zeros(N-1,2*N+2)];zeros(1,3*N+2) 0 0 zeros(1,
N+1);
            zeros(N+1,4*N+5)];

        DB=[1 -1 zeros(1,4*N+3);
            zeros(N-1,4*N+5);
            zeros(1,N-1) -1 1 zeros(1,3*N+4);
            zeros(1,N+1) 1 -1 zeros(1,3*N+2);
            zeros(N,4*N+5);
            zeros(1,2*N+1) -1 1 zeros(1,2*N+2);
            zeros(1,2*N+3) 1 -1 zeros(1,2*N);
            zeros(N-1,4*N+5);
            zeros(1,3*N+2) -1 1 zeros(1,N+1);
            zeros(1,3*N+4) 1 zeros(1,N);
            [zeros(N-1,1) diag(-1*ones(N-1,1)) zeros(N-1,2*N
                +4) diag(lambda/dx^2*ones(N-1,1)) zeros(N
                -1,2)]+[zeros(N-1,3*N+5) diag(-2*lambda/dx^2*
                ones(N-1,1)) zeros(N-1,1)]+[zeros(N-1,3*N+6)
                diag(lambda/dx^2*ones(N-1,1))];
            zeros(1,4*N+4) 1];
        M=diag(ones(4*N+5,1));
        M(1,1)=0;
        M(N+1,N+1)=0;
        M(N+2,N+2)=0;
        M(2*N+3,2*N+3)=0;
        M(2*N+4,2*N+4)=0;
        M(3*N+4,3*N+4)=0;
        for j=3*N+5:4*N+5
            M(j,j)=0;
        end
        DF=[M-(t-t0)*funDF(X)+DB -funF(X)];
    end
end
```

Appendix C

Comparison to the isothermal model

Finally, we present our previous implementation for the isothermal model. Now, the internal energy density equation decouples from the current density equation and can be omitted. However, this introduces the third order differential quantum Bohm potential. Hence, we use ghost grid points $x_{-1} = -1/N$ and $x_{N+1} = 1+1/N$ with the corresponding ghost densities $n_{-1} = n_1$ and $n_{N+1} = n_{N-1}$, which satisfy $n''(0) = 0 = n''(1)$. The density and electric potential are discretized at the grid points x_i and the current density is discretized at the middle points $x_{i-\frac{1}{2}}$, with $J_{i-\frac{1}{2}} = (J_i + J_{i-1})/2$. The discretized isothermal viscous quantum hydrodynamic sytem is given by

$$\left.\begin{aligned}
F_{1,i} &= \frac{\nu}{h^2}(n_{i+1} - 2n_i + n_{i-1}) - \frac{1}{h}(J_{i+\frac{1}{2}} - J_{i-\frac{1}{2}}), \quad i = 1, \dots, N-1, \\
F_{2,i-\frac{1}{2}} &= \frac{\nu}{h^2}(J_{i+\frac{1}{2}} - 2J_{i-\frac{1}{2}} + J_{i-\frac{3}{2}}) - \frac{1}{4h}\left(\frac{(J_{i+\frac{1}{2}} + J_{i-\frac{1}{2}})^2}{n_i} - \frac{(J_{i-\frac{1}{2}} + J_{i-\frac{3}{2}})^2}{n_{i-1}}\right) \\
&\quad - \frac{T}{h}(n_i - n_{i-1}) - \frac{J_{i-\frac{1}{2}}}{\tau} \\
&\quad + \frac{n_i + n_{i-1}}{2h}\Big(V_i - V_{i-1} + V_{B,i} - V_{B,i-1} + B_i - B_{i-1}\Big), \quad i = 1, \dots N, \\
F_{3,i} &= \frac{\lambda^2}{h^2}(V_{i+1} - 2V_i + V_{i-1}) - n_i + C_i, \quad i = 1, \dots N-1,
\end{aligned}\right\} \tag{C.0.1}$$

with the quantum Bohm potential

$$B_i = \frac{\epsilon^2}{2h^2}\sqrt{\frac{n_{i+1}}{n_i}} + \sqrt{\frac{n_{i-1}}{n_i}} - 2. \tag{C.0.2}$$

The boundary conditions are

$$\left.\begin{aligned}
n_{-1} - n_1 &= 0, \quad n_0 - C(0) = 0, \quad n_N - C(1) = 0, \quad n_{N+1} - n_{N-1} = 0, \\
J_{-\frac{1}{2}} - J_{\frac{1}{2}} &= 0, \quad J_{N-\frac{1}{2}} - J_{N+\frac{1}{2}} = 0, \\
V_0 &= 0, \quad V_N - U_0 = 0.
\end{aligned}\right\} \tag{C.0.3}$$

As initial solution for 0V, we suggest solving the isothermal model without a barrier potential. This solution can then be used as initial guess for the system with barrier potential. Lastly, we give the partial derivatives of the functions $F_{j,i}$, $j = 1, 2, 3$, w.r.t. the variables n_i, $J_{i-\frac{1}{2}}$ and V_i, required for the Jacobian matrix

$$\left.\begin{aligned}
\partial_{n_{i-1}} F_{1,i} &= \frac{\nu}{h^2}, \quad \partial_{n_i} F_{1,i} = -\frac{2\nu}{h^2}, \quad \partial_{n_{i+1}} F_{1,i} = \frac{\nu}{h^2}, \\
\partial_{J_{i-\frac{1}{2}}} F_{1,i} &= \frac{1}{h}, \quad \partial_{J_{i+\frac{1}{2}}} F_{1,i} = -\frac{1}{h}, \\
\partial_{n_{i-2}} F_{2,i} &= -\frac{\epsilon^2}{8h^3} \frac{n_i + n_{i-1}}{\sqrt{n_{i-1} n_{i-2}}}, \\
\partial_{n_{i-1}} F_{2,i} &= -\frac{1}{4h} \frac{(J_{i-\frac{3}{2}} + J_{i-\frac{1}{2}})^2}{(n_{i-1})^2} + \frac{T}{h} \\
&\quad + \frac{1}{2h}\left(V_i - V_{i-1} + V_{B,i} - V_{B,i-1} + B_i - B_{i-1}\right) \\
&\quad + \frac{\epsilon^2}{8h^3}(n_{i-1} + n_i)\left(\frac{1}{\sqrt{n_i n_{i-1}}} + \sqrt{\frac{n_i}{n_{i-1}^3}} + \sqrt{\frac{n_{i-2}}{n_{i-1}^3}}\right), \\
\partial_{n_i} F_{2,i} &= \frac{1}{4h} \frac{(J_{i+\frac{1}{2}} + J_{i-\frac{1}{2}})^2}{(n_i)^2} - \frac{T}{h} \\
&\quad + \frac{1}{2h}\left(V_i - V_{i-1} + V_{B,i} - V_{B,i-1} + B_i - B_{i-1}\right) \\
&\quad - \frac{\epsilon^2}{8h^3}(n_{i-1} + n_i)\left(\frac{1}{\sqrt{n_i n_{i-1}}} + \sqrt{\frac{n_{i+1}}{n_i^3}} + \sqrt{\frac{n_{i-1}}{n_i^3}}\right), \\
\partial_{n_{i+1}} F_{2,i} &= \frac{\epsilon^2}{8h^3} \frac{n_i + n_{i-1}}{\sqrt{n_i n_{i+1}}}, \\
\partial_{J_{i-\frac{3}{2}}} F_{2,i} &= \frac{\nu}{h^2} + \frac{1}{2h} \frac{J_{i-\frac{1}{2}} + J_{i-\frac{3}{2}}}{n_{i-1}}, \\
\partial_{J_{i-\frac{1}{2}}} F_{2,i} &= -\frac{2\nu}{h^2} - \frac{1}{\tau} - \frac{1}{2h}\left(\frac{J_{i+\frac{1}{2}} + J_{i-\frac{1}{2}}}{n_i} - \frac{J_{i-\frac{1}{2}} + J_{i-\frac{3}{2}}}{n_{i-1}}\right), \\
\partial_{J_{i+\frac{1}{2}}} F_{2,i} &= \frac{\nu}{h^2} - \frac{1}{2h} \frac{J_{i+\frac{1}{2}} + J_{i-\frac{1}{2}}}{n_i}, \\
\partial_{V_{i-1}} F_{2,i} &= -\frac{n_i + n_{i-1}}{2h}, \quad \partial_{V_i} F_{2,i} = \frac{n_i + n_{i-1}}{2h}, \\
\partial_{n_i} F_{3,i} &= -1, \\
\partial_{V_{i-1}} F_{3,i} &= \frac{\lambda^2}{h^2}, \quad \partial_{V_i} F_{3,i} = -\frac{2\lambda^2}{h^2}, \quad \partial_{V_{i+1}} F_{3,i} = \frac{\lambda^2}{h^2}.
\end{aligned}\right\} \tag{C.0.4}$$

Using the continuation method described in sec. 4.2, we obtain qualitatively similar results compared to [JT06], shown in fig C.1 and C.2. It was already stated in [JT06, JM07], that the isothermal model is not a propper model for resonant tunneling diodes. Additionally, experimental results show a different behavior aswell, see e.g. [KKFR89]. Since our approach gives the same results, we use our algorithm to numerically solve the full viscous quantum hydrodynamic equations with barrier potential. Note however, that the authors of [JT06] gave a plot for the effective current density versus the applied voltage with a voltage up to 0.3V, using the viscosity constant $\nu_0 = 0.00289$, whereas we continued our calculations up to 0.54V. Between 0.3V and 0.54V we observe loops in the current voltage characteristic. Since our algorithm follows a continuous curve where no jumps can occur, these loops may be a natural effect of the isothermal model. However, we observed numerical errors for the full viscous quantum hydrodynamic system for voltages above 0.3V, hence these loops could also be a numerical error. We conclude that our algortihm should be used with care for larger values of the applied voltage.

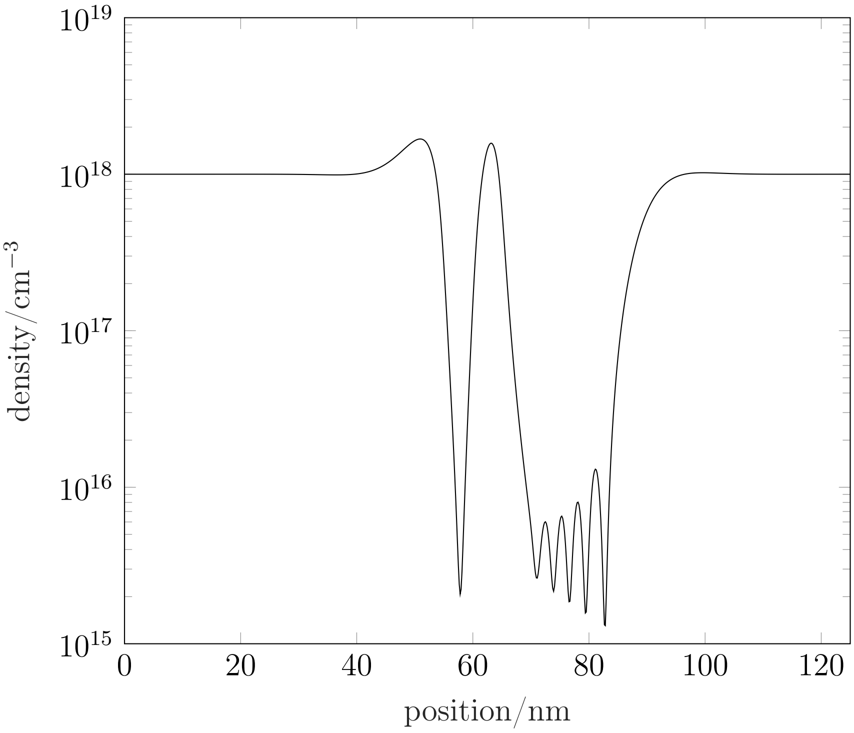

Figure C.1: Electron density of the isothermal model for the applied voltage of 0.54V using 800 grid points.

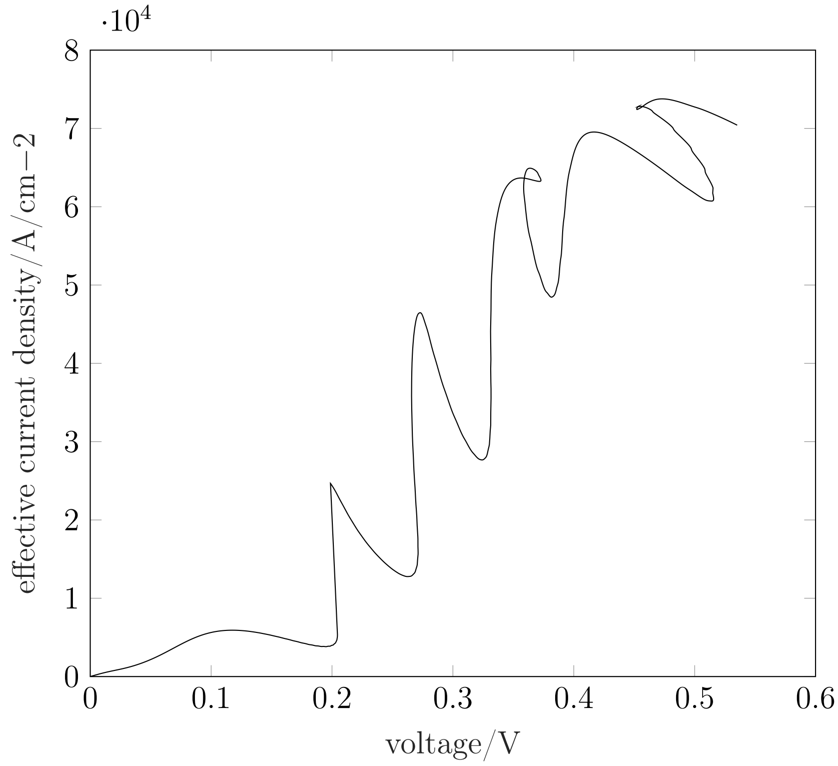

Figure C.2: Current voltage characteristic of a resonant tunneling diode modeled by the isothermal viscous quantum hydrodynamic equations, using 800 grid points.

Appendix D

Jacobian of the full discretized system

Here we give complete Jacobian of the discretized version of the full viscous quantum hydrodynamic system with barrier potential. Alternatively, the Jacobian can be approximated using any difference scheme or interpolation of previously calculated Jacobians, which introduces additional errors.

$$
\begin{aligned}
&\partial_{n_{i-1}} F_{1,i} = \frac{\nu}{h^2}, \quad \partial_{n_i} F_{1,i} = -\frac{2\nu}{h^2}, \quad \partial_{n_{i+1}} F_{1,i} = \frac{\nu}{h^2},\\
&\partial_{J_{i-\frac{1}{2}}} F_{1,i} = \frac{1}{h}, \quad \partial_{J_{i+\frac{1}{2}}} F_{1,i} = -\frac{1}{h},\\
&\partial_{n_{i-1}} F_{2,i} = -\frac{1}{4h}\frac{(J_{i-\frac{1}{2}} + J_{i-\frac{3}{2}})^2}{(n_{i-1})^2} + \frac{\mu}{h} + \frac{1}{2h}(V_i - V_{i-1} + V_{B,i} - V_{B,i-1}),\\
&\quad \partial_{n_i} F_{2,i} = \frac{1}{4h}\frac{(J_{i+\frac{1}{2}} + J_{i-\frac{1}{2}})^2}{(n_i)^2} - \frac{\mu}{h} + \frac{1}{2h}(V_i - V_{i-1} + V_{B,i} - V_{B,i-1}),\\
&\partial_{J_{i-\frac{3}{2}}} F_{2,i} = \frac{\nu}{h^2} + \frac{1}{2h}\frac{J_{i-\frac{1}{2}} + J_{i-\frac{3}{2}}}{n_{i-1}},\\
&\partial_{J_{i-\frac{1}{2}}} F_{2,i} = -2\frac{\nu}{h^2} - \frac{1}{2h}\left(\frac{J_{i+\frac{1}{2}} + J_{i-\frac{1}{2}}}{n_i} - \frac{J_{i-\frac{1}{2}} + J_{i-\frac{3}{2}}}{n_{i-1}}\right) - \frac{1}{\tau},\\
&\partial_{J_{i+\frac{1}{2}}} F_{2,i} = \frac{\nu}{h^2} - \frac{1}{2h}\frac{J_{i+\frac{1}{2}} + J_{i-\frac{1}{2}}}{n_i},\\
&\partial_{ni_{i-1}} F_{2,i} = \frac{2}{h}, \quad \partial_{ni_i} F_{2,i} = -\frac{2}{h},\\
&\partial_{V_{i-1}} F_{2,i} = -\frac{n_i + n_{i-1}}{2h}, \quad \partial_{V_i} F_{2,i} = \frac{n_i + n_{i-1}}{2h},
\end{aligned}
$$

$$
\begin{aligned}
\partial_{n_{i-1}} F_{3,i} &= -\frac{1}{2h} \frac{\left(J_{i-\frac{1}{2}} + J_{i-\frac{3}{2}}\right) ni_{i-1}}{(n_{i-1})^2} \\
&+ \frac{\nu}{8h^2} n_i \left(\frac{J_{i+\frac{3}{2}} + J_{i+\frac{1}{2}}}{n_{i+1}} - \frac{J_{i-\frac{1}{2}} + J_{i-\frac{3}{2}}}{n_{i-1}} \right) \frac{J_{i-\frac{1}{2}} + J_{i-\frac{3}{2}}}{(n_{i-1})^2} \\
&- \frac{1}{4h} \frac{J_{i-\frac{1}{2}} + J_{i-\frac{3}{2}}}{(n_{i-1})^2} (2ni_i + \mu n_i), \\
\partial_{n_i} F_{3,i} &= \frac{\nu}{16h^2} \left(\frac{J_{i+\frac{3}{2}} + J_{i+\frac{1}{2}}}{n_{i+1}} - \frac{J_{i-\frac{1}{2}} + J_{i-\frac{3}{2}}}{n_{i-1}} \right)^2 \\
&- \frac{\mu}{4h} \left(\frac{J_{i+\frac{3}{2}} + J_{i+\frac{1}{2}}}{n_{i+1}} - \frac{J_{i-\frac{1}{2}} + J_{i-\frac{3}{2}}}{n_{i-1}} \right) + \frac{1}{\tau}, \\
\partial_{n_{i+1}} F_{3,i} &= \frac{1}{4h} \frac{\left(J_{i+\frac{3}{2}} + J_{i+\frac{1}{2}}\right) ni_{i+1}}{(n_{i+1})^2} \\
&- \frac{\nu}{8h^2} n_i \left(\frac{J_{i+\frac{3}{2}} + J_{i+\frac{1}{2}}}{n_{i+1}} - \frac{J_{i-\frac{1}{2}} + J_{i-\frac{3}{2}}}{n_{i-1}} \right) \frac{J_{i+\frac{3}{2}} + J_{i+\frac{1}{2}}}{(n_{i+1})^2} \\
&+ \frac{1}{4h} \frac{J_{i+\frac{3}{2}} + J_{i+\frac{1}{2}}}{(n_{i+1})^2} (2ni_i + \mu n_i), \\
\partial_{J_{i-\frac{3}{2}}} F_{3,i} &= \frac{1}{4h} \frac{ni_{i-1}}{n_{i-1}} - \frac{\nu}{8h^2} \frac{n_i}{n_{i-1}} \left(\frac{J_{i+\frac{3}{2}} + J_{i+\frac{1}{2}}}{n_{i+1}} - \frac{J_{i-\frac{1}{2}} + J_{i-\frac{3}{2}}}{n_{i-1}} \right) \\
&+ \frac{1}{4h} \frac{2ni_i + \mu n_i}{n_{i-1}}, \\
\partial_{J_{i-\frac{1}{2}}} F_{3,i} &= \partial_{J_{i-\frac{3}{2}}} F_{3,i}, \\
\partial_{J_{i+\frac{1}{2}}} F_{3,i} &= -\frac{1}{4h} \frac{ni_{i+1}}{n_{i+1}} + \frac{\nu}{8h^2} \frac{n_i}{n_{i+1}} \left(\frac{J_{i+\frac{3}{2}} J_{i+\frac{1}{2}}}{n_{i+1}} - \frac{J_{i-\frac{1}{2}} + J_{i-\frac{3}{2}}}{n_{i-1}} \right) \\
&- \frac{1}{4h} \frac{2ni_i + \mu n_i}{n_{i+1}}, \\
\partial_{J_{i+\frac{3}{2}}} F_{3,i} &= \partial_{J_{i+\frac{1}{2}}} F_{3,i}, \\
\partial_{ni_{i-1}} F_{3,i} &= \frac{\nu}{h^2} + \frac{1}{4h} \frac{J_{i-\frac{1}{2}} + J_{i-\frac{3}{2}}}{n_{i-1}}, \\
\partial_{ni_i} F_{3,i} &= -2\frac{\nu}{h^2} - \frac{1}{2h} \left(\frac{J_{i+\frac{3}{2}} + J_{i+\frac{1}{2}}}{n_{i+1}} - \frac{J_{i-\frac{1}{2}} + J_{i-\frac{3}{2}}}{n_{i-1}} \right) - \frac{2}{\tau}, \\
\partial_{ni_{i+1}} F_{3,i} &= \frac{\nu}{h^2} - \frac{1}{4h} \frac{J_{i+\frac{3}{2}} + J_{i+\frac{1}{2}}}{n_{i+1}}.
\end{aligned}
$$

Beruflicher Werdegang

Anstellungen

04/2018-31/12/2023	Wissenschaftlicher Mitarbeiter an der Universität Rostock am Institut für Mathematik
01/2016-06/2016	Wissenschaftliche Hilfskraft an der Universität Rostock am Institut für Physik

Ausbildung

Studium	der Physik an der Universiät Rostock (2012-2017) M.Sc. (09/2017)
Schule	Grundschule und Gymnasium (2000-2012) Abitur am Ostseegymnasium Rostock (06/2012)

Selbstständigkeitserklärung

Ich versichere hiermit an Eides statt, dass ich die vorliegende Arbeit selbstständig angefertigt und ohne fremde Hilfe verfasst habe, keine außer den von mir angegebenen Hilfsmitteln und Quellen dazu verwendet habe und die den benutzten Werken inhaltlich und wörtlich entnommenen Stellen als solche kenntlich gemacht habe.

Rostock, den 15. September 2023